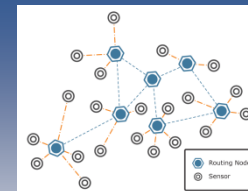




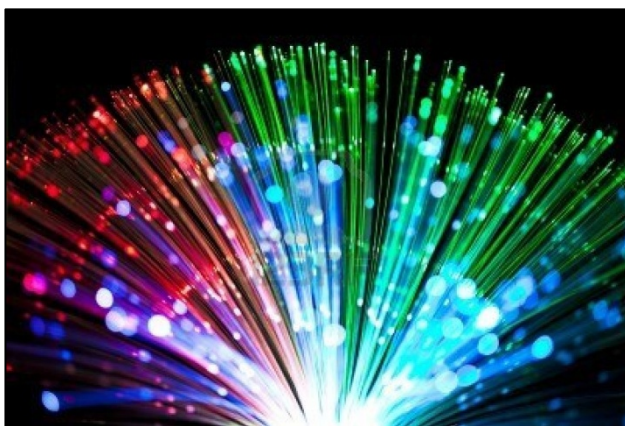
Optoelectronics Group, Engineering Department
University of Sannio, Benevento (Italy)



Fiber Optic Sensors for Industrial Applications *Perspectives, Challenges and New Trends*



*Andrea Cusano, Optoelectronic Division
University of Sannio*

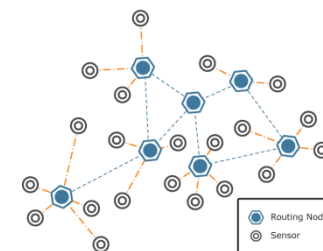


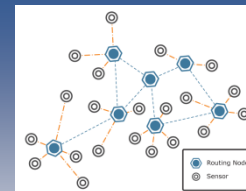
University of Padova, Dept. of Information Engineering



2013 Summer School of Information Engineering
Bressanone (Brixen, BZ), Italy -- June 30 – July 6, 2013

Sensors and sensors networks



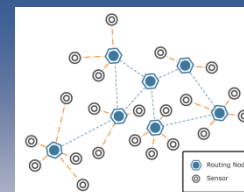


Outline

- *Introduction*
- *Fiber Optic Sensors*
- *Fiber Bragg Grating Sensors*
- *Industrial Applications: Case Studies*
- *A new Vision: Lab on Fiber Technology*
- *Conclusions*



Optoelectronics Group, Engineering Department
University of Sannio, Benevento (Italy)

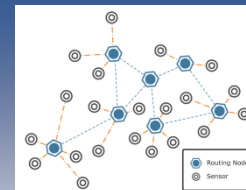


OPTOELECTRONICS group
University of Sannio



University of Sannio
Department of Engineering
BENEVENTO





Optoelectronics Group Members

Full Professor

- Prof. Antonello Cutolo

Associate Professors

- Prof. Andrea Cusano
- Prof. Giovanni Vito Persiano
- Prof. Stafania Campopiano

Assistant Professor

- Dr. Marco Consales
- Dr. Agostino Iadicicco

Post-doc Researchers

- Dr. Marco Pisco
- Dr. Armando Ricciardi
- Dr. Alessio Crescitelli

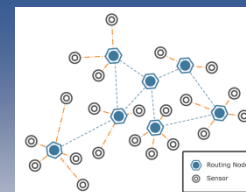
- Dr. Massimo Moccia
- Dr. Giuseppe Quero
- Dr. Giuseppe Lanza
- Dr. Francesco Bruno

Ph. D. Students

- Ing. Antonio Iele (3rd year)
- Ing. Alberto Micco (1st year)
- Ing. Gaia Berruti (1st year)
- Ing. Antonella Chiuchiolo (1st year)

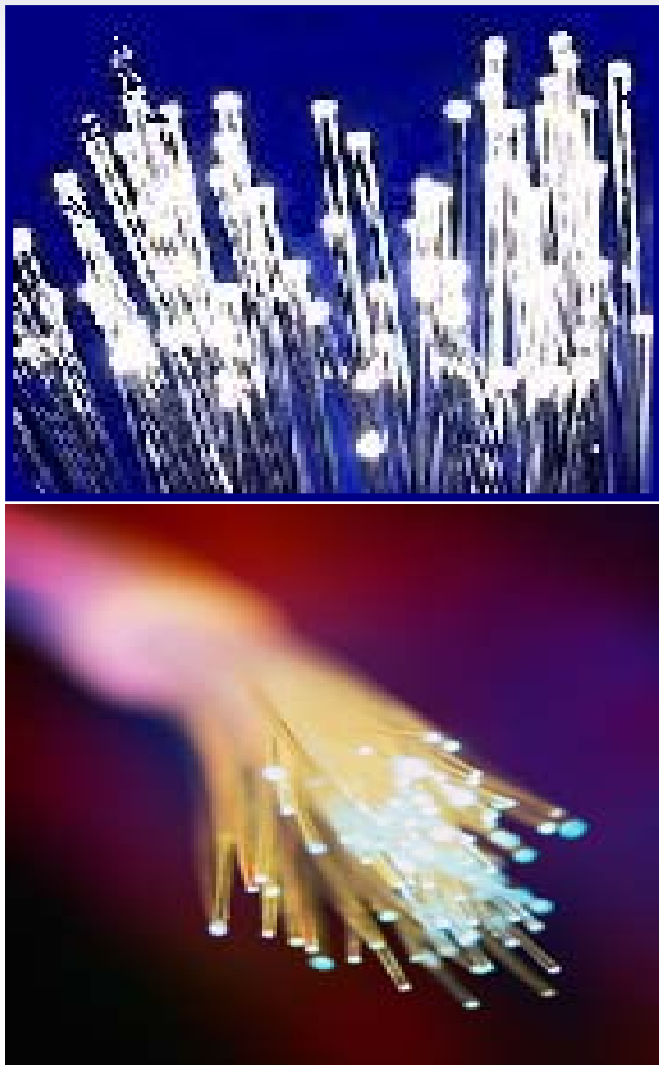
Administrative

- Dott. Paola Ambrosino



Spin-off Companies

NAME	YEAR	CORE BUSINESS
<p>Optosmart s.r.l.</p>  <p>OPTOELECTRONIC AND SMART SYSTEMS</p>	2005	Design and development of fiber optic sensor systems for structural and environmental monitoring applications.
<p>Optoadvance s.r.l.</p> 	2011	Design and development of fiber optic sensors for musical and biological applications.



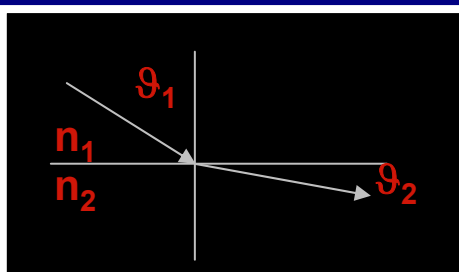
Optical Fiber

- ❑ a filament of transparent dielectric material, glass or plastic
- ❑ usually cylindrical in shape
- ❑ a guidance system for light

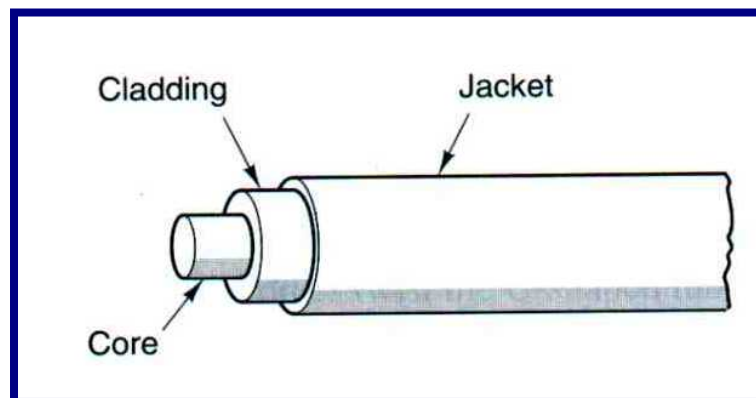
Optical Fiber

SNELL'S LAW:

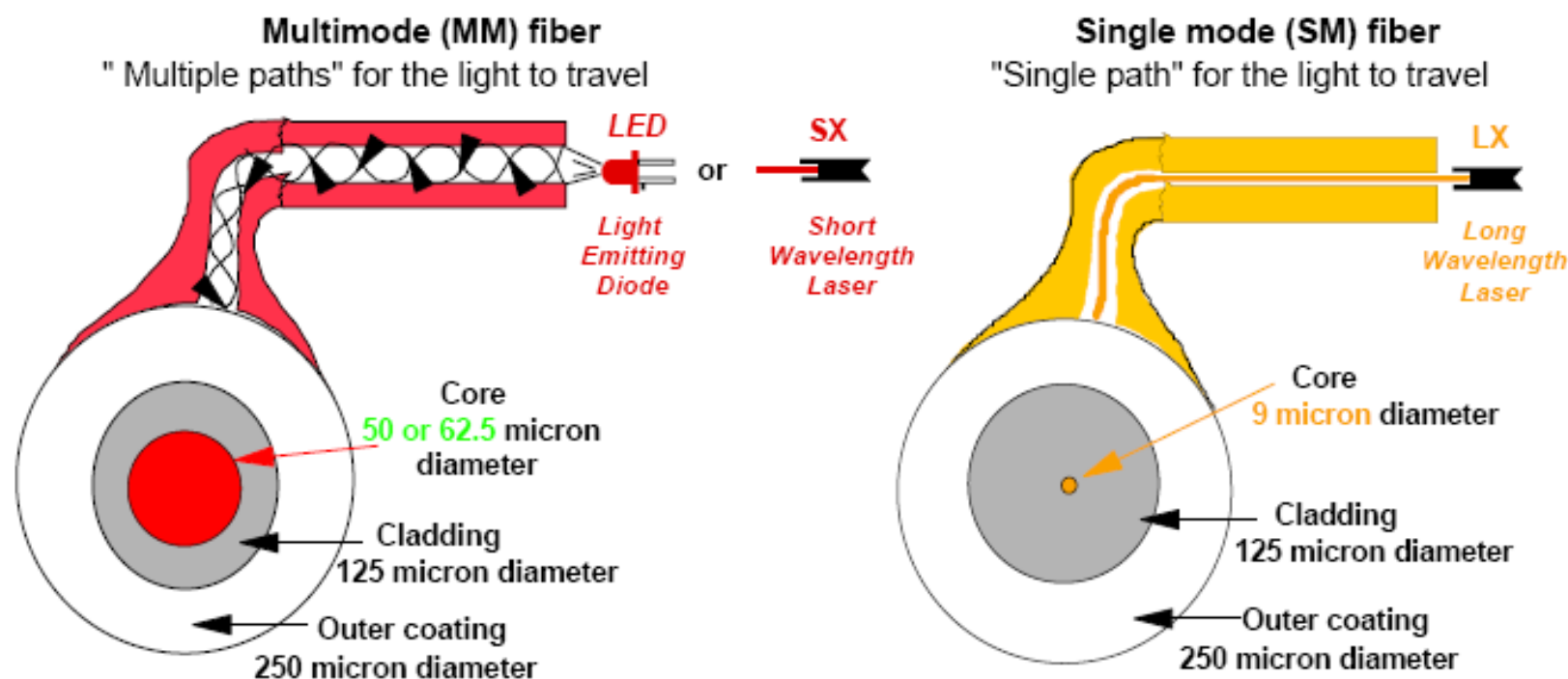
$n_1 \sin \vartheta_1 = n_2 \sin \vartheta_2$
where n is the refractive index



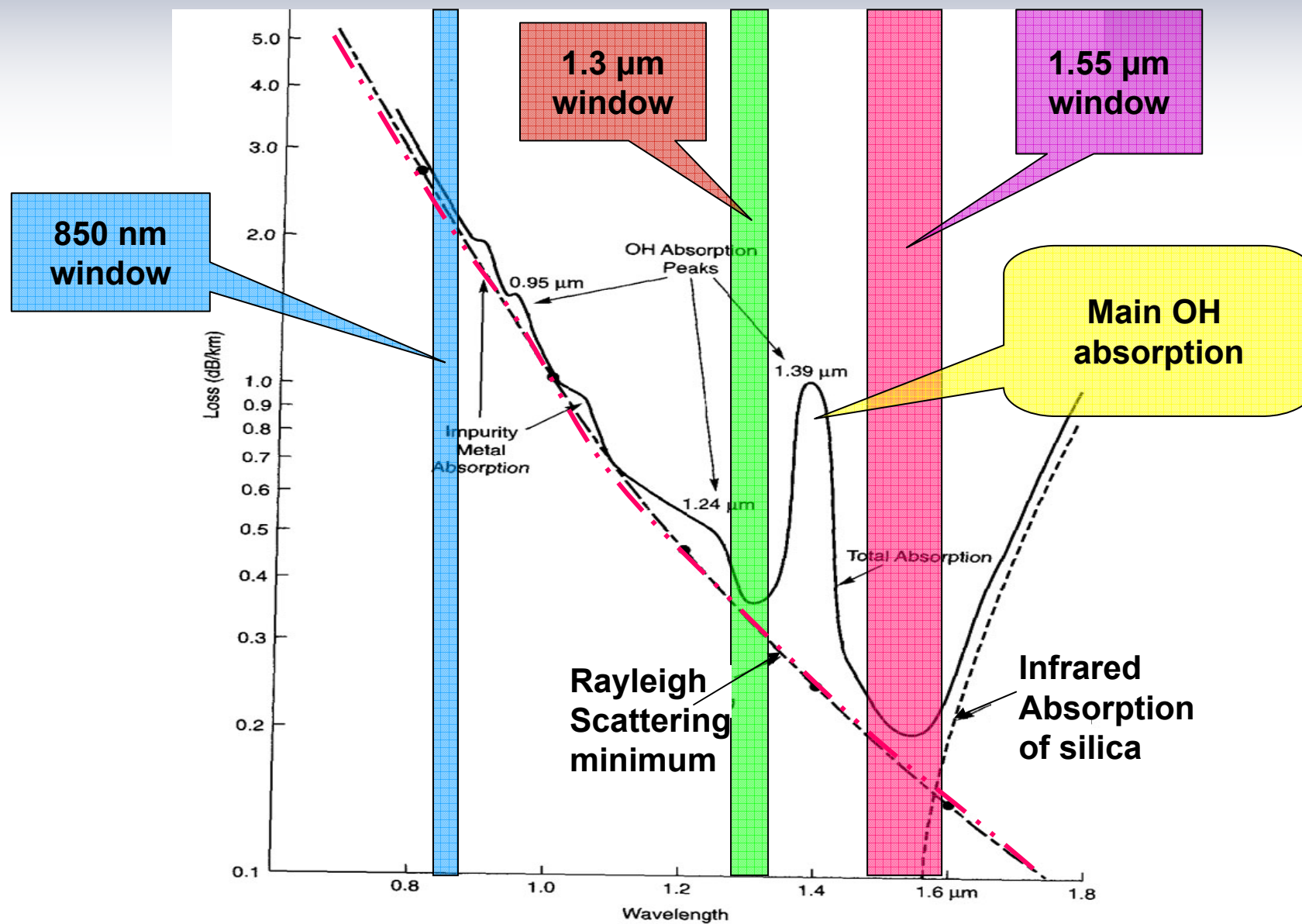
- Guidance is achieved through total internal reflection at the core-cladding interface
- Core, transparent dielectric material, surrounded by another dielectric material with a lower refractive index called cladding. ($n_1 > n_2$)
- In practice, there is a third protective layer called jacket.



Fiber Optic Technology

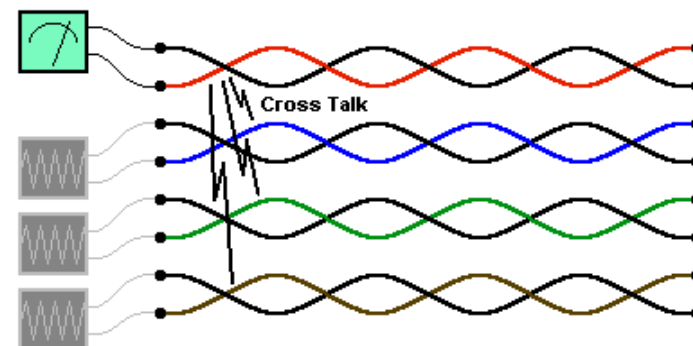


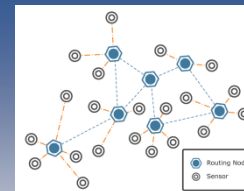
For comparison purposes
this is the relative size of a
human hair (@ 70 microns)



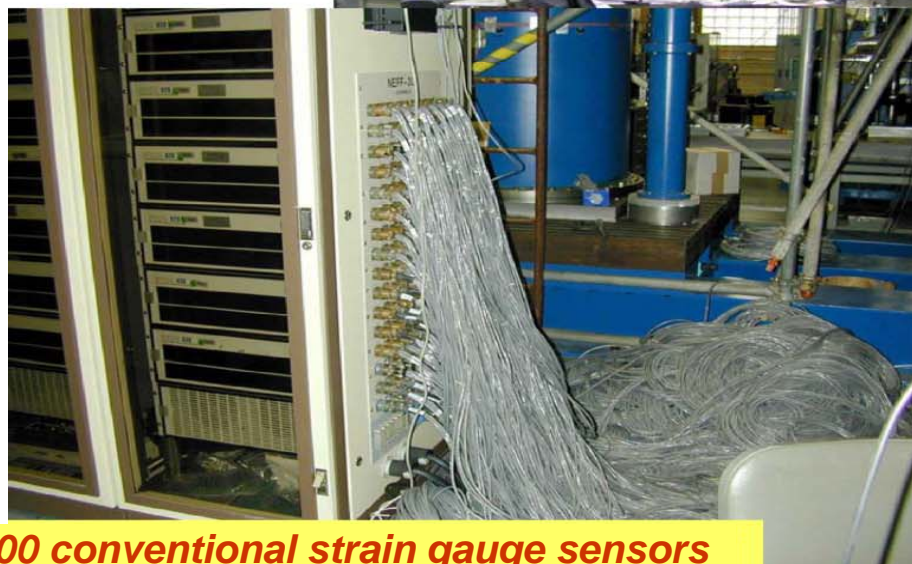
- ❑ Capacity: much wider bandwidth
- ❑ Crosstalk immunity
- ❑ Immunity to static interference
 - Lightning
 - Electric motor
 - Fluorescent light
- ❑ Higher environment immunity
 - Weather, temperature, etc.
- ❑ Safety: Fiber is non-metallic
 - No explosion, no shock
- ❑ Longer lasting
- ❑ Security: tapping is difficult
- ❑ Economics: Fewer repeaters
 - Low transmission loss (dB/km)
 - Fewer repeaters
 - Less cable

Optical Fiber Advantages





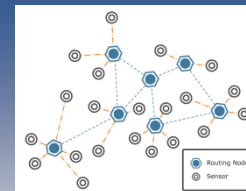
Why Fiber Optic Sensors?



400 conventional strain gauge sensors

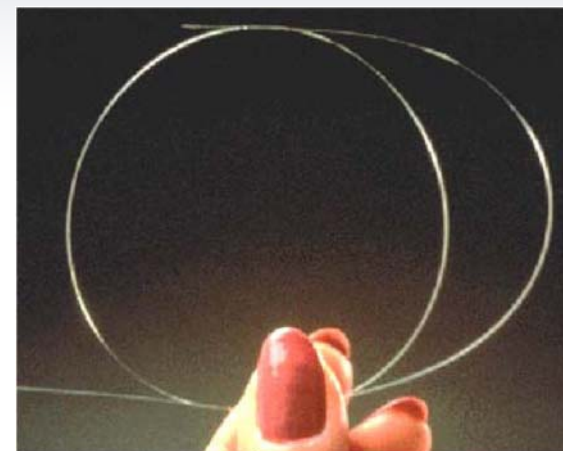


3000 fiber optic FBG strain sensors

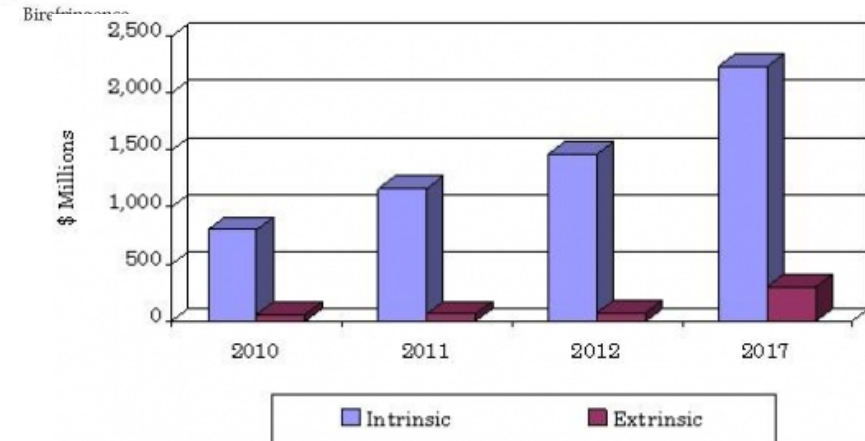
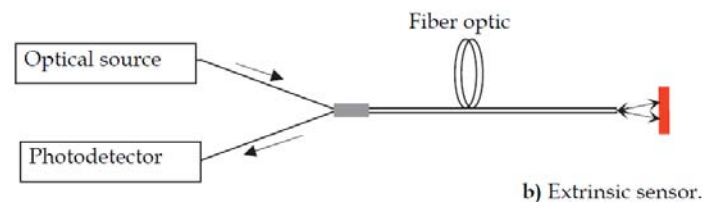
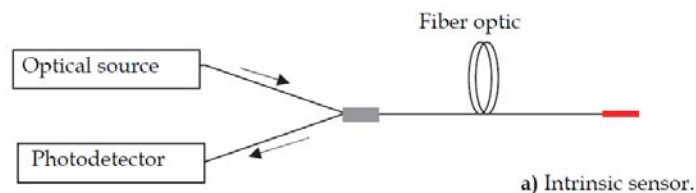
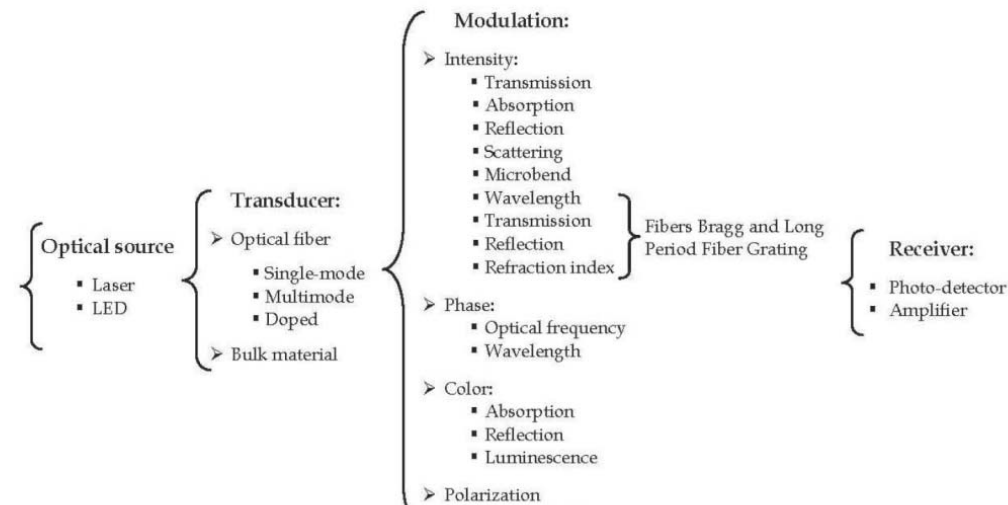
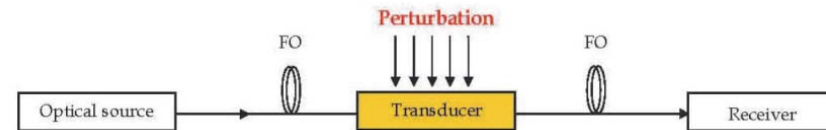


Advantages of Fiber Optic Sensors

- *Galvanic isolation*
- *EMI immunity*
- *Intrinsically safe*
- *Passive: no need for electrical power*
- *Possibility of remote, multiplexed operation*
- *Small size and lightweight*
- *Integrated telemetry: fiber itself is a data link*
- *Wide bandwidth*
- *High sensitivity*

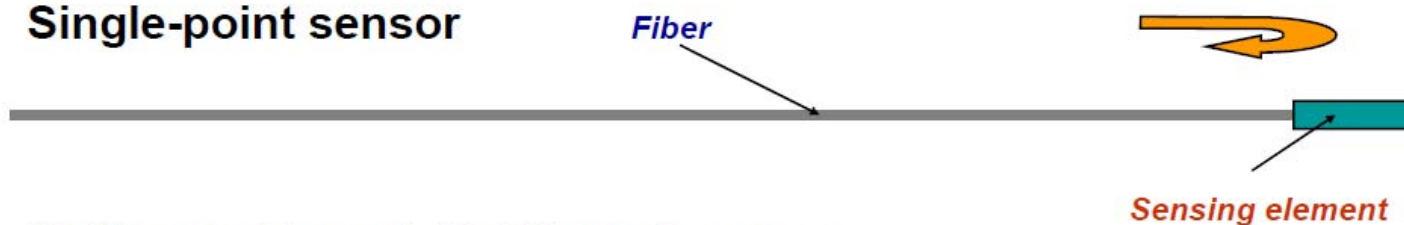


Fiber Optic Sensors: Fundamentals

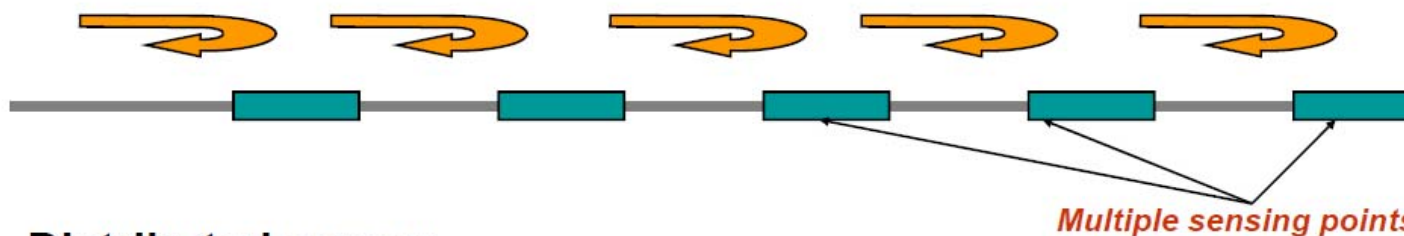


Fiber Sensors Configurations

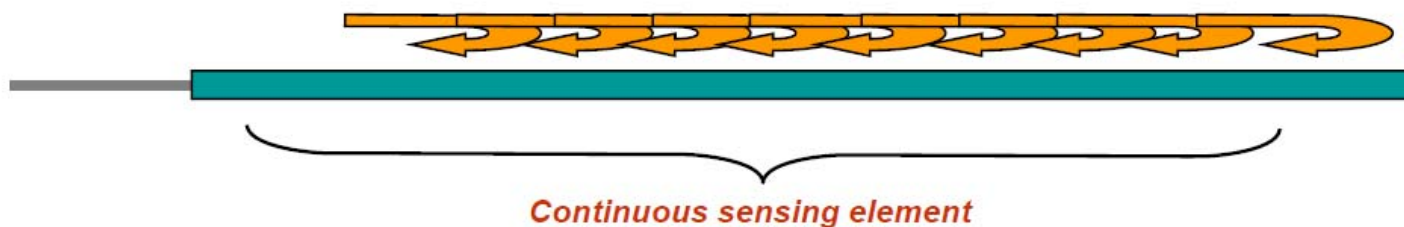
Single-point sensor



Multi-point (quasi-distributed) sensor



Distributed sensor



Extrinsic Optical Fiber Sensors (EOFS)



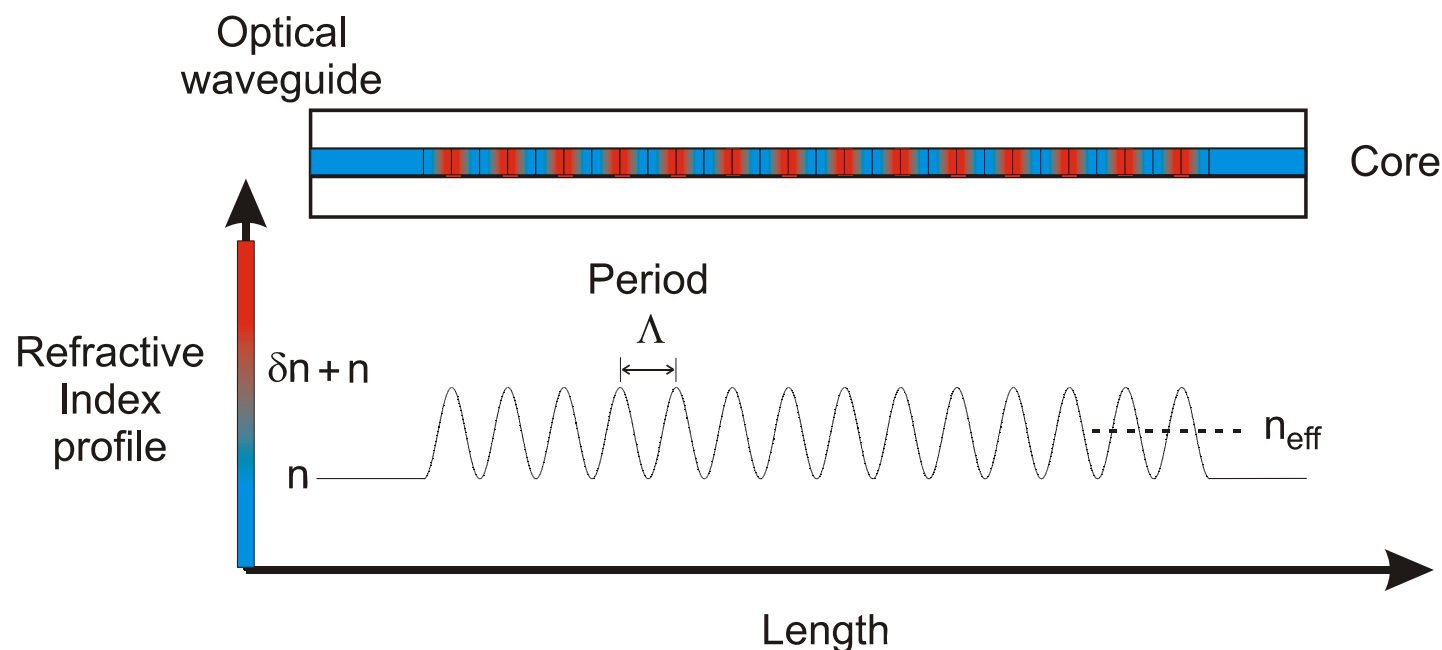
Intrinsic Optical Fiber Sensors (IOFS)



~ Bragg grating fundamentals ~

What is a Bragg grating?

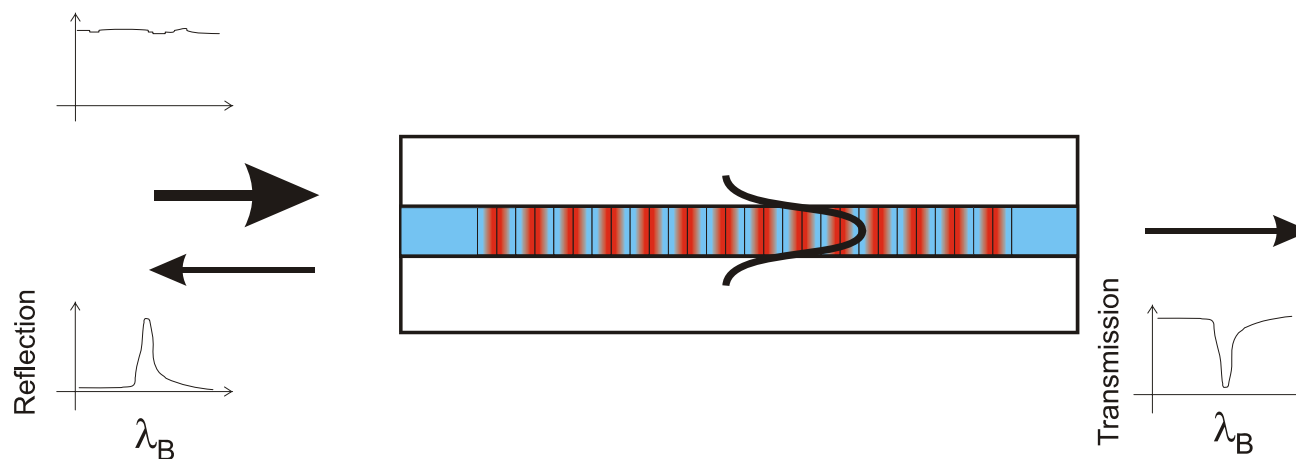
- A periodic or almost periodic structure consisting of a variation of for example the refractive index along the length of a waveguide.



~ Bragg grating fundamentals ~

What does it do?.

- Coupling of a forward propagating core-mode to a backward propagating core-mode.
- Acts as a band-rejection filter passing all wavelengths that are not in resonance with the grating and reflecting the wavelength that satisfies the Bragg condition.



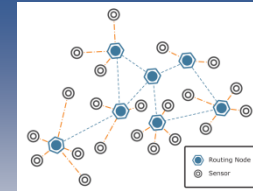
~ Bragg grating fundamentals ~

Why?.

- A small Fresnel reflection from each low-high, high-low refractive index transition.

$$r = \left(\frac{n - (n + \delta n)}{n + (n + \delta n)} \right)^2 = \left(\frac{\delta n}{2n + \delta n} \right)^2 \approx 10^{-9}$$





~ Bragg grating fundamentals ~

Parameters related to a Bragg grating.

- Strong overall reflection is achieved when each of the reflected contributions add in-phase (phase coherence/matching).

$$\beta = k \cdot n_{eff} = \frac{2\pi}{\lambda} \cdot n_{eff} \quad (\text{Propagation constant})$$

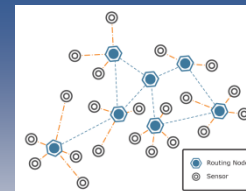
$$\delta = \beta \cdot \Lambda \quad (\text{phase of the propagating wave})$$

For each of the reflected contribution to add in phase

$$\delta = m \cdot 2\pi \quad (m \text{ positive integer})$$

\Downarrow

$$\underline{\lambda_B \cdot m = 2 \cdot n_{eff} \cdot \Lambda} \quad (\text{Bragg condition})$$



BRAGG GRATINGS : Theory

- Grating couples two modes in a fiber

- e.g: forward -> backward
- Coupling strength given by κ :

$$\kappa \propto \int E_n^*(x) \Delta n(x) E_m(x) dx$$

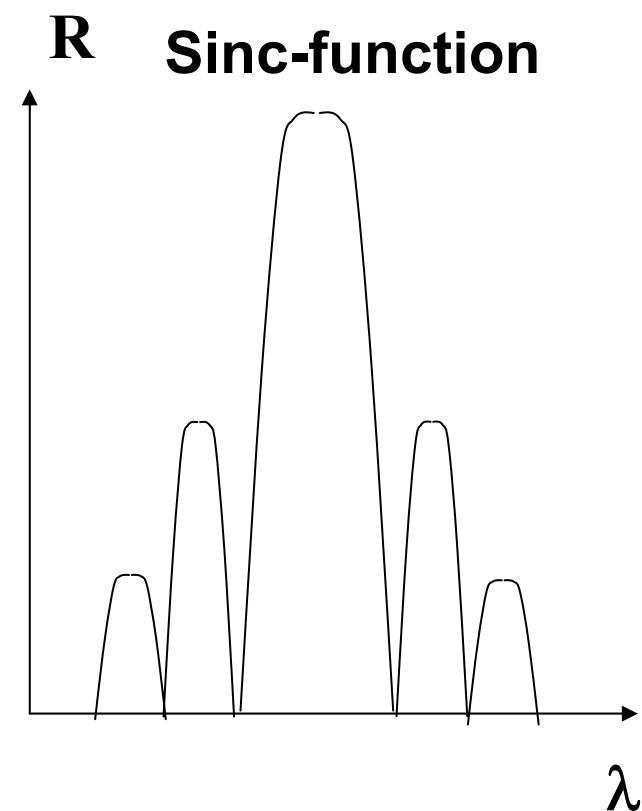
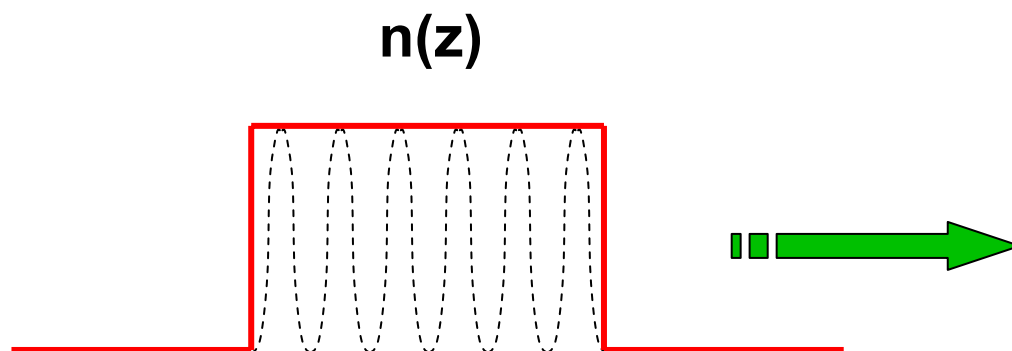
- E_n and E_m are the electric fields related to mode n and m respectively
- Grating length L , for complete power transfer

Maximum
Reflectance
Conditions

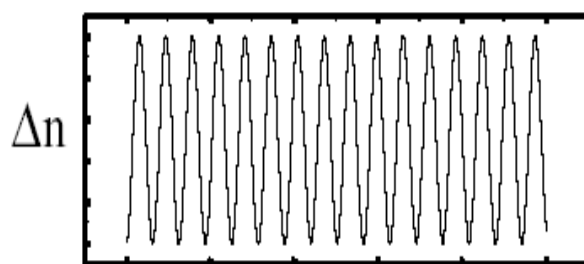
$$L = \frac{\pi}{2 |\kappa|}$$

BRAGG GRATINGS APPROXIMATION

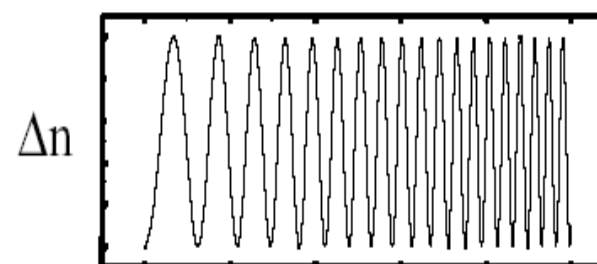
- ❑ Reflection spectrum a F. T. of the index profile
- ❑ Grating starts and stops abruptly
- ❑ F. T. of square function is a sinc function



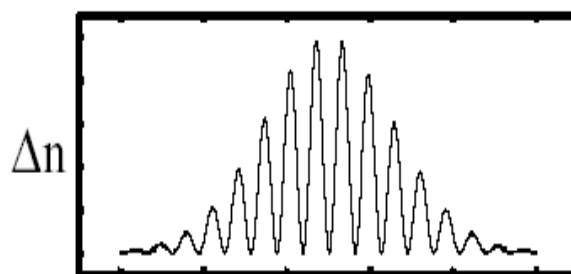
Suitable refractive index modulation can provide different spectral characteristics



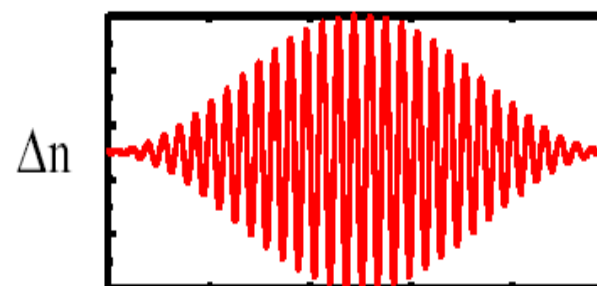
Uniform Profile : Uniform
Bragg Grating Period (typical).



Chirp : Non-Uniform
Bragg Grating Period.



Apodization : Tailored
Spatial Exposure.

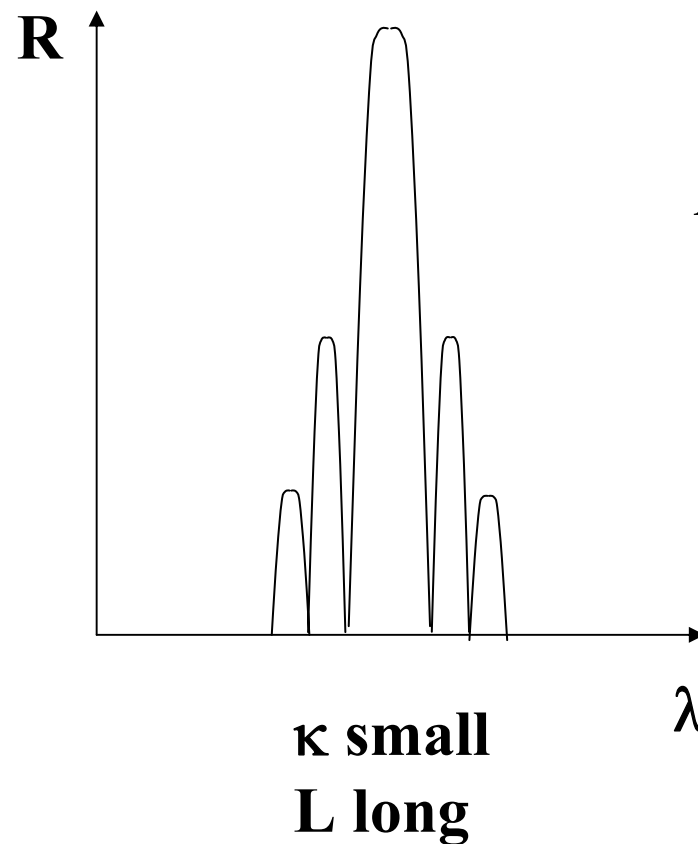
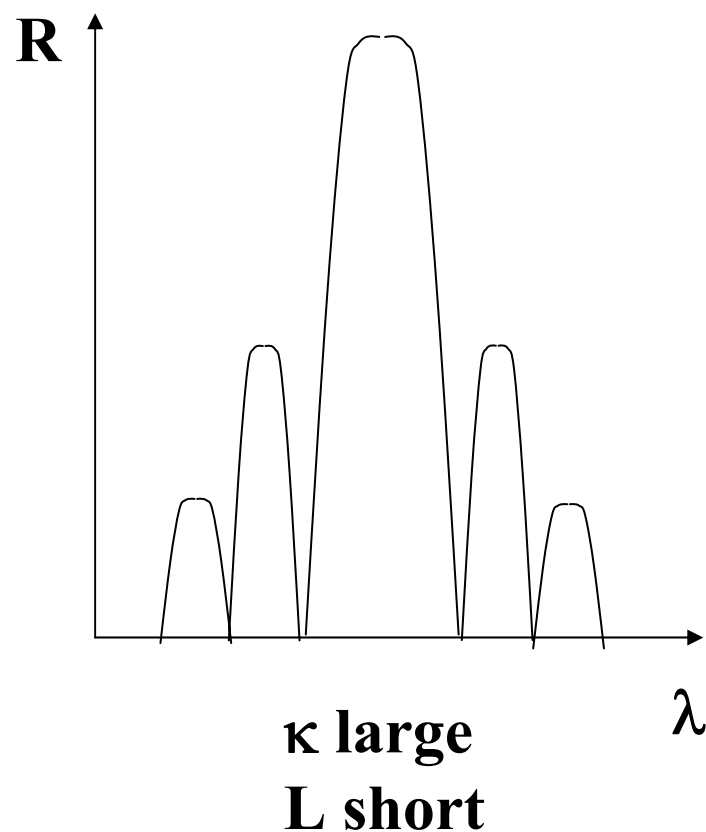


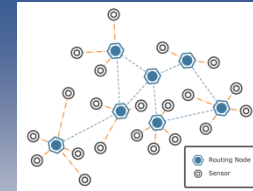
Apodization : Tailored
Spatial Exposure.

BRAGG GRATINGS : Bandwidth

Maximum
Reflectance
Conditions

$$L = \frac{\pi}{2 |\kappa|}$$

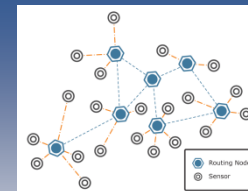




Achieving Refractive Index Changes

- **Create defects in glass**
 - Increase absorption (in UV)
 - Affect the refractive index n through Kramers-Kronig relations
- **Densification of glass**
 - Increase the refractive index n directly

Both strategies can be implemented using light exposure



Photosensitivity in Germania doped silica fibers

Non linear effect which permits the index of refraction in the core of the fiber to be increased by exposure to intense laser radiation

Without Hydrogen

Index change: up to 10^{-3}

*Defects absorb light
and form new bonds*

*Writing by pumping defect bands:
240 nm, 330 nm, also 193 nm*

Hydrogen loaded

Index change: up to 10^{-2}

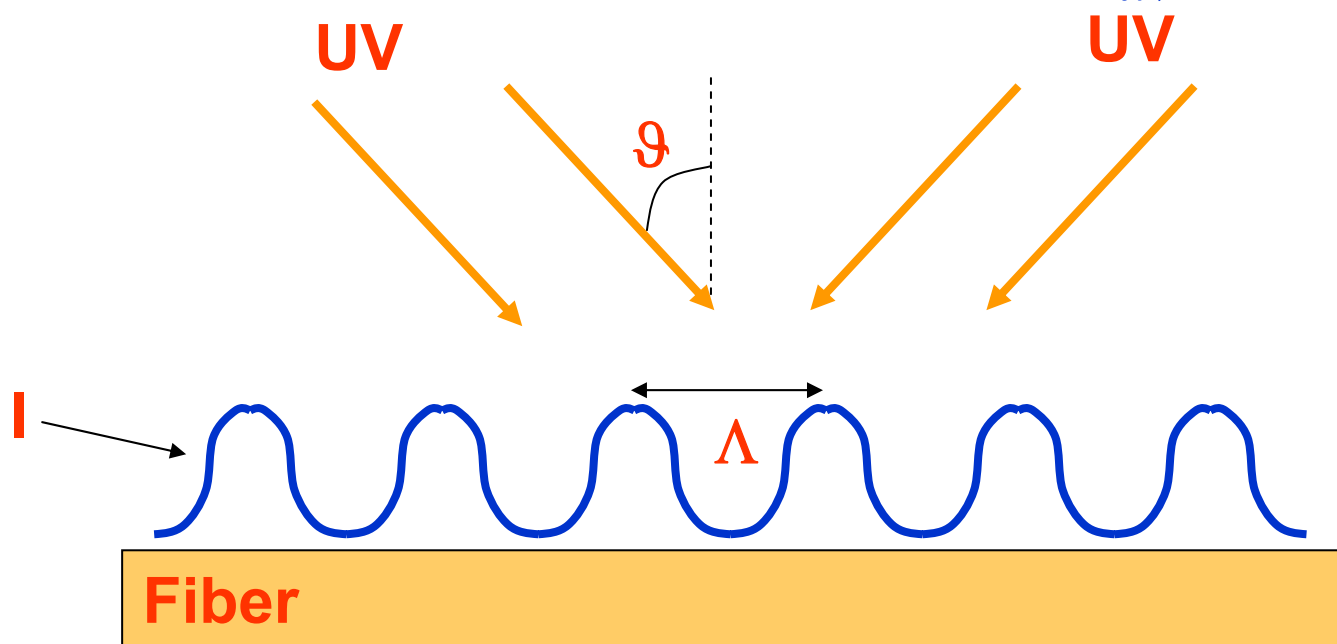
*Photochemical reaction of
hydrogen with Ge-O bonds*

*Edge of fundamental absorption:
<310 nm (the shorter the better)*

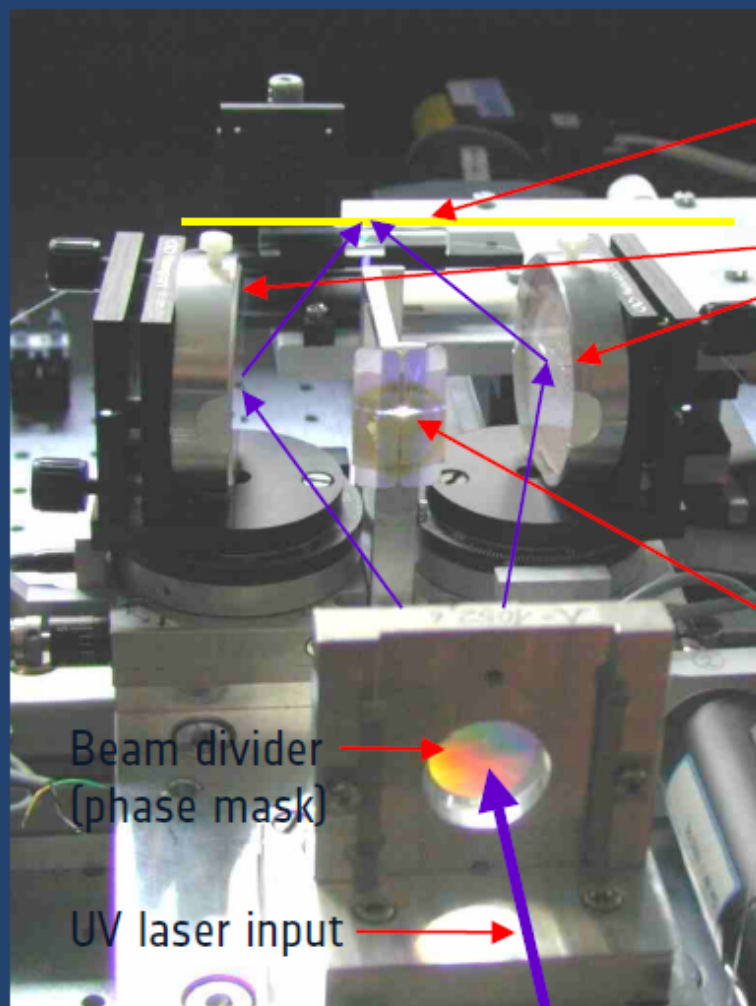
Gratings Manufacturing: The Holographic Method

- Interfering UV beams:
 - Sinusoidal Δn

$$\Lambda = \frac{\lambda_{uv}}{2n_{uv} \sin \theta}$$



Talbot Interferometer



Optical fibre

2 mirrors (adjustable),
directing diffracted beams
of +1st and of -1st order,
for superposition
at optical fibre.

Blocking of 0th order

Beam divider
(phase mask)

UV laser input

FABRICATION : Phase Mask

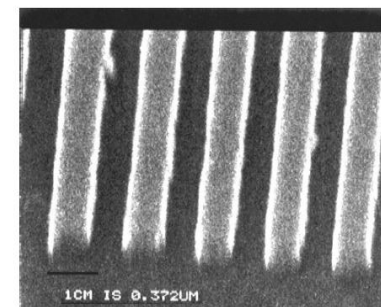
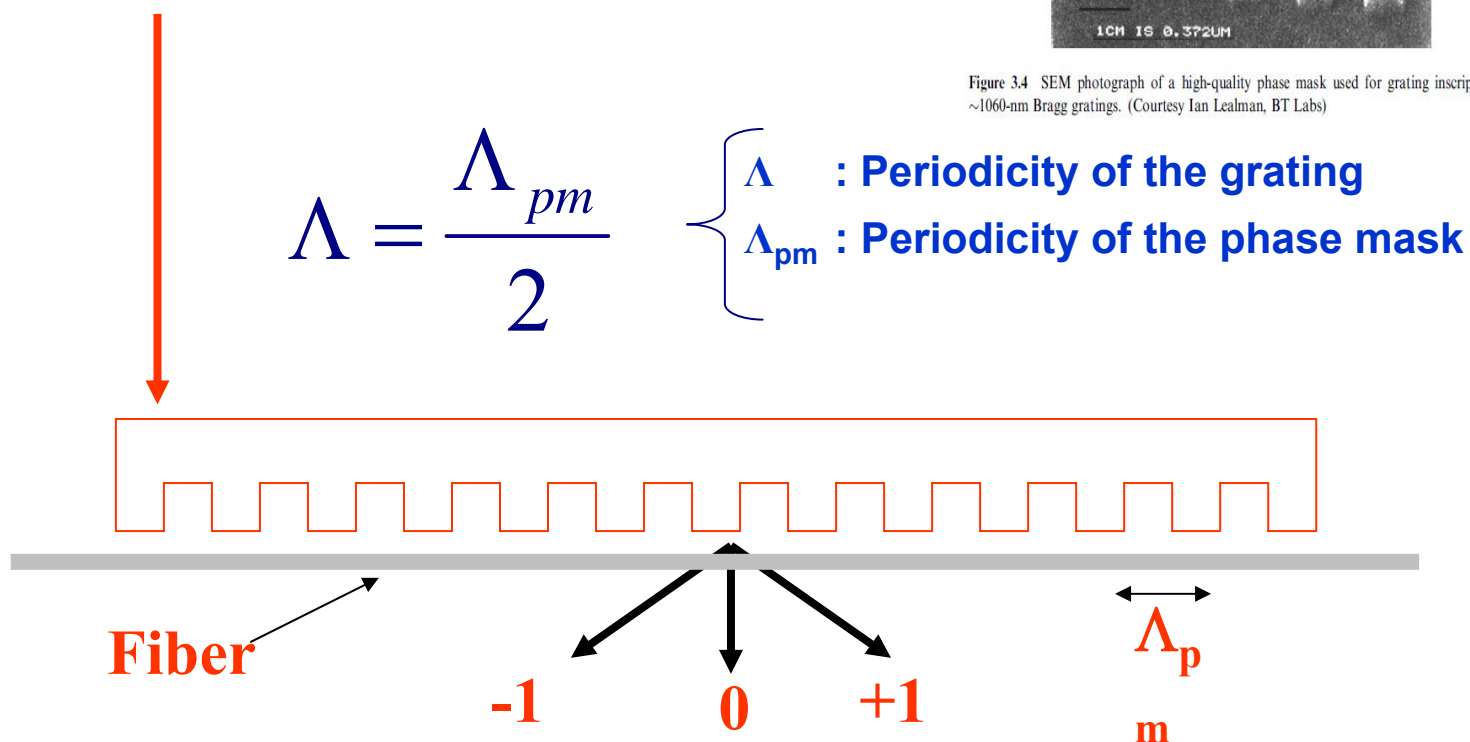
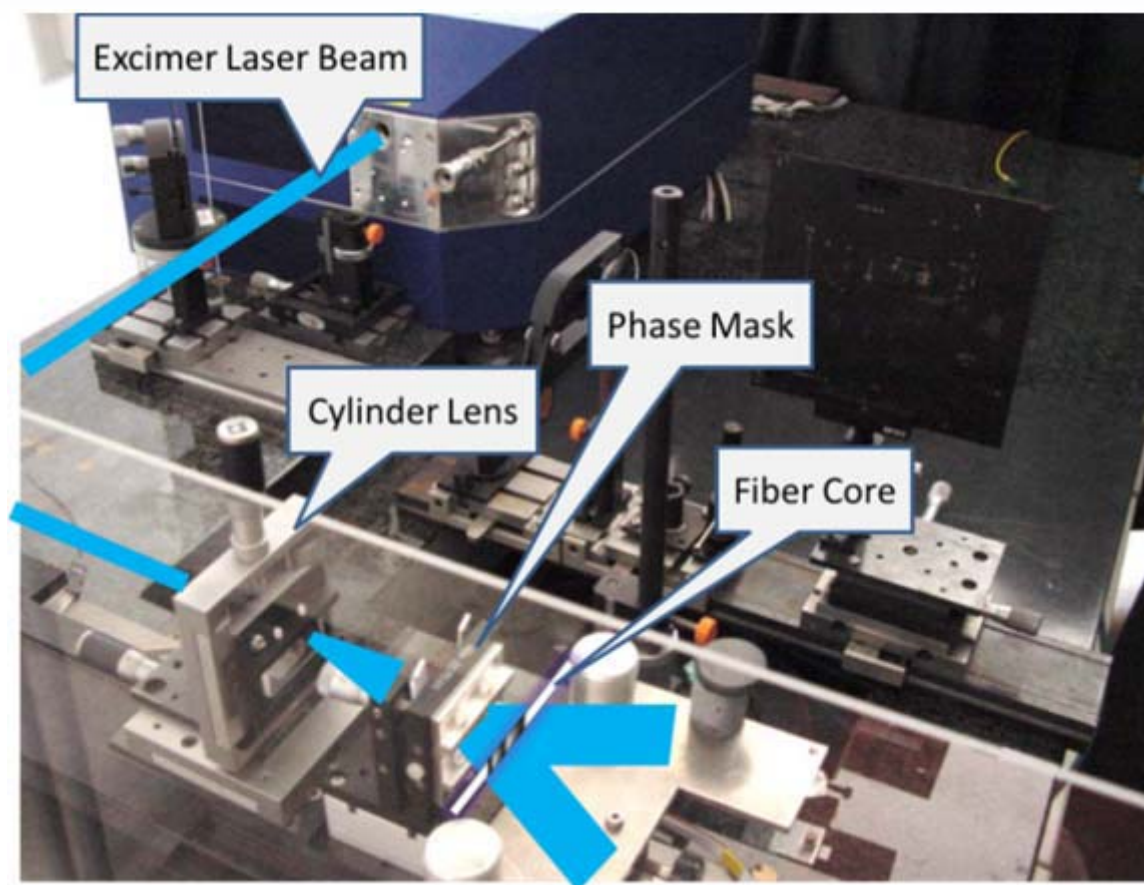


Figure 3.4 SEM photograph of a high-quality phase mask used for grating inscription of ~1060-nm Bragg gratings. (Courtesy Ian Lealman, BT Labs)



Phase Mask: A practical Set-up

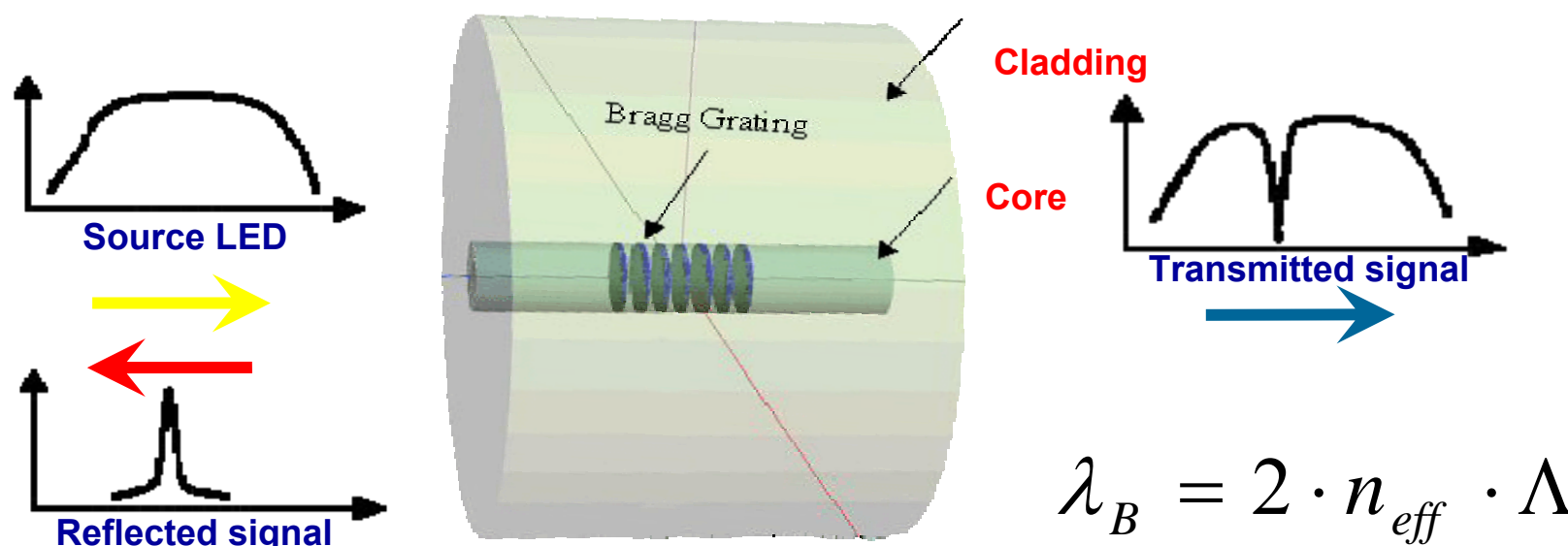


Fiber Bragg gratings in Single Mode Optical Fibers

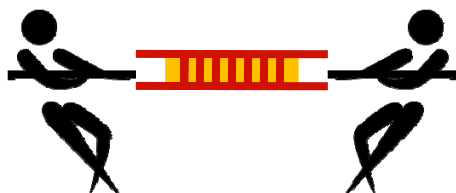
Parameters related to a Bragg grating.

A. Cusano et al., «Fiber Bragg Grating Sensors: Recent Advancements, Industrial Applications and Market Exploitation», **Bentham Science Publishers**, 2011
ISBN: 160805084X,

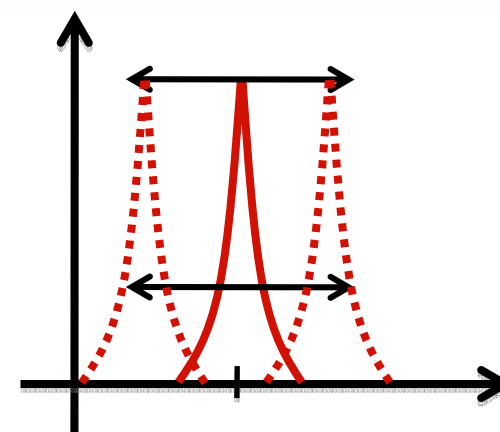
- $n_{\text{eff}} \sim 1.455$ in silica.
- “Short” period grating to operate in lowest order mode ($m=1$) with Bragg wavelength $\lambda_B \sim 1550\text{nm}$, $\Lambda \sim 500\text{nm}$.
- Typical index changes, $\delta n \sim 10^{-5} - 10^{-3}$.
- Typical lengths, 1cm – 10cm, some types $\sim 1\text{m}$.



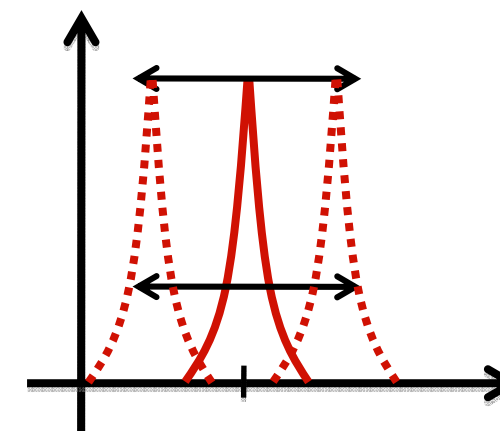
Temperature & Strain

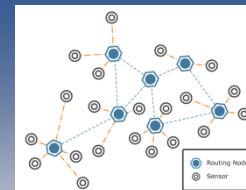


Strain
Changes Λ via
direct
deformation
and n via
elasto optic
effect



Temperature
Change n via
thermo optic
effect and Λ
via thermal
expansion





Temperature Sensitivity

$$\left(\frac{\Delta \Lambda}{\Lambda} \right)_T = \alpha \Delta T$$

Thermal
Expansion Effect

$$\left(\frac{\Delta n}{n} \right)_T = \frac{1}{n} \cdot \frac{\partial n}{\partial T} \Delta T$$

Thermo Optic
Effect

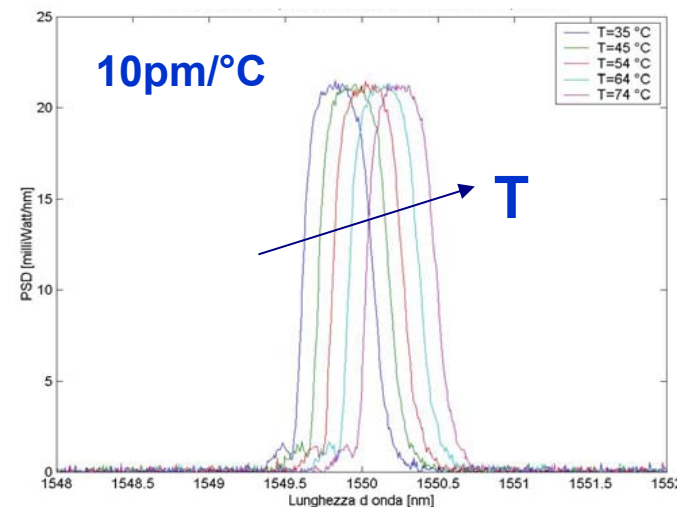
$$\left(\frac{\Delta \lambda_B}{\lambda_B} \right)_T = \left(\frac{\Delta \Lambda}{\Lambda} \right)_T + \left(\frac{\Delta n}{n} \right)_T = \left(\alpha + \frac{1}{n} \cdot \frac{\partial n}{\partial T} \right) \Delta T = S_T \Delta T$$

S_T : Temperature Sensitivity

$5.8 \cdot 10^{-6} / K^{-1} @ \lambda_B = 1550 \text{ nm}$

With :

α : Optical fiber core temperature expansion coefficient
 Λ : Periodicity of the grating
 n : Optical fiber core refractive index



STRAIN SENSITIVITY

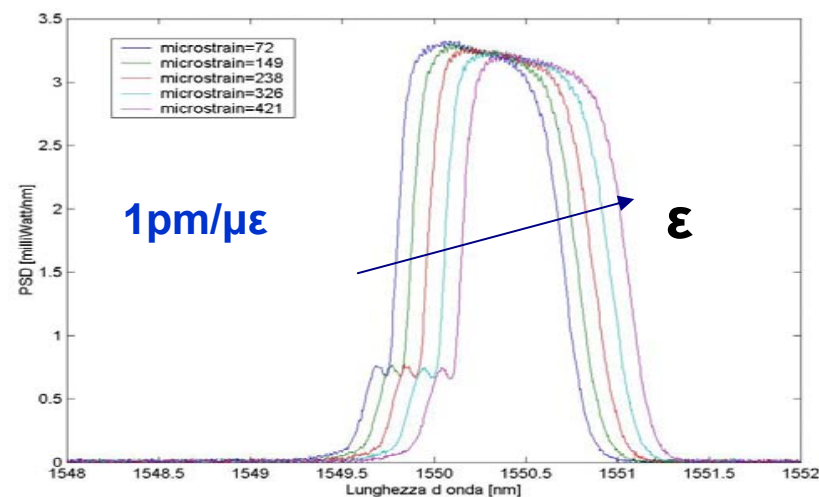
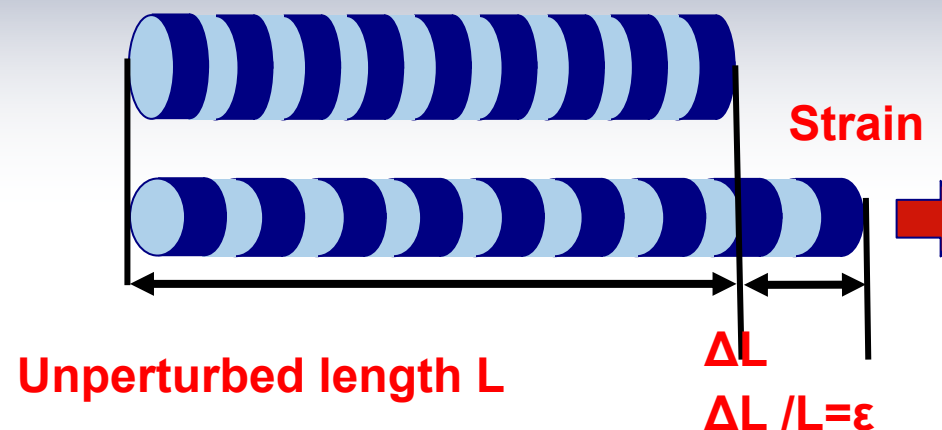
Axial Strain

$$\begin{cases} \varepsilon_1 = \varepsilon \\ \varepsilon_2 = \varepsilon_3 = -\nu\varepsilon \end{cases}$$

ν : Poisson ratio



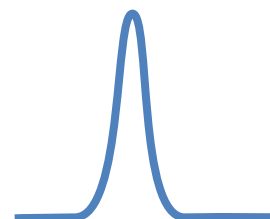
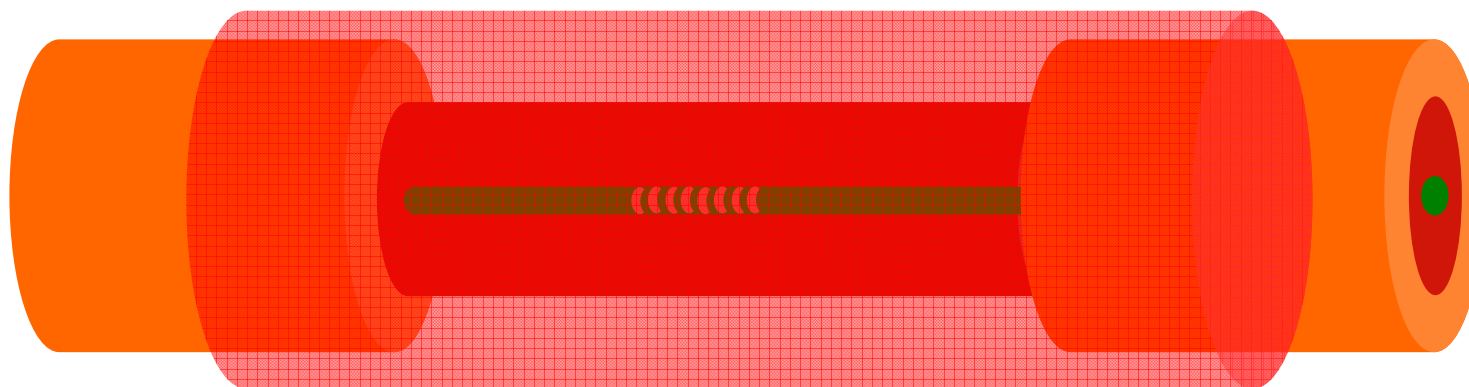
$$\left(\frac{\Delta\lambda_B}{\lambda_B} \right)_\varepsilon = \left(\frac{\Delta\Lambda}{\Lambda} \right)_\varepsilon + \left(\frac{\Delta n}{n} \right)_\varepsilon = \left\{ 1 - \frac{n^2}{2} [p_{12} - \nu \cdot (p_{11} + p_{12})] \right\} \varepsilon_1 = S_\varepsilon \varepsilon$$



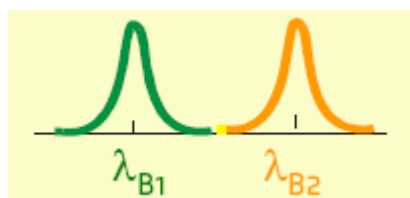
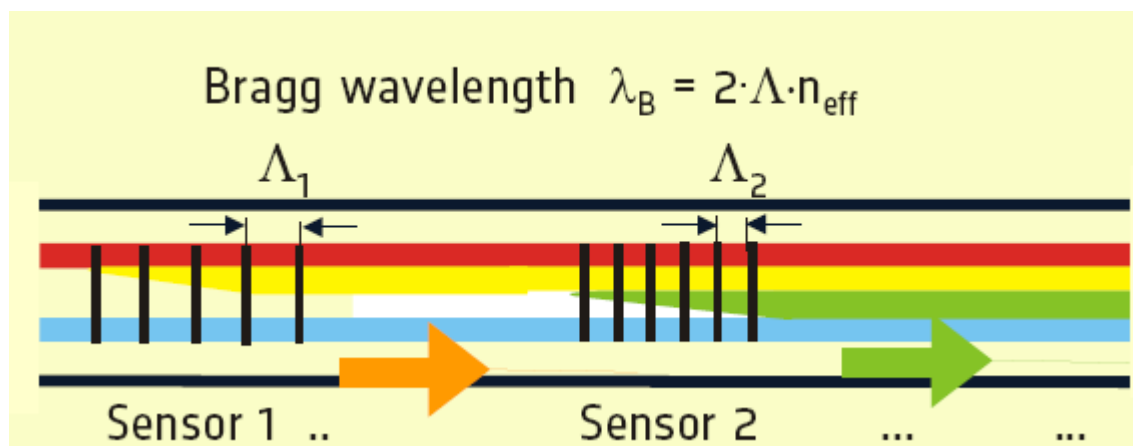
Strain Sensitivity $[(\Delta\lambda_B/\lambda_B)/\varepsilon]$:
 $8,0 \cdot 10^{-7} \mu\varepsilon^{-1}$ @ $\lambda_B = 1550 \text{ nm}$

FBGs AS MULTIFUNCTIONAL SENSORS

- **Functionalization:** integration with appropriate materials and suitable packaging (i.e. mechanical packaging, magnetostrictive, polymeric coatings) to measure a number of physical, chemical and biological parameters (i.e. magnetic field, humidity, cryo temperatures, acoustic waves, weight, chemical and biological analytes)



Fibre Bragg Grating Sensor and Multiplexing Principle



Hundreds of FBG sensors can be realized within a single optical fibers by changing the grating period

$$\lambda_{B-i} = 2n \Lambda_i$$

Maximum number of sensors is ruled by taking into account the spectral range of the light source and the maximum expected wavelength shift of each sensor according to:

$$N < \Delta\lambda_{\text{Source}} / \Delta\lambda_{\text{BMAX}}$$

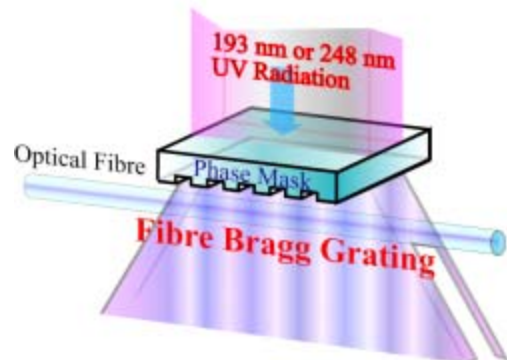
FBG Sensors: A Standardised Technological Platform

... **An attractive sensing solution:**

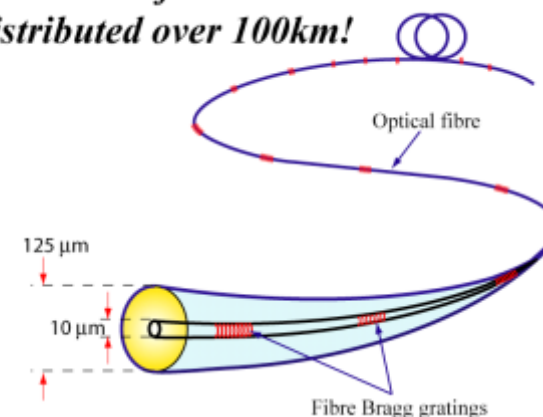
- **Wavelength Encoded**
- **Self Referencing**
- **Linear Output**
- **Small and Lightweight**
- **WDM & TDM Multiplexing**
- **Mass Producible**

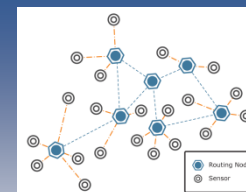
Reflective & Transmission Operation

- **Single & Multi Point Sensing**
- **Multi Parameter Sensing**
- **Long Range**
 - **Reasonable Cost**
 - **Durable**



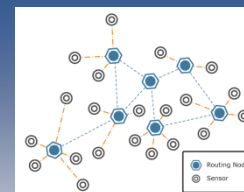
*Hundreds of sensors
distributed over 100km!*





FBG TECHNOLOGY EVOLUTION: Major Milestones

- 1978 — Discovery of photosensitivity in fibers (K.O. Hill)
- 1989 — UV side-writing technique (Meltz, Morey & Glenn)
- 1993 — Mask writing technique (K. O. Hill)
 - Hydrogen loading photosensitization (Lemaire)
- 1995 — Commercial FBG production (3M, Bragg Photonics, Innovative Fibers, Indx, etc...)
 - First commercial FBG interrogator (Electro-Photonics)
- 1997 — Deployment of FBGs in WDM systems (Ciena)
- 2000 — Advanced FBG instrumentation (Micron Optics)
- 2003 — Commercial reel-to-reel FBG arrays (LxSix, Sabeus)
- 2007 — First pre-packaged FBG strain gauge (Micron Optics)
 - First strain gauge company to offer FBG sensors (HBM)
- 2009 — Standardization efforts (W. R. Habel *et al.* BAM Institute-Jena Germany)
- 2010 — First FBG sensors installation at CERN (University of Sannio & Optosmart)
- 2013 — First Certified FBG Sensing System for Weighing in Motion (Ansaldo STS, University of Sannio & Optosmart)



FBG-Based Sensors & Arrays: Multiple Parameters & Suppliers



Accelerometer



Displacement meter



Strain meter



Pressure meter



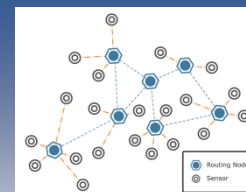
Thermometer



Tilt Meter

Reliability is the main
commercial issue





Applications: Segment Areas



Oil & Gas

- Reservoir monitoring
- Downhole P/T sensing
- Seismic arrays



Energy Industry

- Power plants
- Boilers & Steam turbines
- Power cables
- Turbines
- Refineries



Aerospace

- Jet engines
- Rocket propulsion systems
- Fuselages



Underwater

- Leaks in subsea pipeline monitoring
- Flood detection
- Hydrophone



Civil

- Bridges
- Dams
- Road
- Tunnels
- Land slides

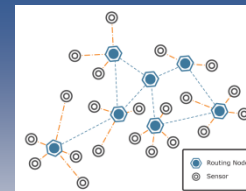
Transportation

- Rail monitoring
- Weight in motion
- Carriage safety



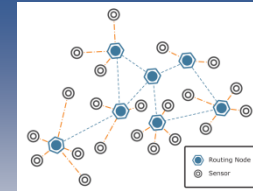


Optoelectronics Group, Engineering Department
University of Sannio, Benevento (Italy)



Smart Railways Using Fiber Optic Technology





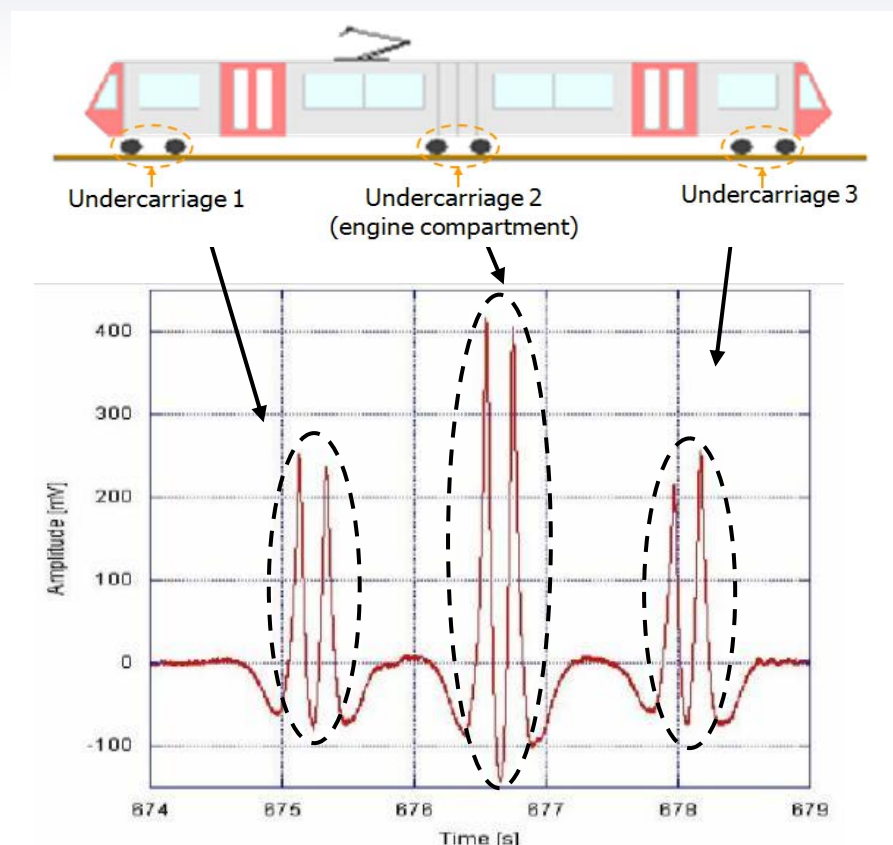
Needs and Requirements

- Increasing need for improved **safety**, **reliability** and **efficiency** in the worldwide railway industry;
- Monitoring of railway traffic and in particular rail truck integrity;
- Require the Development of **smart monitoring systems** for real-time and continuous monitoring of the structural and operational conditions of rail tracks;
- Advantages for railway industry: reduced maintenance costs, optimized performance and capacity;
- Railway monitoring requires **extensive sensor networks** (1,000s of sensors) for multifunctional measurements (strain, vibration, velocity, temperature, acceleration, weighing in motion, traffic status, structural health ...).



Feasibility: Year 2007 "Tel Station (Bz)

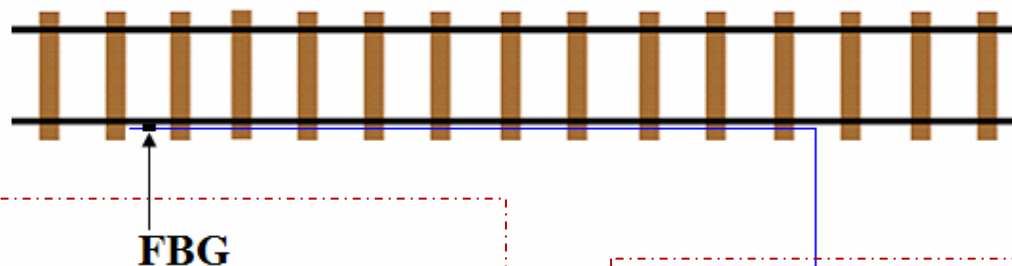
"Bare FBG" glued to the rail



A Single FBG glued to the rail, can provide useful information about:

- occupation state, train, velocity, acceleration, axle counting, weighing in motion,

December 2007 - June 2008: "Nervi (Ge) Station" First Packaged Sensors



Bare FBG



Package FBG

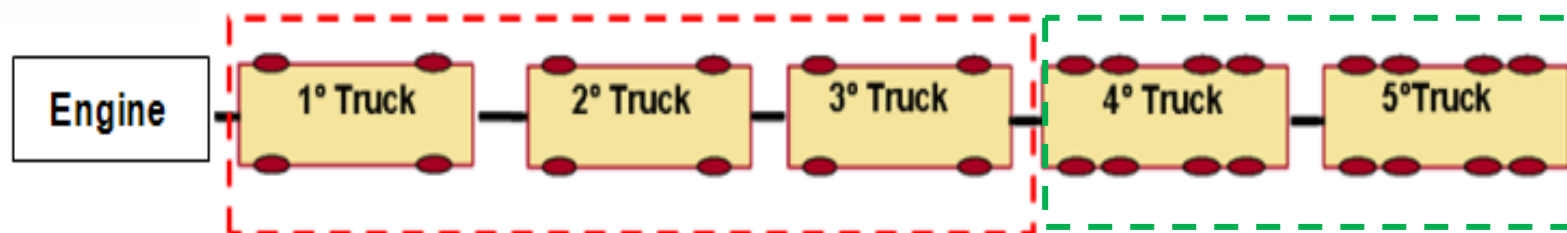


**CONTROL
ROOM**

Interrogator system & measure setup



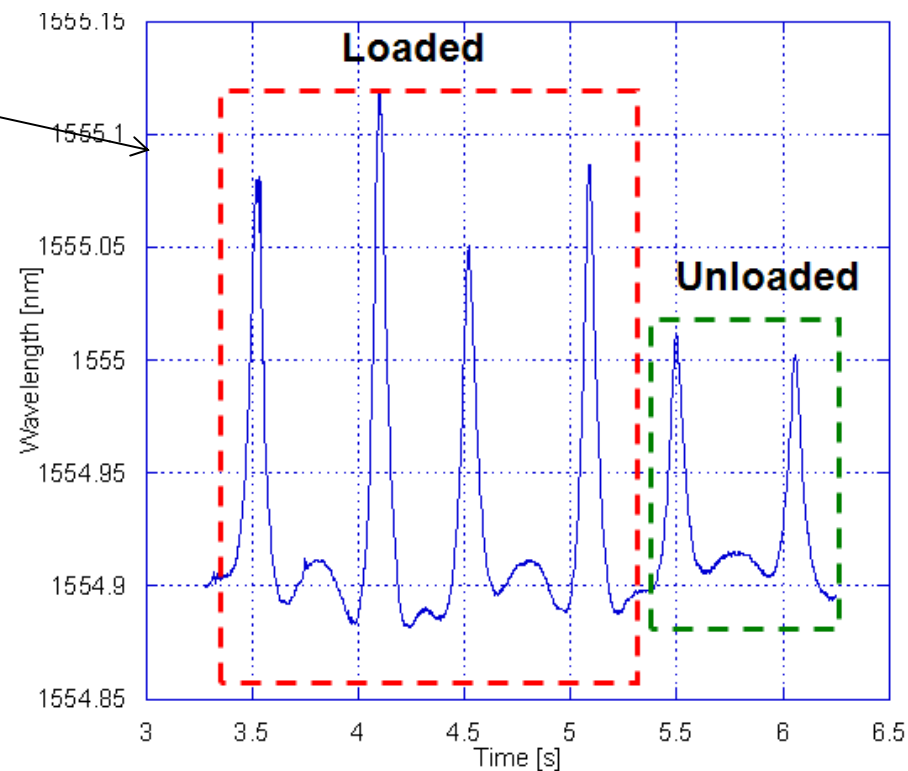
Test train with loaded and unloaded trucks



Truck loaded with concrete cube



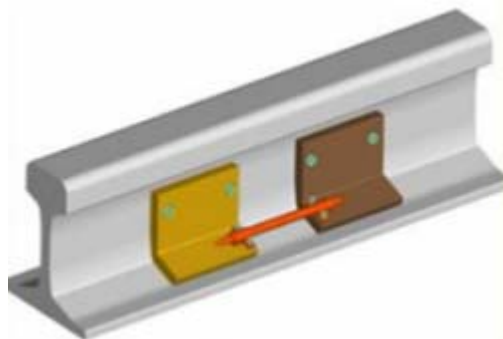
FBG soldered on the rail



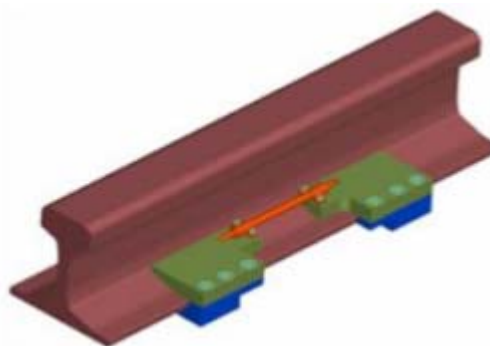
Sensors Packaging Engineering: November 2008 - December 2010 "Sezze Romano (LT) Station"

FBGs anchored to the rail, using customised metallic kit

Anchor solution A

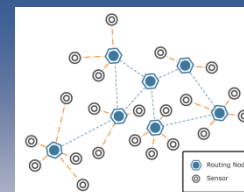


Anchor solution B



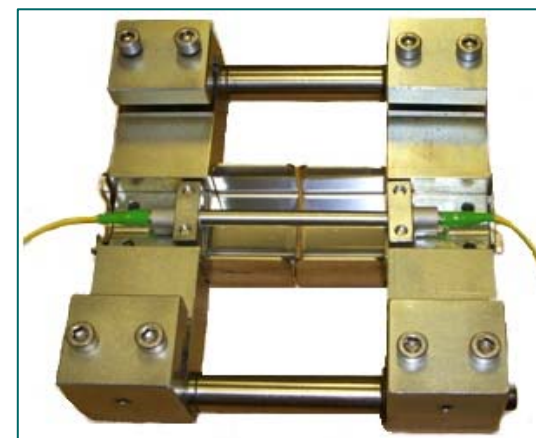
Anchor solution C





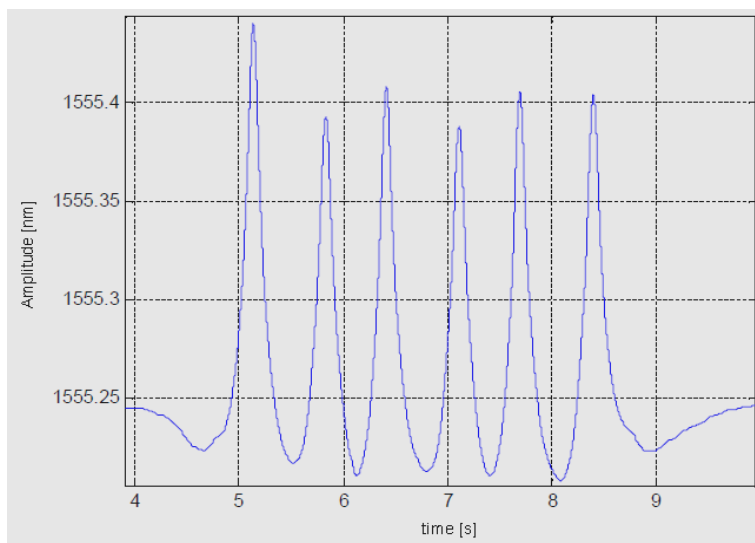
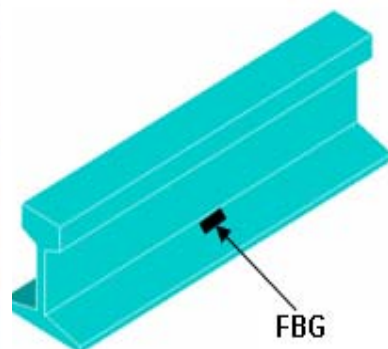
March 2011 - September 2012 : "Marcianise Station": Optimised Packaged Sensors

- Noninvasive
- No drilling of the rail
- Reduced installation time
- Easily removable

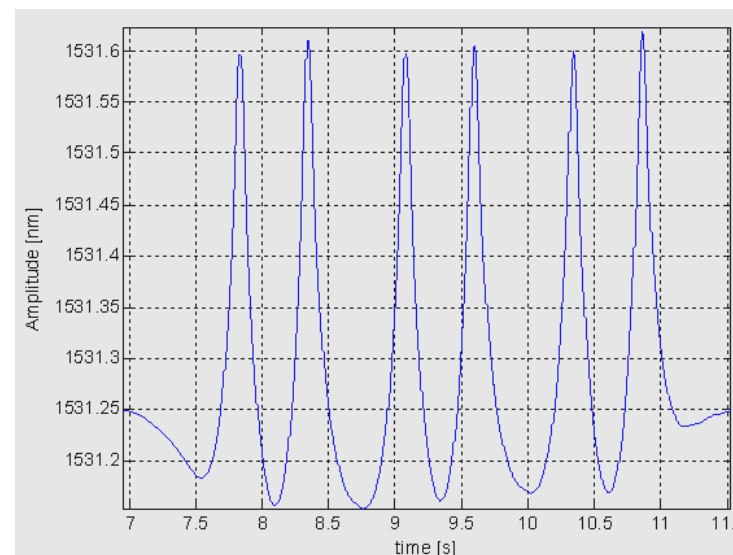
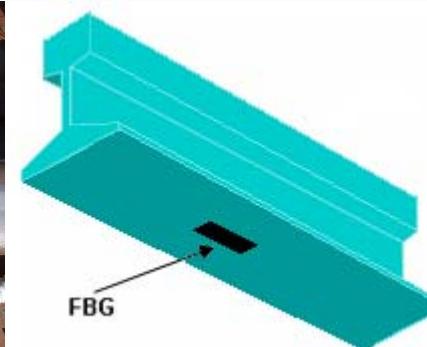
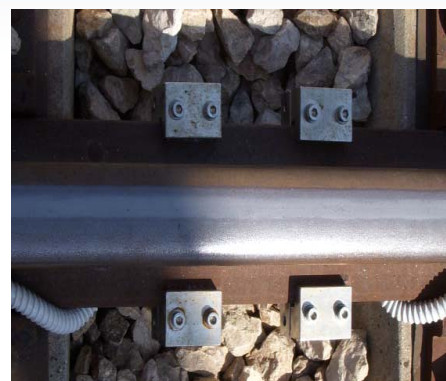


Improved Performances

TWBCS packaging and positioning doubles sensitivity



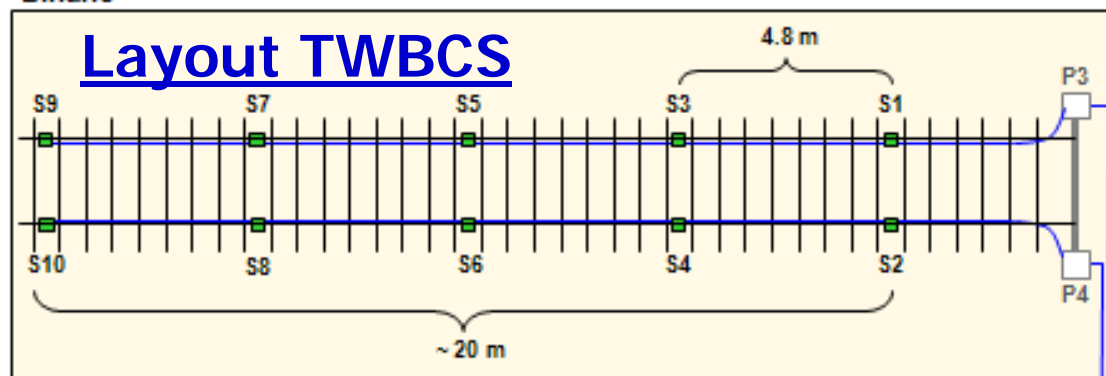
shift: ~ 200 pm per pulse



shift: ~ 400 pm per pulse

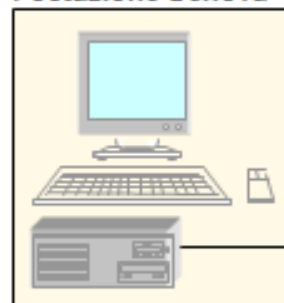
Year 2013 :TWBCS First Industrial Release

Binario



- Sensors Number: 10
- Sensorised Section length: 20m
- Fiber optic cabling ensures total electrical insulation

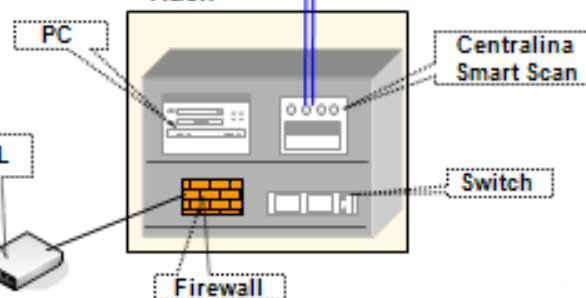
Postazione Genova



Modem AD SL

Modem AD SL

Rack



Certification Tests

Mechanical tests



- Vibrations: up to 280 m/s^2
- Shock: $2500 \text{ m/s}^2/1\text{ms}$

Solar irradiation tests



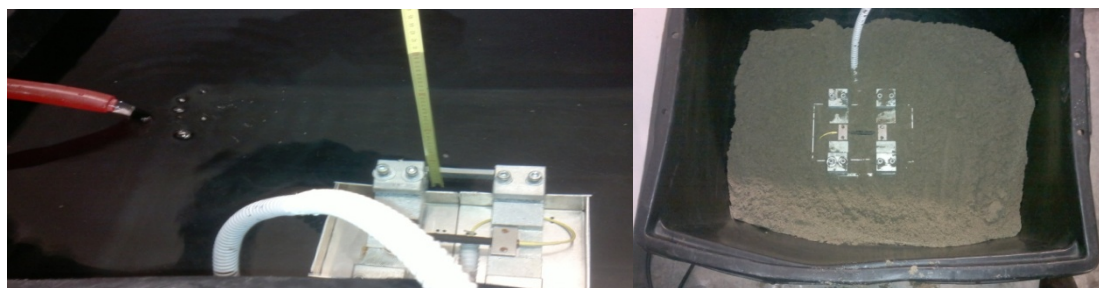
Maximum level of solar radiation : 1120 W/m^2 .
Temperature: 60°C

Climatic tests



- Temperature changes : $-40^\circ\text{C} \div +85^\circ\text{C}$
- Hot dry test: 70°C , U.R. $\leq 60\%$
- Hot wet test: 55°C , U.R. 95%
- Cold test: -25°C

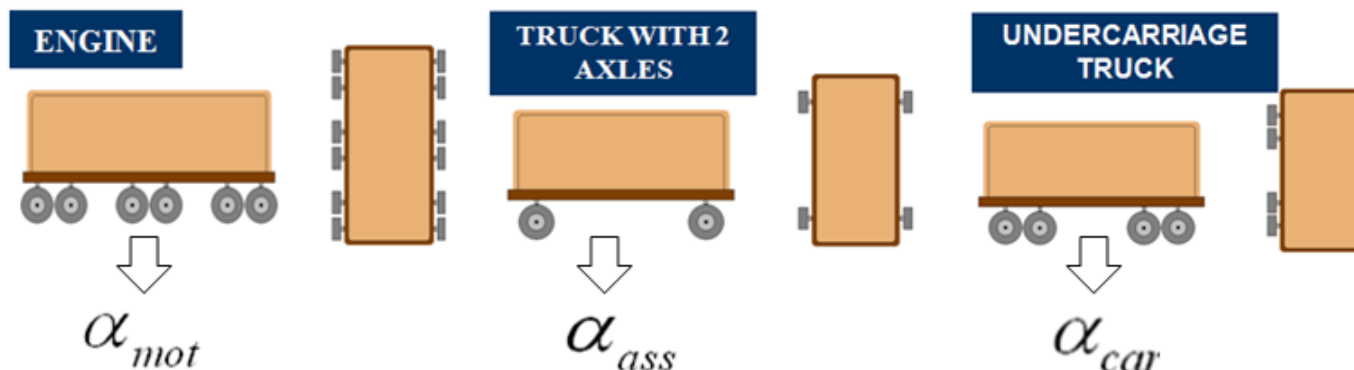
Immersion tests in sand and water



300 liters of water (h 50 cm) – 75 kg of sand (h 30 cm)

On line calibration

Calibration of FBG using all the typologies of trucks



To determinate the weight of the engine compartment :

$$P_{mot} = \alpha_{mot} * \sum_{i=1}^6 A_i$$

To determinate the weight of axles :

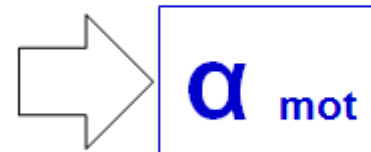
$$P_{ass} = \alpha_{ass} * A_{ass}$$

To determinate the weight of undercarriages truck :

$$P_{car} = \alpha_{car} * \sum_{i=1}^2 A_i$$

Calibration of FBG using only engine rail truck





α_{mot}

TWBCS (Train Weight Balance Control System)

Output

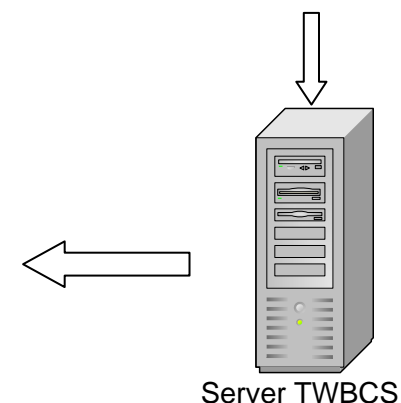
"A_110919_215919_total.html"

Risultato TWBCS					
Scalo Mercè Maddaloni/Marcianise					
Data e Ora 110919_215919					
Velocità 9[km/h]					
Numero Vagoni 24					
ID Vagone	Carrelli	Assi	Sbil. Longitudinale %	Sbil. Trasversale %	Carico [kg]
0	1	6	50	49	106890
1	2	4	52	48	57710
2	2	4	50	49	72364
3	2	4	46	50	57884
4	2	4	48	48	61336
5	2	4	49	49	70462
6	2	4	49	50	73094
7	2	4	49	51	63936
8	2	4	50	50	65042
9	2	4	49	53	70926
10	2	4	54	47	77308
11	2	4	52	47	74750
12	2	4	49	47	75178
13	2	4	49	48	58012
14	2	4	49	49	74880
15	2	4	49	50	71944
16	2	4	49	50	74254
17	2	4	50	53	64844
18	2	4	49	49	65300
19	2	4	49	48	71950
20	2	4	49	49	64818
21	2	4	51	49	59256
22	2	4	53	51	72226
23	1	6	50	48	106518
Peso Totale Convoglio 1710882 [kg]					



"A_110919_215919_wheel.html"

Risultato TWBCS		
Scalo Mercè Maddaloni/Marcianise		
Data e Ora 110919_215919		
Velocità 9[km/h]		
Numero Vagoni 24		
ID Asse	Carico DX [kg]	Carico SX [kg]
0	9012	8803
1	9012	8803
2	9012	8803
3	9012	8803
4	9012	8803
5	9012	8803
6	7840	7426
7	7840	7426
8	7037	6552
9	7037	6552
10	9184	8918



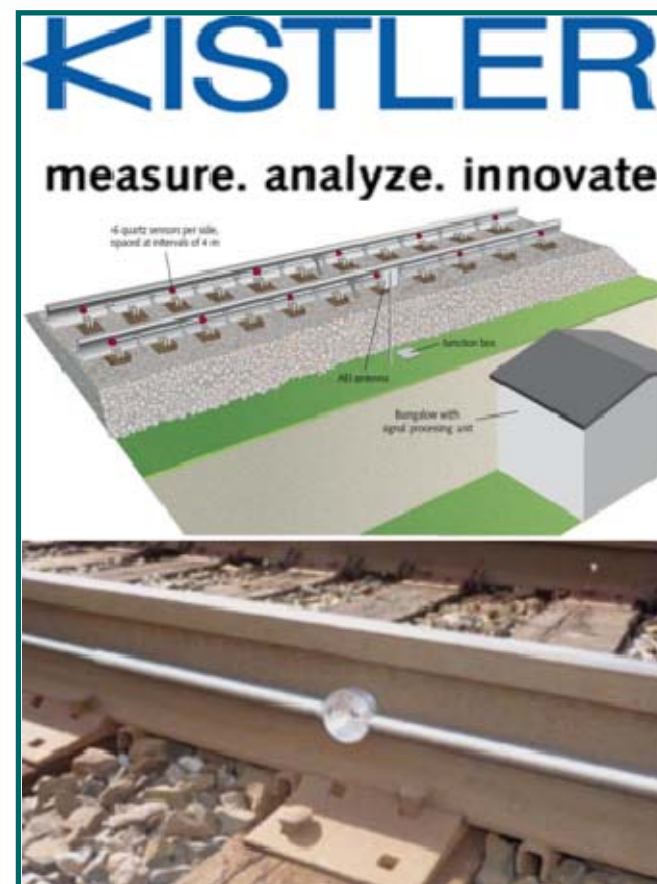
- Weight for Wheel;
- Weight for Wagon;
- Type of wagon;
- Info about train composition

TWBCS : Performances and Certification

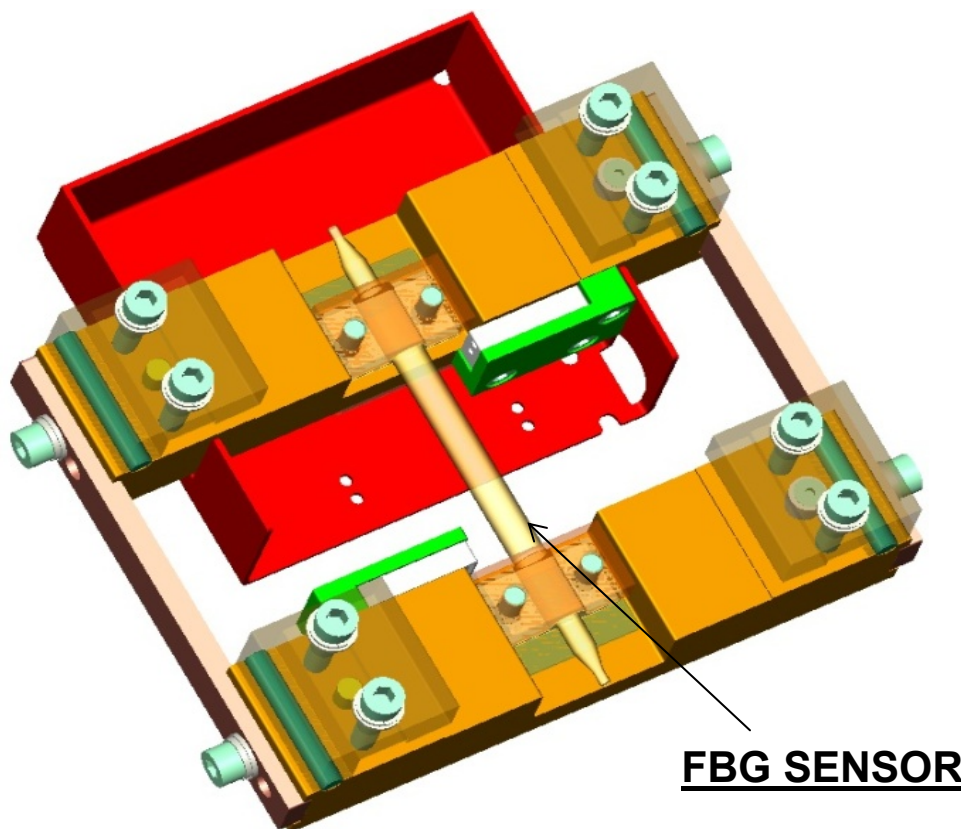
- Number of transits examined : 100

	Error Mean %	
Typology	FBG	KISTLER
Engine Truck	1	8
Undercarriages Truck	6	4
Truck with 2 axles	2	7

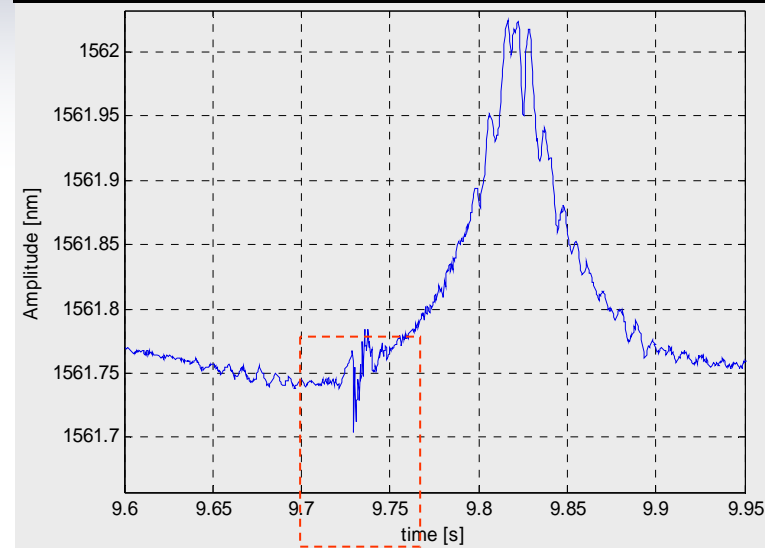
**KISTLER USES QUARTZ SENSOR,
INSTALLED BY DRILLING OPERATIONS**



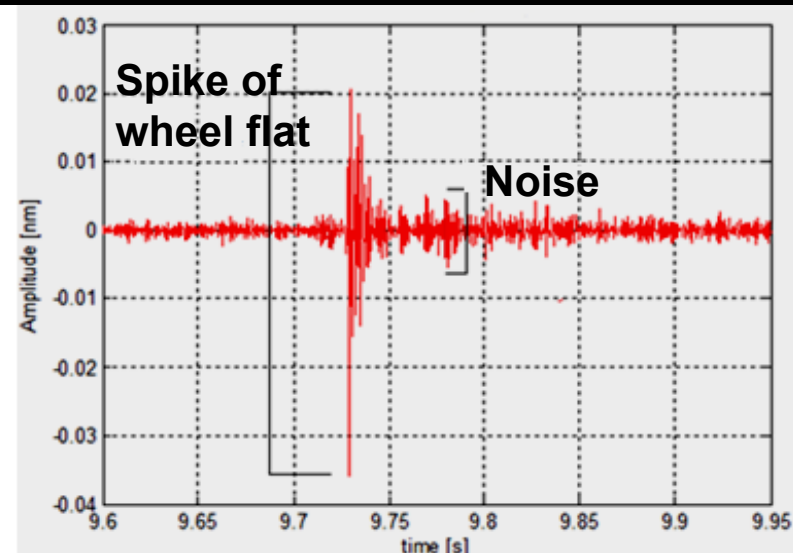
Add Functionality: Wheel flat detection



FBG SENSOR RESPONSE: RAW DATA

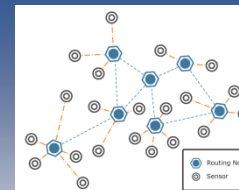


AFTER ELIMINATING STATIC CONTRIBUTE





Optoelectronics Group, Engineering Department University of Sannio, Benevento (Italy)



*Innovative Technologies for
Safety and Security of Railway
Systems*



investiamo nel vostro futuro

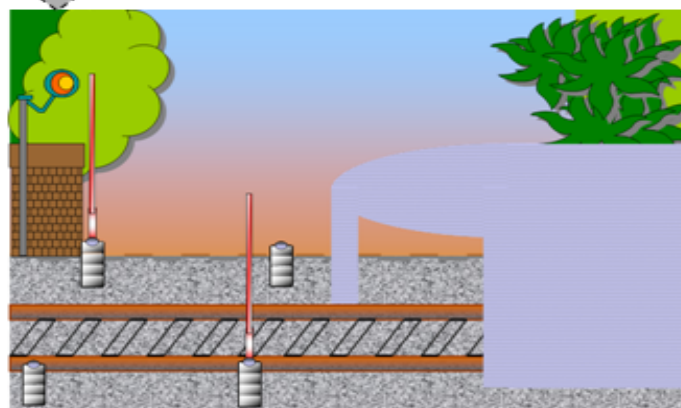
PON Ricerca: 2012-2015
10MEuro

Main Partners



Optical Fibers: A Unique Multifunctional Technological Platform

Weight in motion



Temperature monitoring (rail/tunnel)



Wheelflat detection



Landslide

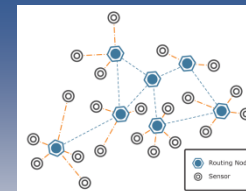


Anti - intrusion system





Optoelectronics Group, Engineering Department
University of Sannio, Benevento (Italy)



RESEARCH PROJECT "ASSO"

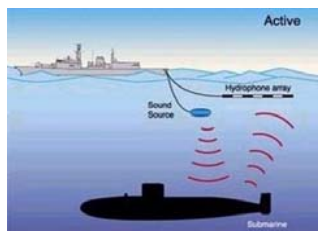
- Supported by Italian Ministry of University and Research
- Funding : 7 M€
- Duration: 3 years

In collaboration with:



Aim: *To get high-performance opto-acoustic antennas, based on Fiber Bragg Grating (FBG) technology, for military, environmental and industrial underwater applications*

Military applications

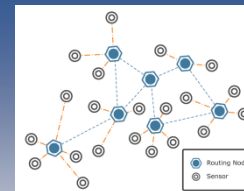


Marine environmental monitoring



Medical





Comparison with Traditional Hydrophones

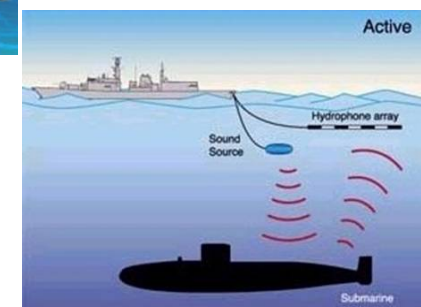
Marine environmental monitoring

Traditional hydrophones

- *Electromagnetic sensitivity*
- *Water seepages*
- *Heavy and bulky*



Military applications



Fiber optic hydrophones

- *Immunity to Electromagnetic Interferences*
- *Light and small*
- *No electric connections*
- *Remote monitoring*
- *Multiplexing capability*

Medical



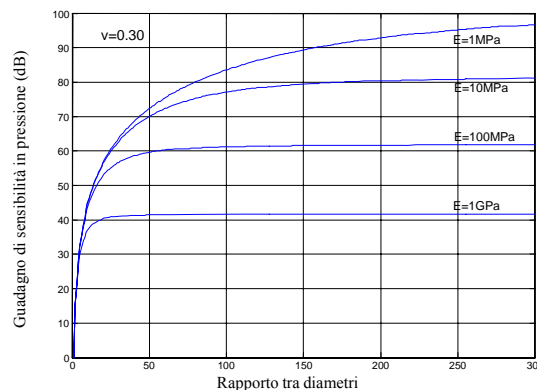
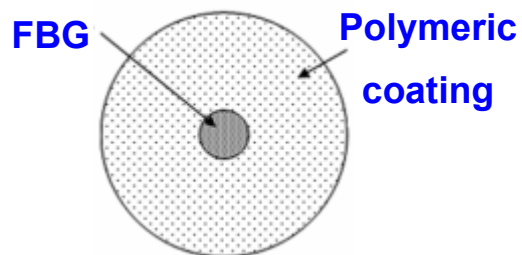
HYDROSTATIC ANALYSIS

Pressure Sensitivity in FBGs

FBGs exhibit low pressure sensitivity essentially due to the high Young module of the optical fibre material (tens of GPa) which converts the effects of high pressures applied on the grating in weak deformations.

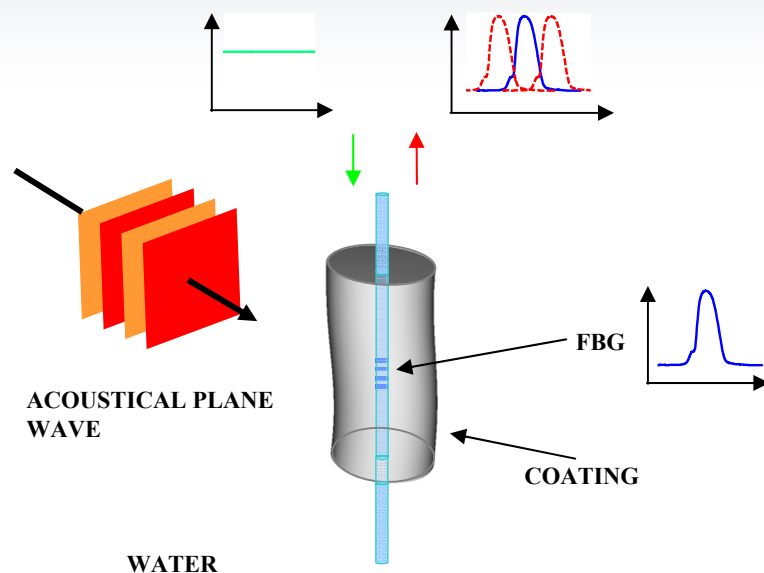
Solution

Fiber optic hydrophone: FBG coated with a polymeric coating



A proper choice of elastic and geometrical properties of the coating allows a significant sensitivity enhancement

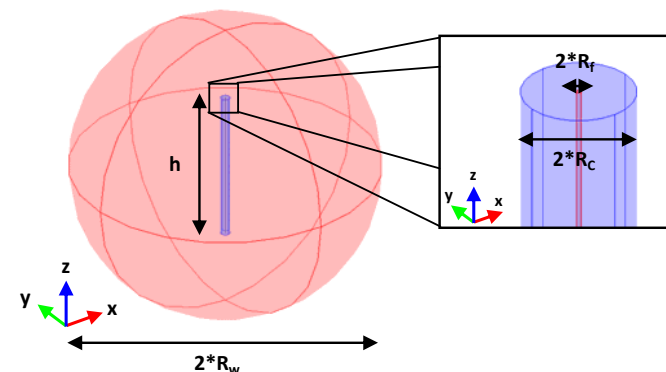
DYNAMIC ANALYSIS: ACOUSTIC WAVE DETECTION



FBG hydrophones based on standard FBGs
coated by a ring shaped overlay

We studied, via full-wave numerical simulations, the complex opto-acousto-mechanical interaction among an incident acoustic wave traveling in water, the optical fiber surrounded by the ring shaped coating, and the FBG inscribed in the fiber

FEM geometry



- COMSOL Multiphysics™ is used as FEM solver

The 3D geometry is composed by an inner cylinder (fiber), an outer cylinder (coating) and a sphere (truncated water domain)

- The acoustical frequency range is 0.5 – 30 kHz

OPTO-ACOUSTIC-MECHANICAL: AN INTEGRATED DESIGN TOOL

COMSOL Multiphysics™ solve the problem with appropriate boundary conditions

Acoustics

(acoustic wave propagation)

$$\nabla^2 p + \left(\frac{\omega}{c}\right)^2 p = 0$$

ω angular freq., p pressure,
 c sound speed

Mechanics

(elastic wave propagation)

$$\mu \nabla^2 \mathbf{u} + (\tilde{\lambda} + \mu) \nabla (\nabla \cdot \mathbf{u}) + \rho \omega^2 \mathbf{u} = -\tilde{\mathbf{f}}$$

\mathbf{u} displacement, $\tilde{\mathbf{f}}$ load,
 $\tilde{\lambda}, \mu$ Lamè const., ρ density

Optics

(Bragg wavelength shift with strain)

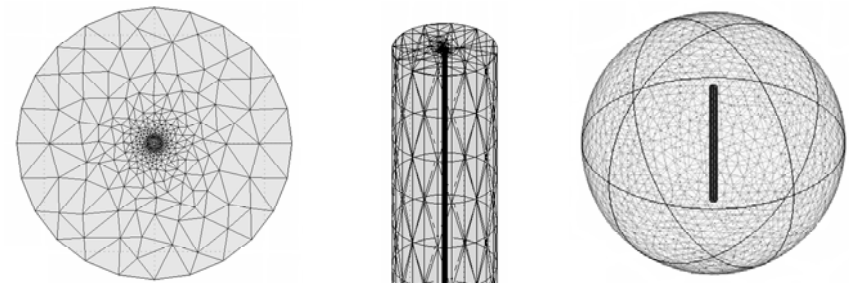
$$\frac{\Delta \lambda}{\lambda} = \varepsilon_z - \frac{n_{eff}^2}{2} (p_{11} \varepsilon_x + p_{12} (\varepsilon_z + \varepsilon_y))$$

ε_i strain comp., λ Bragg wavelength,
 p_{ij} elasto-optic coeff., n_{eff} effective refr.ind.

Boundary conditions

- Inner/outer cylinder
 - Continuity of stresses and displacements
- Coating/water
 - Pressure in static equilibrium with stress normal to boundary
 - Normal displacement of solid and fluid are equal
 - No tangential stresses occurs
- Water sphere surface
 - No reflection of incident waves

Geometry discretization



MATERIAL SELECTION: LOW FREQUENCIES

Project “ASSO” defines among the needs and requirements two operating frequency ranges for the underwater acoustic sensors:

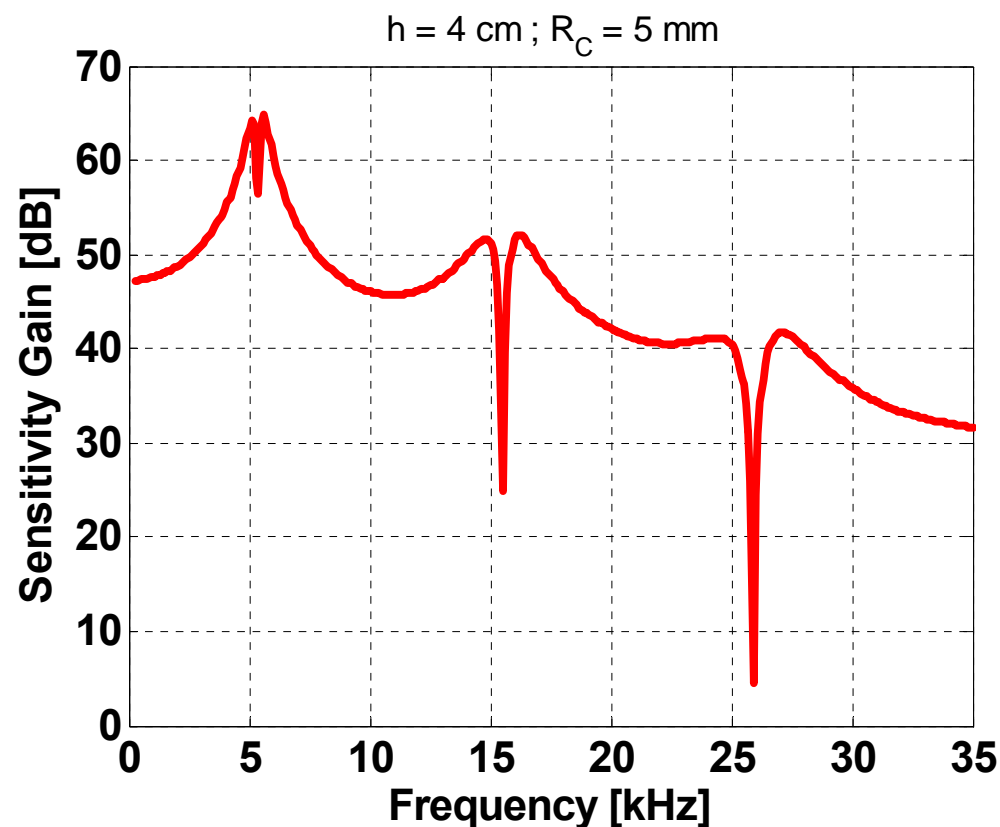
- a “low” frequency range 0-15 kHz
- a “high” frequency range 15-30 kHz

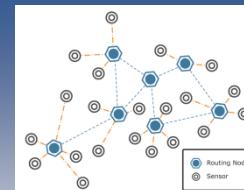
vonRoll

DAMIVAL 13650

$E = 200 \text{ MPa}$
 $\nu = 0.4$
 $\rho = 1180 \text{ kg/m}^3$
 $\eta = 0.1$

- Thermosetting polyurethane resin
- Perfect fiber bonding
- Waterproof





MATERIAL SELECTION: HIGH FREQUENCIES

HUNTSMAN

ARALDITE DBF

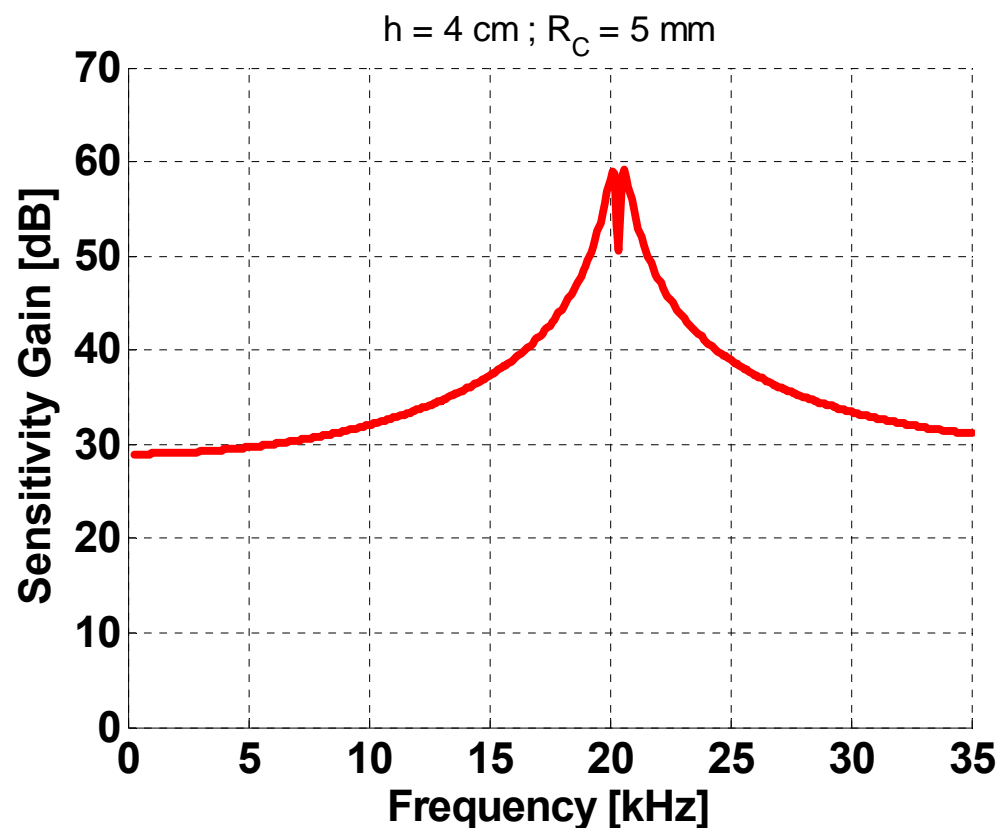
$E = 2.9 \text{ GPa}$

$\nu = 0.345$

$\rho = 1100 \text{ kg/m}^3$

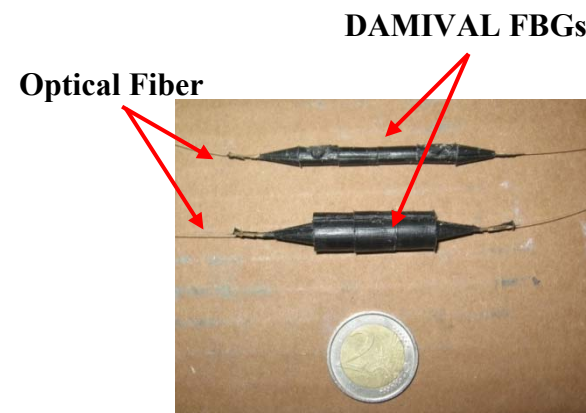
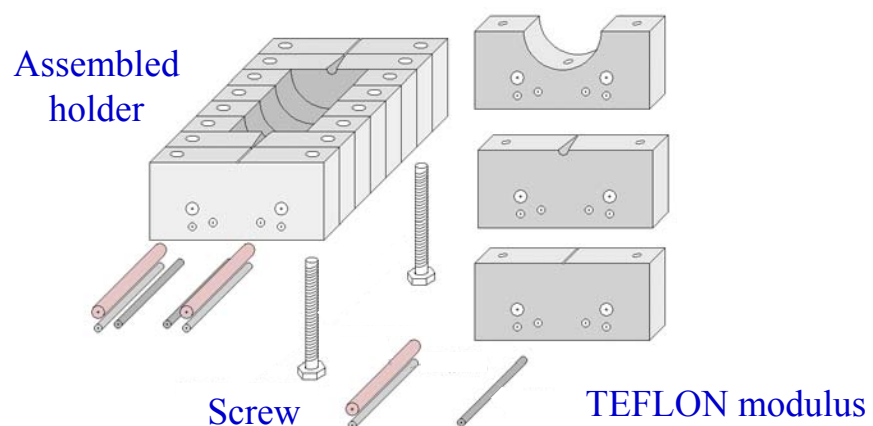
$\eta = 0.02$

- Low viscosity epoxy resin
- Adhesive resin
- Perfect fiber bonding

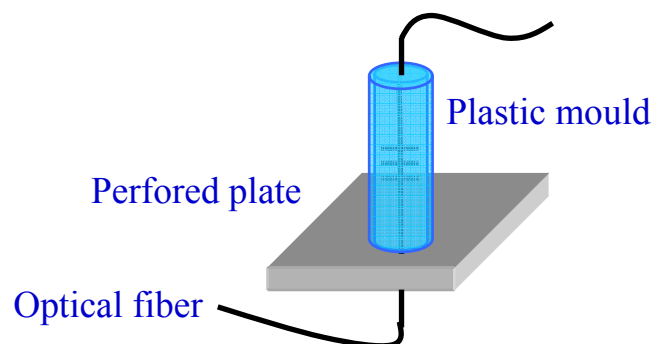


FIRST OPTO-ACOUSTIC ANTENNAS

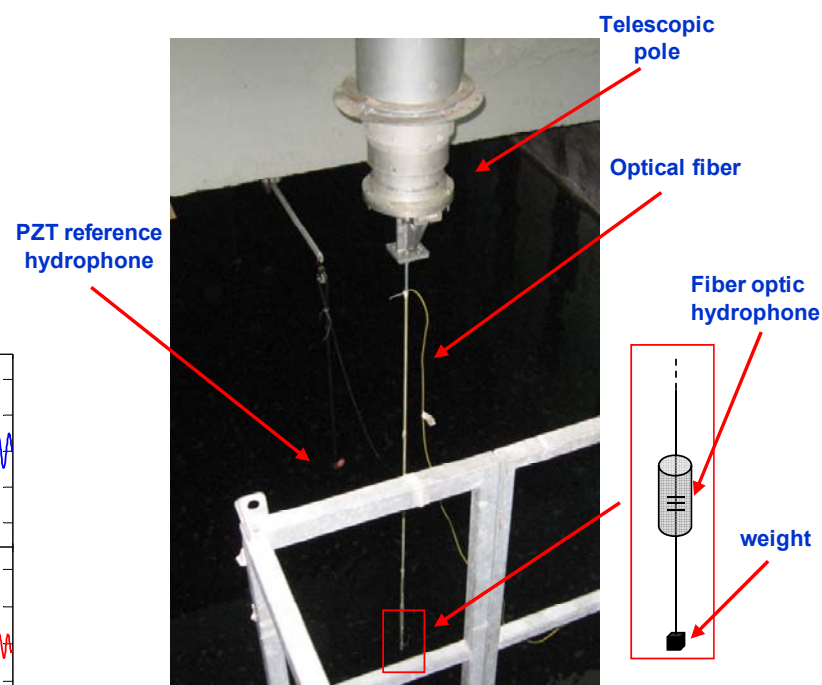
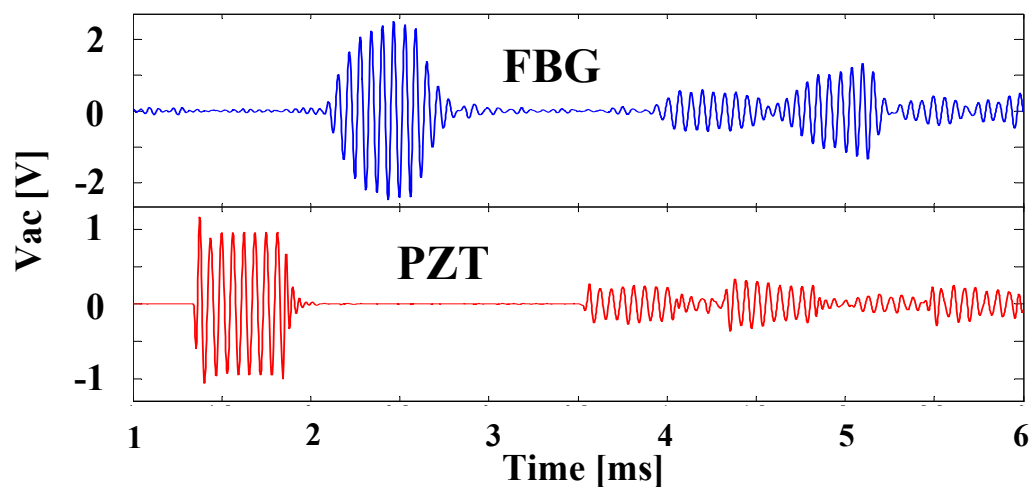
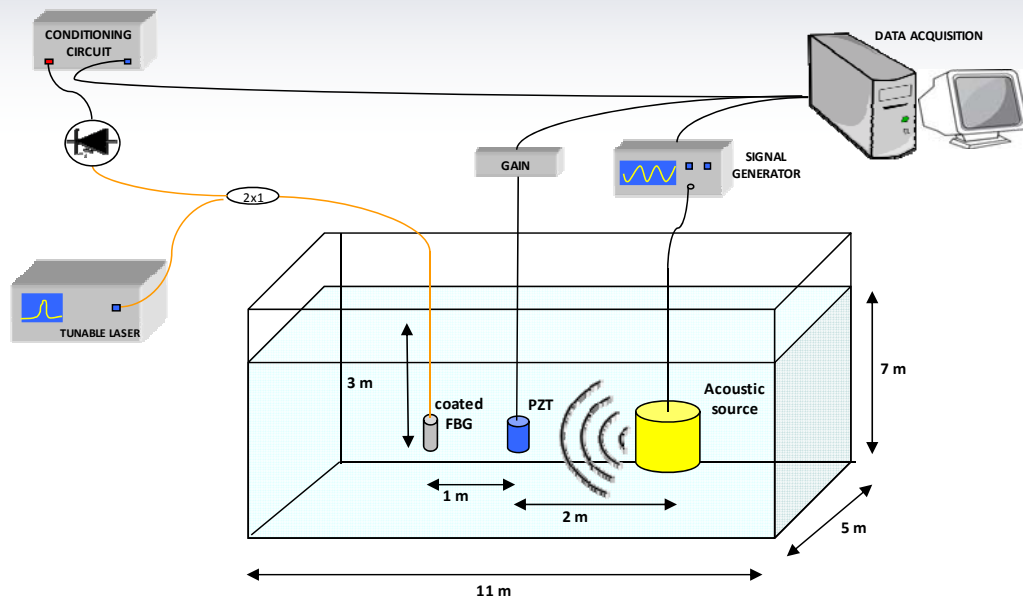
A TEFLON® modular holder was properly designed to fabricate DAMIVAL cylindrical coatings with different sizes.



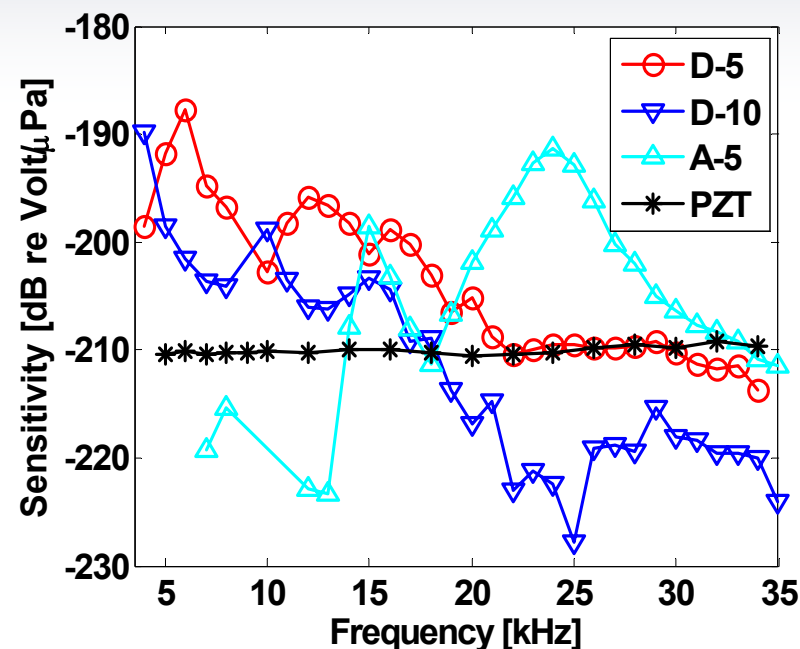
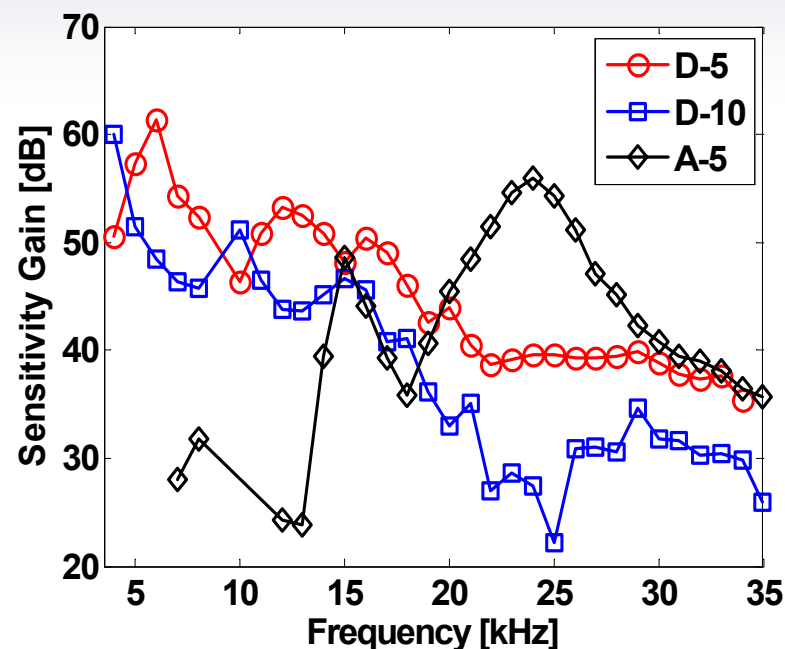
A cylindrical holder was properly designed to fabricate ARALDITE coatings.



EXPERIMENTAL VALIDATION



SENSOR PERFORMANCES



- Sensors with Damival coating are more sensitive than PZT in the frequency range 4-20kHz
- Sensors with Araldite coating are more sensitive than PZT in the frequency range 15-35kHz
- Sensitivity improvement with respect to bare FBG of 2-3 order of magnitude
- Sensitivity comparable or higher than traditional PZT and other photonic technologies at the state of the art

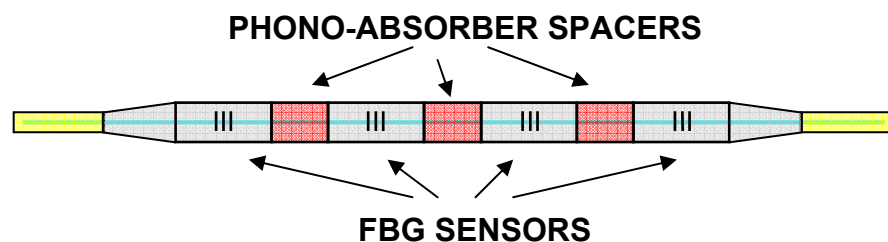
TOWARDS INDUSTRIALIZATION

Flexible array :

Material : Damival

Array : 4x1

Sensors : D-5



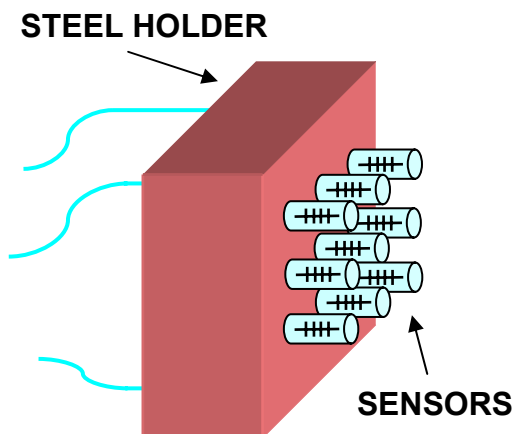
Phono-absorber spacers keep FBG sensors mechanically and acoustically separated

Rigid array :

Material : Araldite

Array : 4x4

Sensors : A-5



OFFSHORE PRELIMINARY TEST

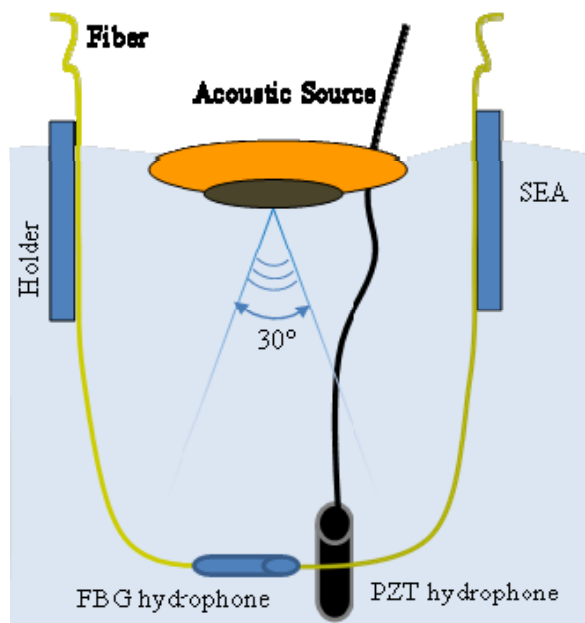
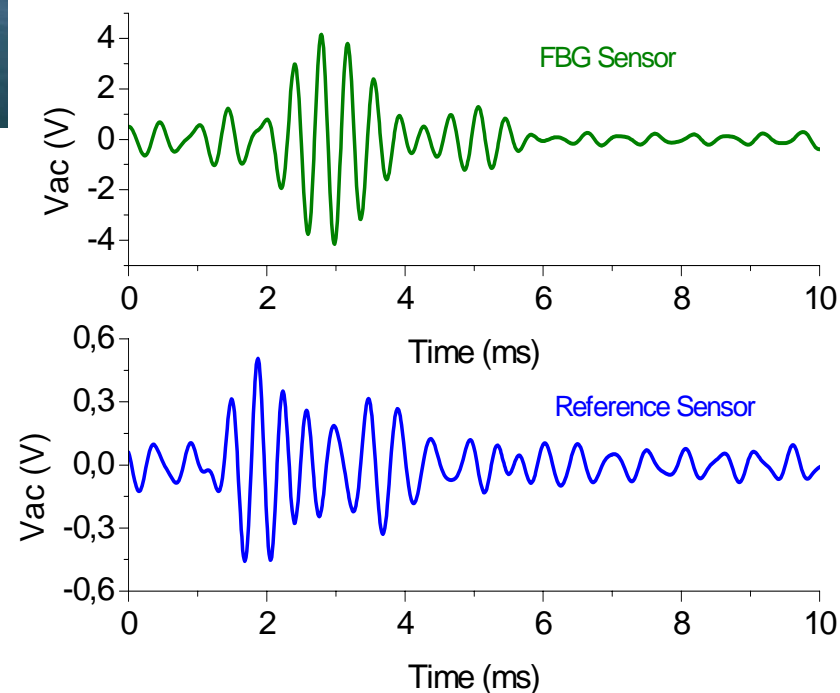


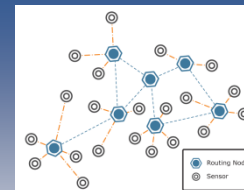
PZT



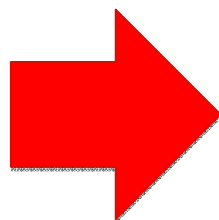
- Port of Baia, Napoli
- FBG Sensor: D-5
- Sea environment with high noise

Sensor time response





Fiber Optic Sensors for High Energy Physics Applications



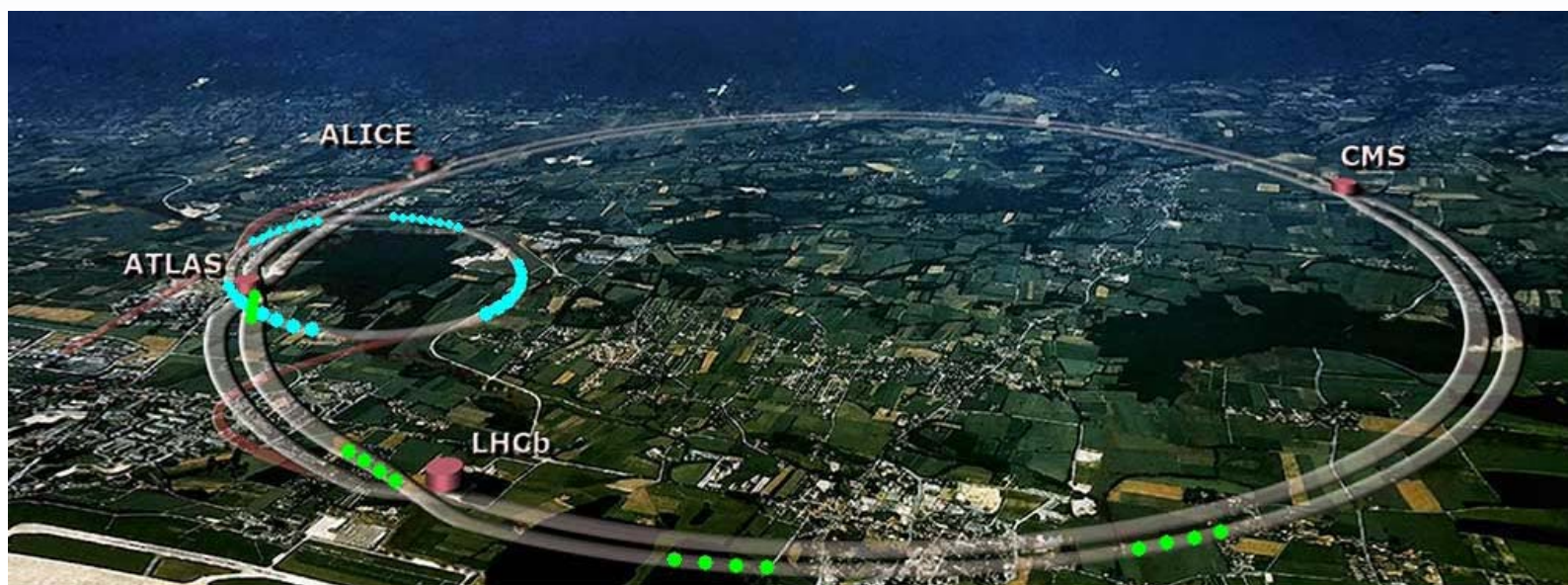
Fiber Optic Sensor
Community
(academic and
industrial partners)

CMS Collaboration @ CERN



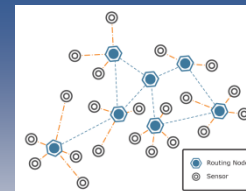
FOS4HEP Project

High Energy Physics at CERN



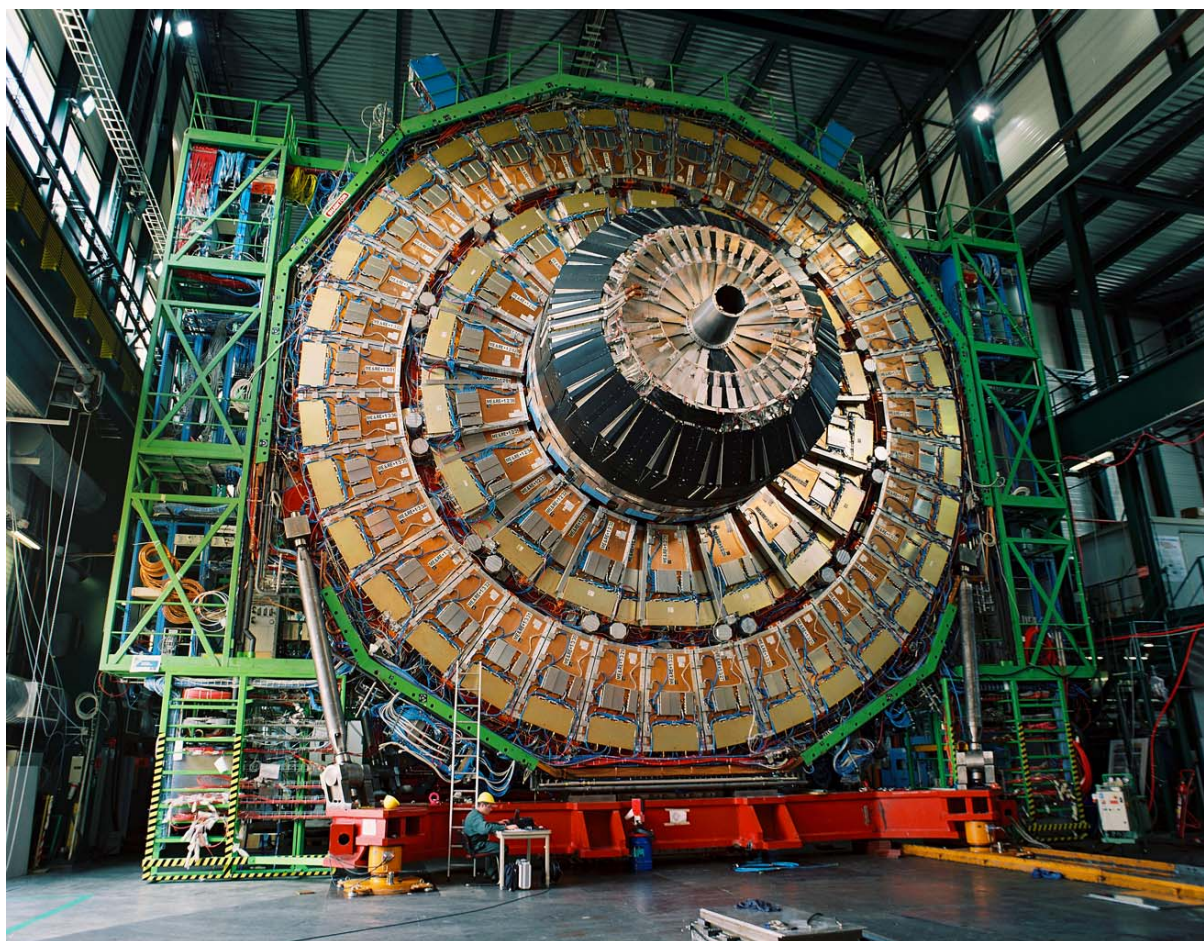
**CERN (European Organization for Nuclear
Research) from 1954**
**Large Hadron Collider (LHC) housed in a 27 km
tunnel and 100 m underground**
4 main experiments running





CMS: Needs and Requirements

Compact because it is “small” for its enormous weight,
muon for one of the particles it detects, and **solenoid** for the
coil inside its huge superconducting magnet.



Needs:

Thousands of sensors for
the monitoring and control
of CMS operations

(SAFETY and SECURITY are
fundamental in these types
of experiments operating in
extreme conditions)

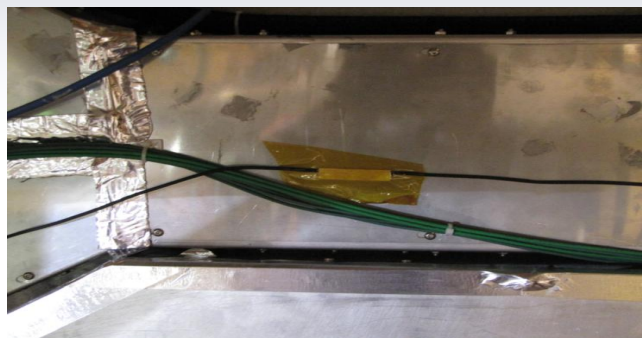
Parameters to be detected:

Temperature, Humidity,
pressure, magnetic induced
strain, displacements
magnetic field, gases, cryo
sensors, and many others

Requirements:

Reduced cabling
Radiation Hardness
Electromagnetic immunity

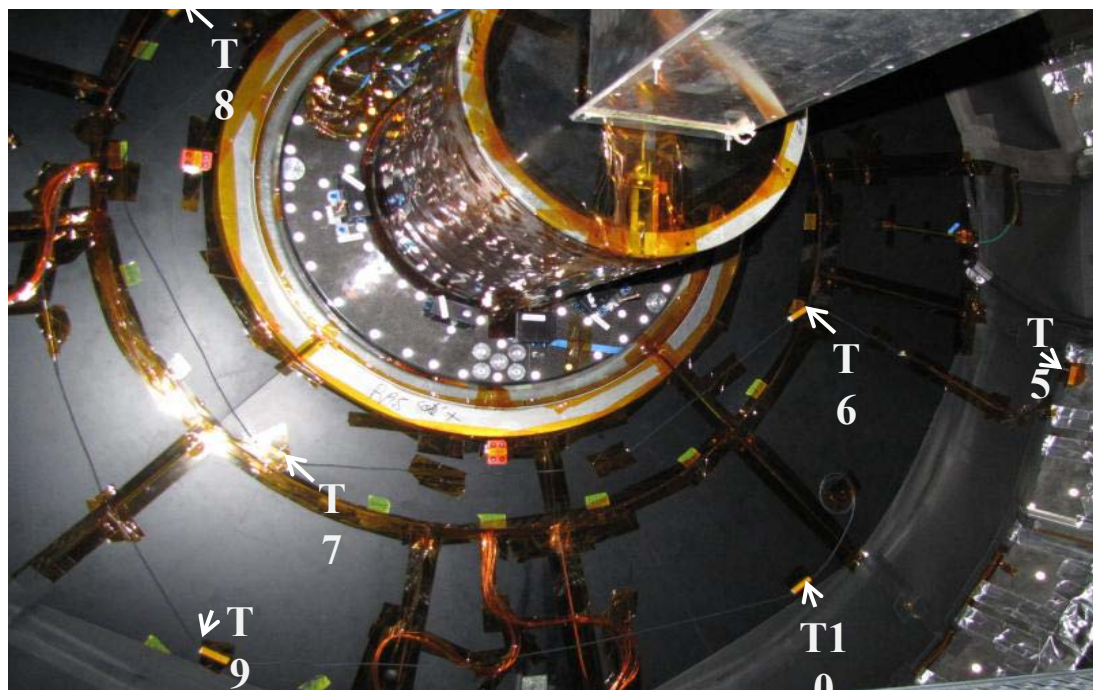
Fiber Optic Temperature Sensors at CMS



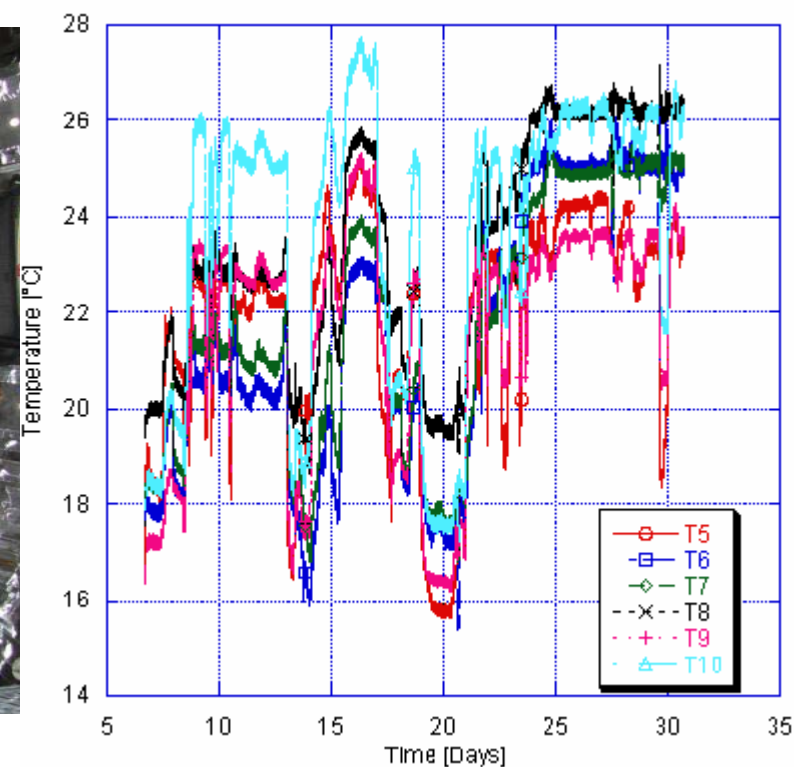
**Ceramic packaging for
radiation hardness**

**Coating absence on
FBGs to avoid radiation
induced cracking and
aging**

A. Saccomanno, A. Cusano et al, **IEEE
Sensors Journal**, 12(12), 3392- 3398 (2012)



F3 July 06-30 T5, T6, T7, T8, T9, T10

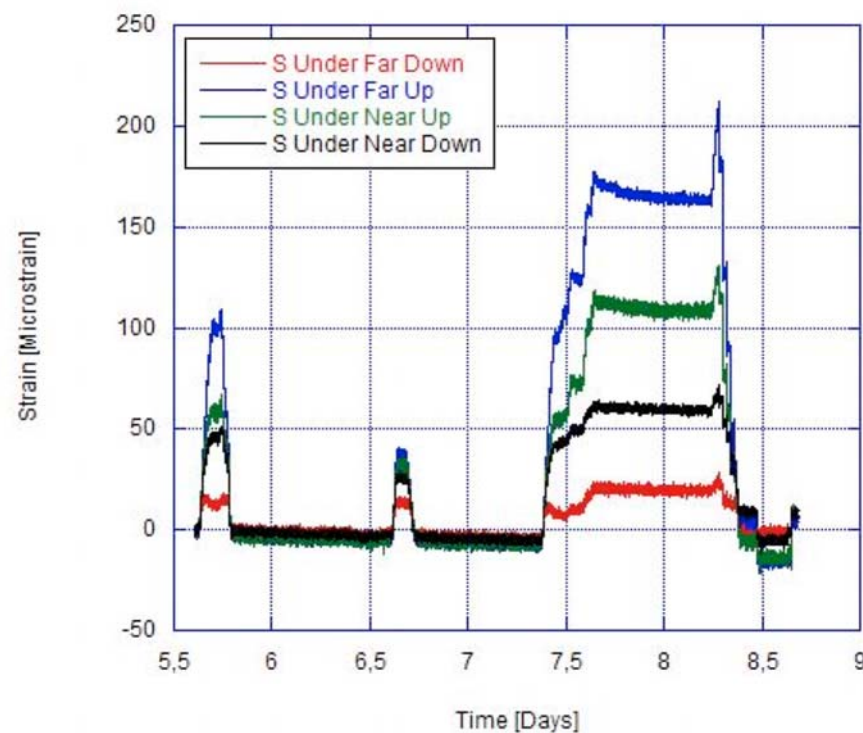


Strain Monitoring at CMS

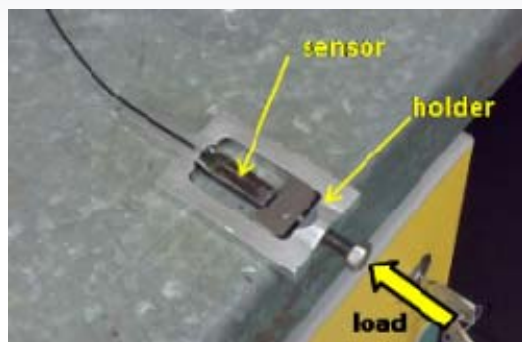


High B field causes strain within iron structures leading to possible structure re-shaping

This effect is very dangerous since it can cause the damaging of the beam pipe leading to catastrophic explosions

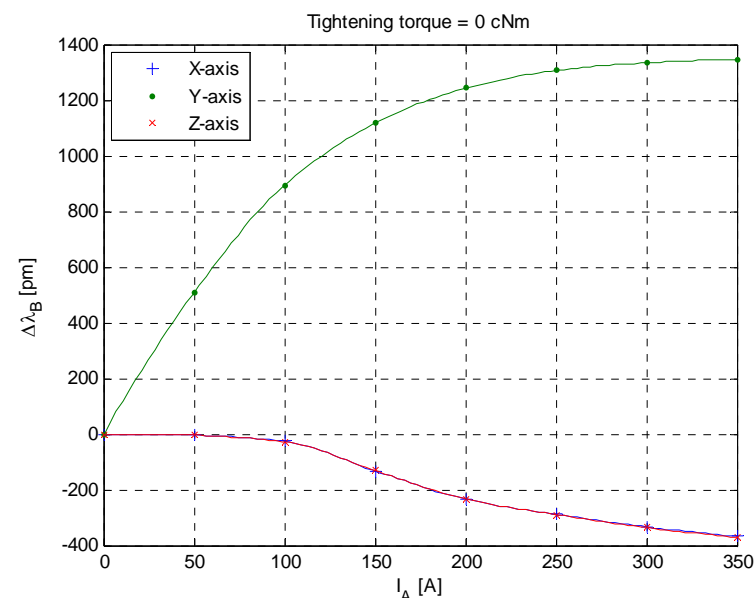
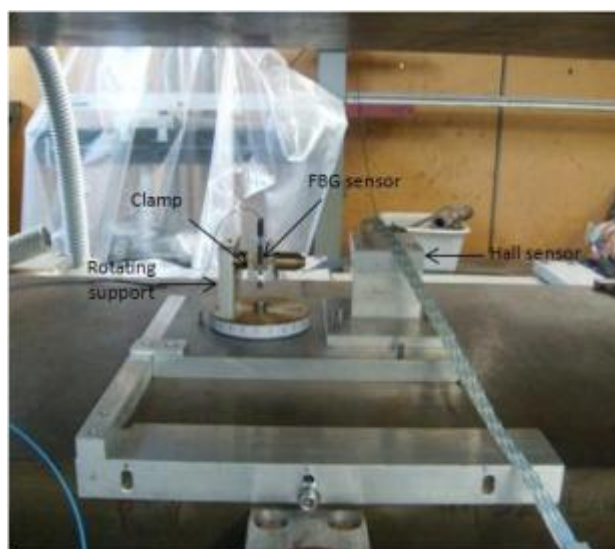


Fiber Optic Magnetic Field Sensors at CMS



Magnetic field measurement by magnetostrictive materials using.

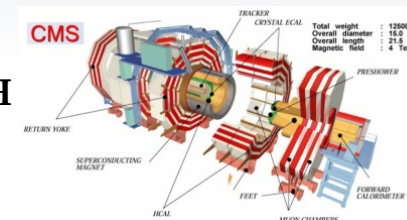
They deform in the presence of magnetic field and an optical FBG converts mechanical deformations in optical signal; then, the optical interrogator replies the size magnetic measuring



“Effect of the Anisotropic Magnetostriction on Terfenol-D Based Fiber Bragg Grating Magnetic Sensors,” G. Lanza, G. Breglio, M. Giordano, A. Gaddi, S. Buontempo, A. Cusano, *Sensors & Actuators: A. Physical* 172 (2011) pp. 412-419

Humidity Sensors Issues in HEP Trackers

- ✓ Low mass and Small dimensions
- ✓ Insensitivity to magnetic field
- ✓ Operation at temperature down to -40°C and response to the full range $[0, 100]\% \text{ RH}$
- ✓ Reduced number of wires
- ✓ High long term stability and/or possibility of an easy remote recalibration
- ✓ Radiation resistance to dose up to 1 Mgy



Miniaturized humidity sensors used at CERN

HIH 4000 series by Honeywell



Capacitive
Small Size
Inexpensive

3 wires for each RH measuring point
Accuracy of 3,5%RH
Response time 15s
Minimum operation temperature -40°C
NOT Radiation hard



Precon HS2000

PIN DIAGRAM
(Front View)



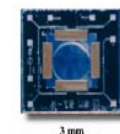
Pin # 1 2 3 4

Pin 1	Temperature Out (0 to Vsupply)
Pin 2	Power (2 to 5.5 volt)
Pin 3	RH Out (0 to Vsupply)
Pin 4	Ground

Capacitive
Small Size
Easy in use
Direct reading of Dew Point
NOT radiation hard
Sensitive to B fields



Hygrometrix HMX



Resistive
Small size
Tolerant to radiations
Extremely low response
Complex chain of read-out over long distances
Highly not linear signal
NOT AVAILABLE on the market any more

For HEP detectors, multi-point distributed measurements and insensitivity to electro-magnetic noise and resistance to ionizing radiations are a MUST.

NOWADAYS THERE IS NO MINIATURIZED HUMIDITY SENSOR ON THE MARKET WELL SUITED FOR HEP DETECTOR APPLICATIONS

FBG as Humidity Sensor

- Bare FBGs are insensitive to humidity.
- Use of a sensitive material as coating of the FBG to induce a mechanical effect.
- Hygroscopic polymers swell upon adsorption of water molecules.



Development of humidity sensor by coating the FBG with a polyimide film.

Water molecules absorbed by
the hygroscopic coating



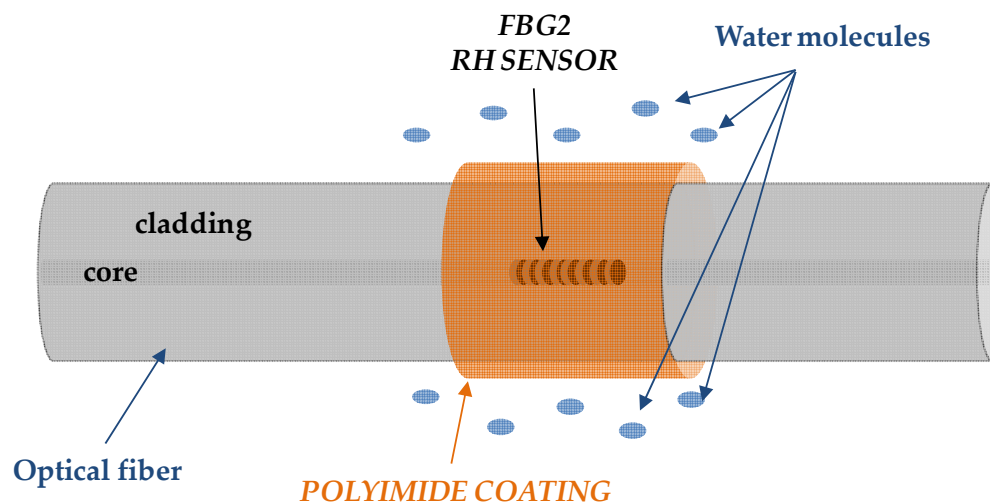
Coating expansion
("Swelling")



Strain induced
on the FBG



Bragg wavelength shift
($\Delta\lambda_B$)

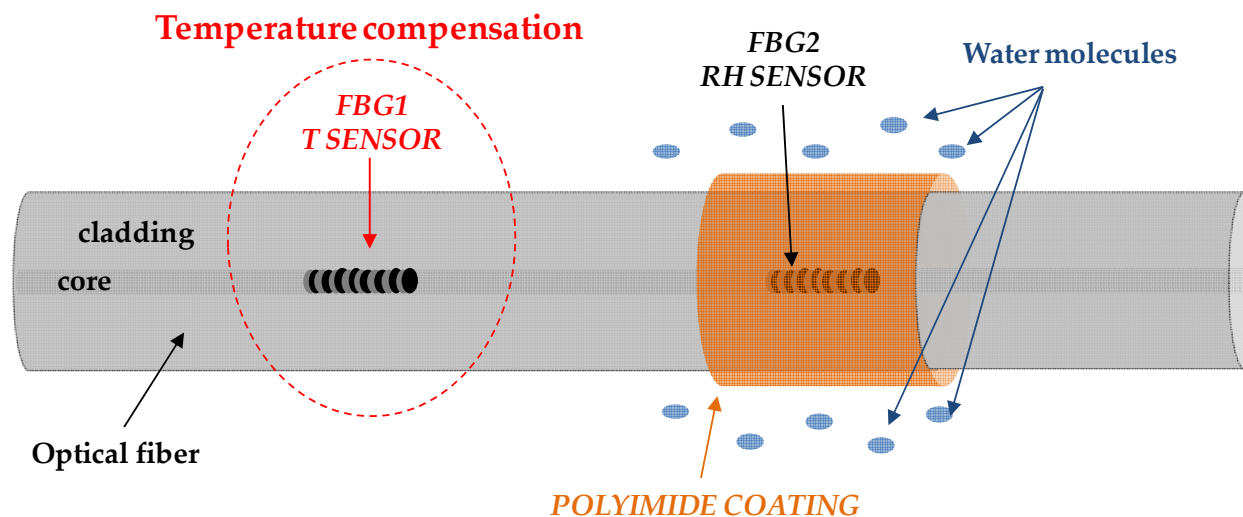


Temperature compensation

Polyimide-coated FBGs are also sensitive to temperature:

$$\Delta\lambda_B = f(\Delta T, \Delta RH) = S_T(T, RH) \cdot \Delta T + S_{RH}(T, RH) \cdot \Delta RH$$

- A temperature compensation scheme is required to extract RH measurements from the sensor readings, that can be simply accomplished by using an uncoated FBG (on the same fiber)



2011: FBGs as humidity sensors in HEP applications

FBGs coated by a Polyimide (PI) layer

Sensors and Actuators B 177 (2013) 94–102

Radiation hard humidity sensors for high energy physics applications using polyimide-coated fiber Bragg gratings sensors

G. Berruti^a, M. Consales^a, M. Giordano^b, L. Sansone^b, P. Petagna^c, S. Buontempo^d,
G. Breglio^c, A. Cusano^{a,*}

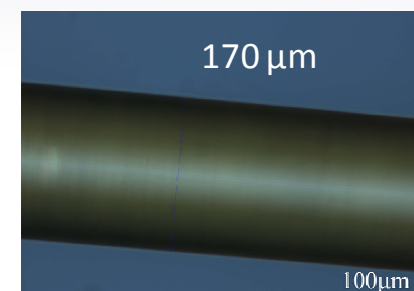
^a Optoelectronic Division, Department of Engineering, University of Sannio, Benevento, Italy

^b Institute for Composite and Biomedical Materials, CNR, Portici, Italy

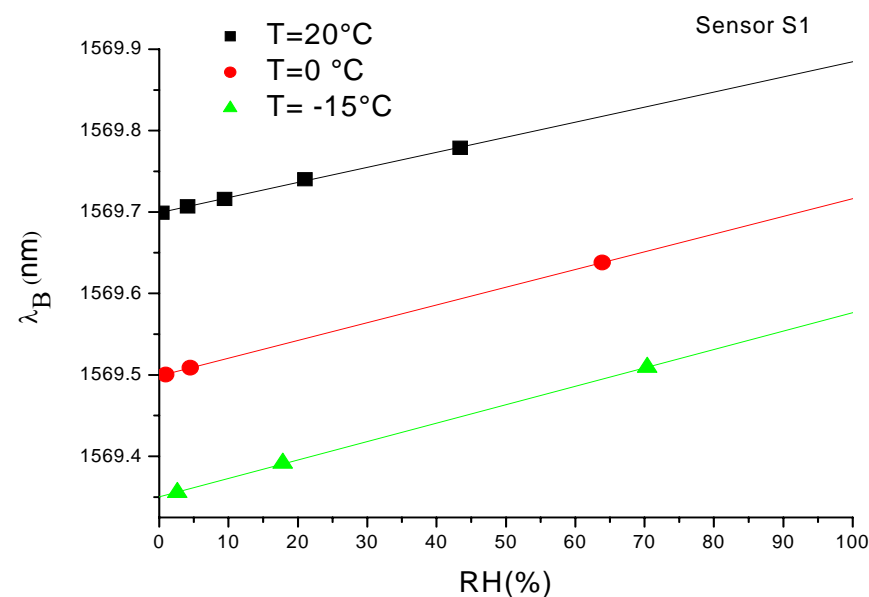
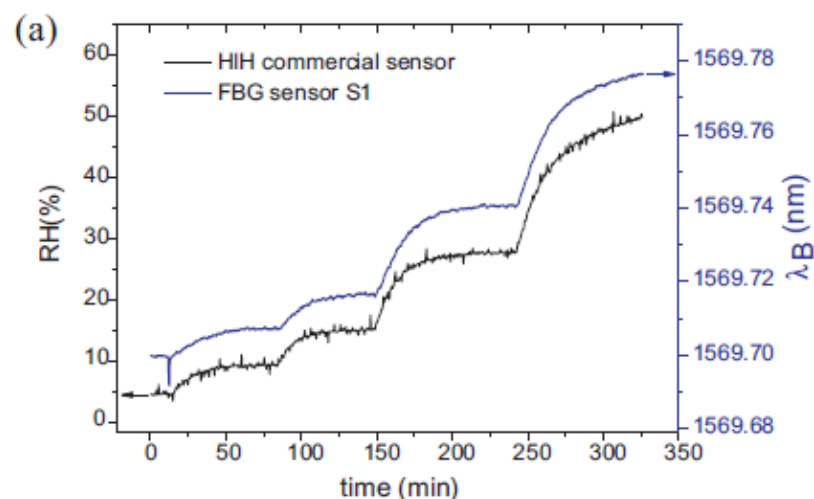
^c European Organization for Nuclear Research, CERN, Genève, Switzerland

^d Istituto Nazionale di Fisica Nucleare, Sezione di Napoli, Via Cinthia, 80126 Napoli, Italy

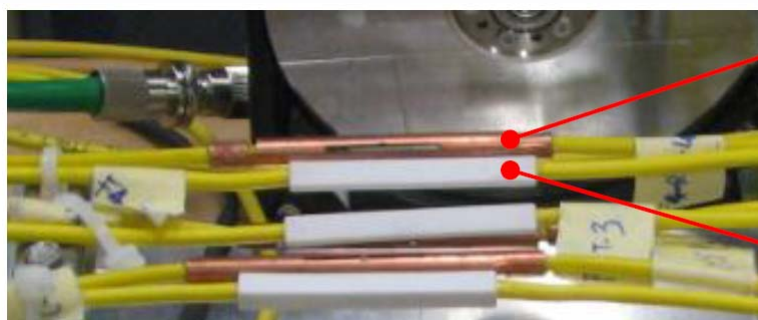
* Department of Biomedical, Electronic and Telecommunication Engineering, University of Naples Federico II, Napoli, Italy



Optical microscope image of a FBG sensor coated by a ~23µm-thick PI layer



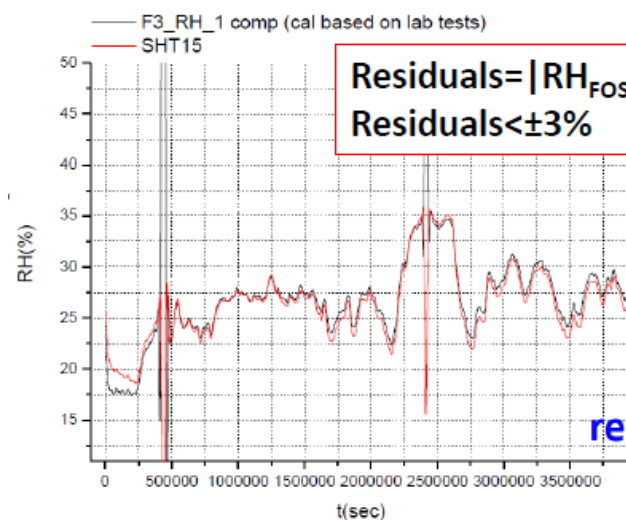
R&D PROGRAMME@CERN



RH-FOS SENSOR

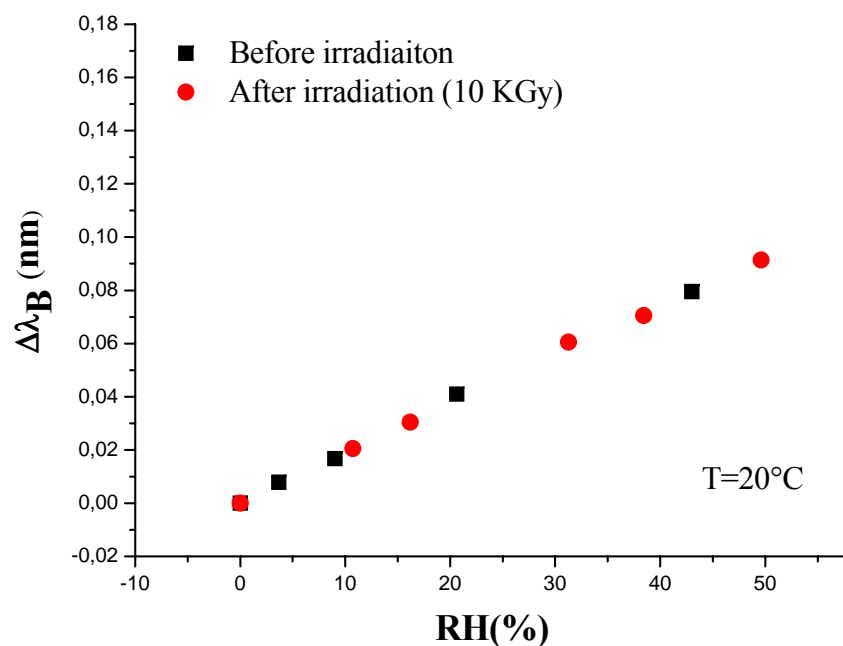
T-FOS SENSOR

- Arrays pre-irradiated at 10 kGy ionizing irradiation dose
- FBG conveniently protected in a special casing
- Calibration of the arrays performed in the climatic chamber using a special cylindrical support
- After the calibration, arrays installed in CMS as first application of this technology to the “real world”

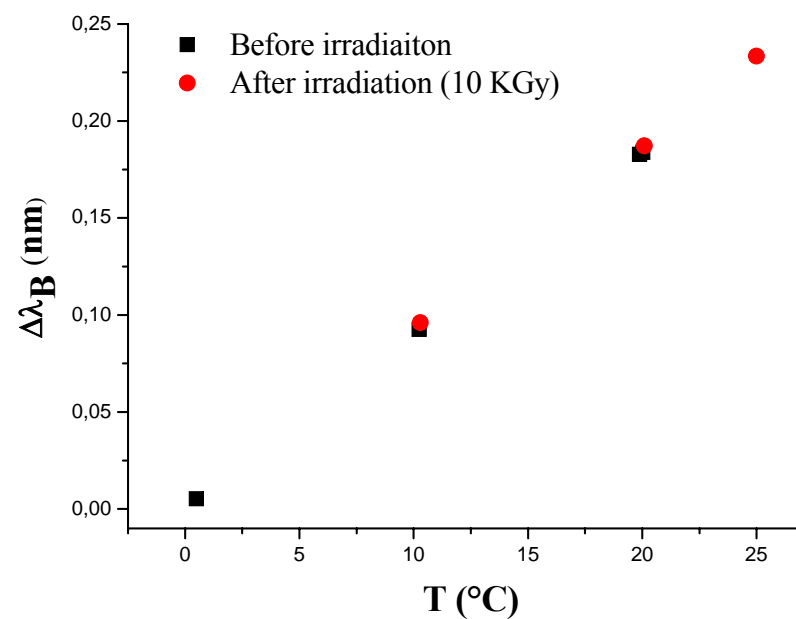


Results seem to be
very
compatible to RH
analogic sensor
readings present in the
same box!!!

Pre and Post irradiation characteristic curves (after a 10kGy dose)

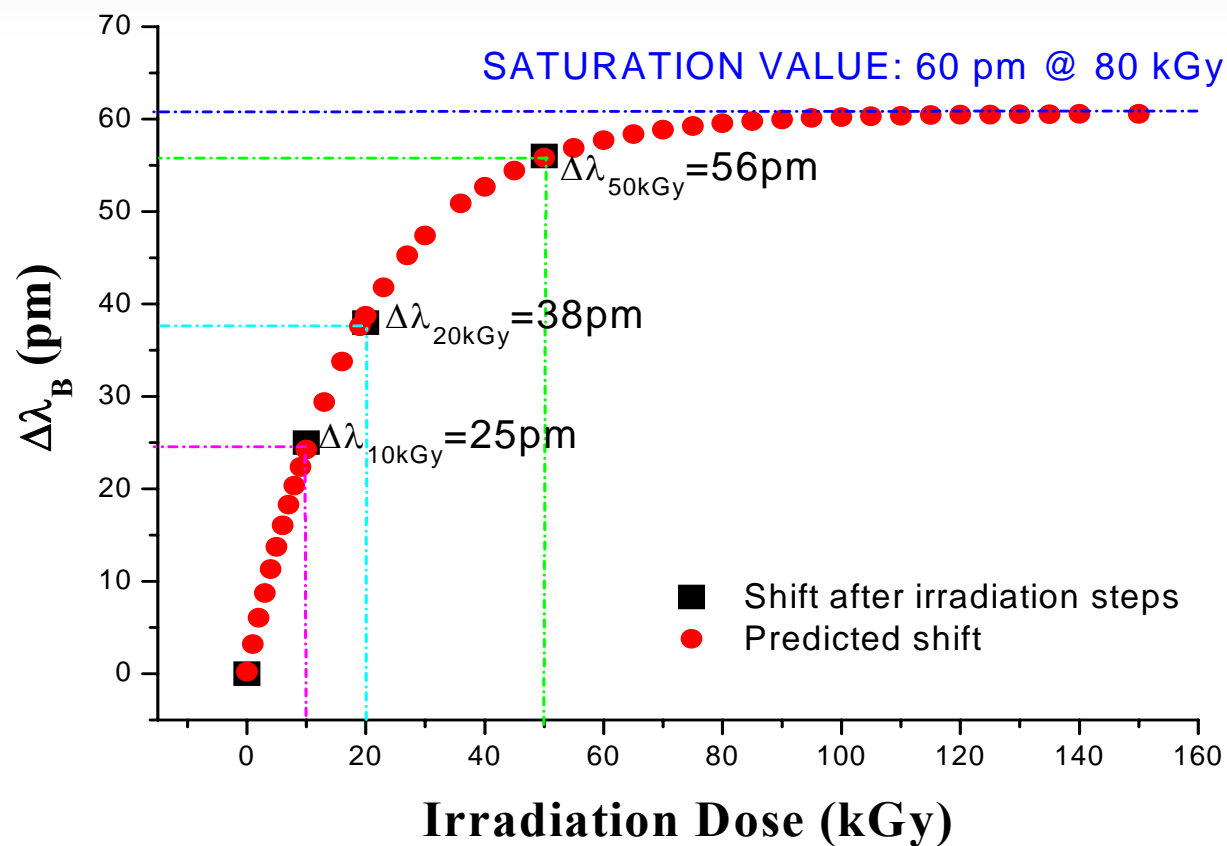


$\Delta\lambda_B$ vs RH before and after the irradiation process



$\Delta\lambda_B$ vs T before and after the irradiation process

$\Delta\lambda_B$ vs Irradiation dose



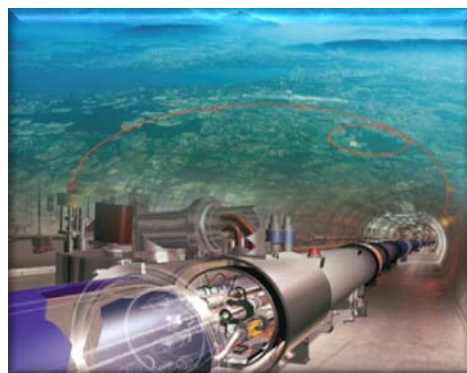
Commercial electronic hygrometer resulted definitely damaged after the 10 kGy dose.

Cryo-Sensors for superconducting magnets

Needs and requirements

A large number of sensors and electronic devices located inside the 27- km LHC tunnel able to withstand the **radiation** and **cryogenic** environment:

Cryogenic Thermometers
to monitor and to control the
temperature in the wide
range 1.9 - 300 K



Electrical Strain Gauges
to monitor and to control the
stress profile from the
assembly to the operation of
the magnet

A lot of wires needed!

Potentials for the use of fibers for temperature and strain

- Immunity to electromagnetic interference in high field environment
- reduction of instrumentation (wires, connections, read out system)
- low heat in-leak into the bath
- improvement of workplace safety in the upgraded tunnel by monitoring the temperature over long length (Wavelength Division Multiplexing)

Temperature sensors: working principle

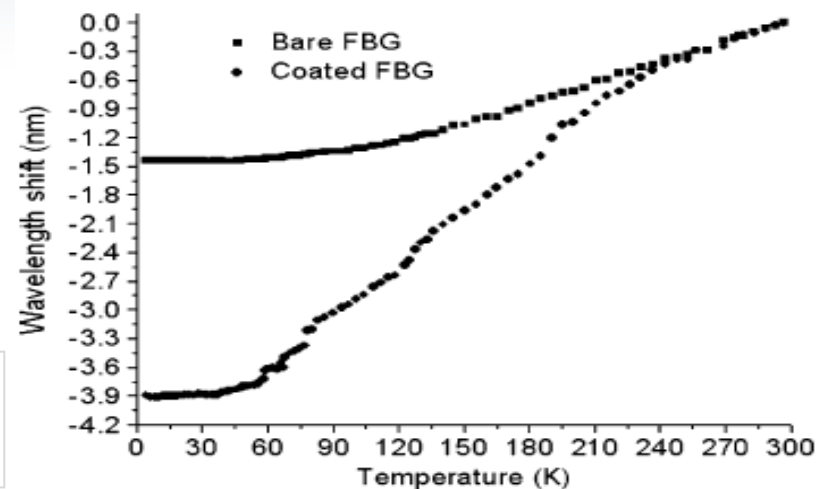
Poor FBG sensitivity at Cryo

Temperatures

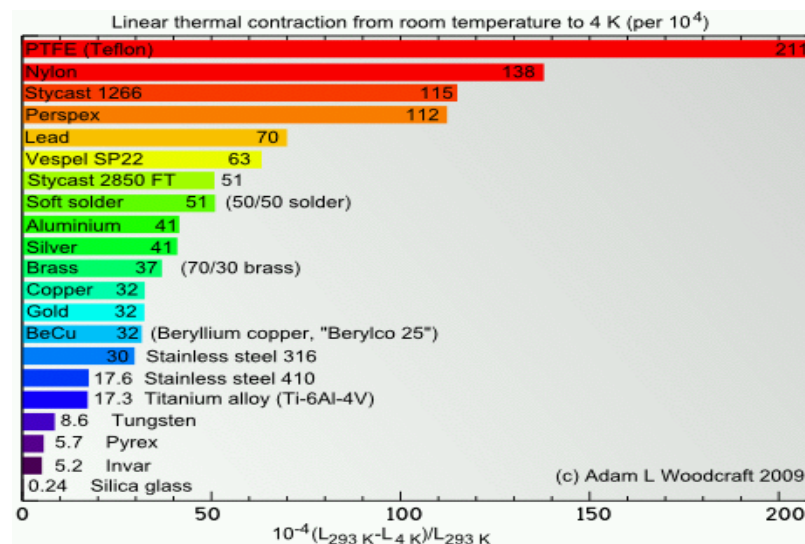
8 - 12 pm/K @ room T

< 0.1 pm/K below 40 K

Hongjie Zhang, Fanping Deng, Qiuliang Wang, Luguang Yan, Yingming Dai, and Keeman Kim, Development of Strain Measurement in Superconducting Magnet Through Fiber Bragg Grating, IEEE TRANSACTIONS ON APPLIED SUPERCONDUCTIVITY, VOL. 18, NO. 2, JUNE 2008;



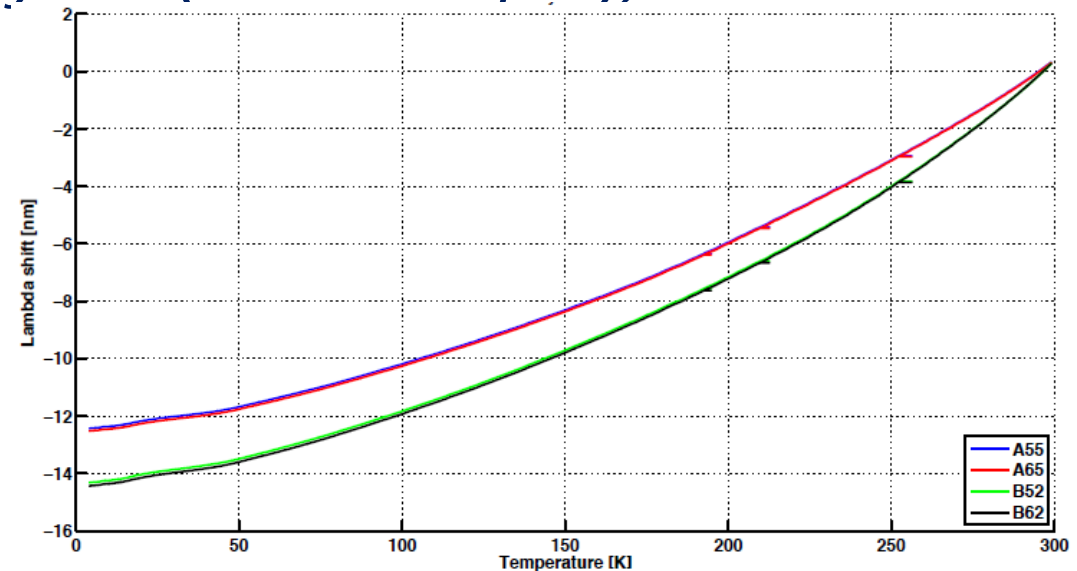
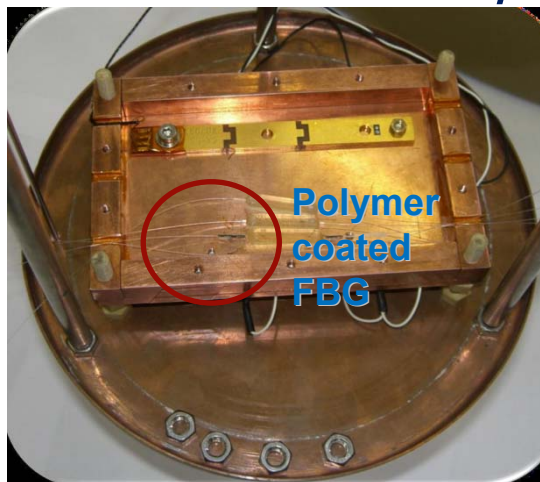
A suitable material with a large thermal expansion coefficient at cryogenic temperature is needed



Embedded Temperature sensors

Polymer coating can be easy and cheap, it makes the FBG sensors very competitive in terms of fabrication and production

Tests at 4.2 K have been carried out on FBGs coated with different polymers (PMMA and Epoxy)



- The analysis shows a strong non linearity within the range 4-10 K but a good feasibility of the coating technique up to 10 K

Strain Cryo-Sensors: Feasibility study

*Preliminary tests have been carried out **gluing** the FBGs on the Aluminum structure of the magnet and comparing them with resistive strain gauges:*

- **Cooldown:** the magnet is lowered inside the cryostat and cooled down up to 1.9 K
- **Training:** the magnet is powered with high current in order to investigate the strain when quenches (transition from superconducting to resistive state) occur.

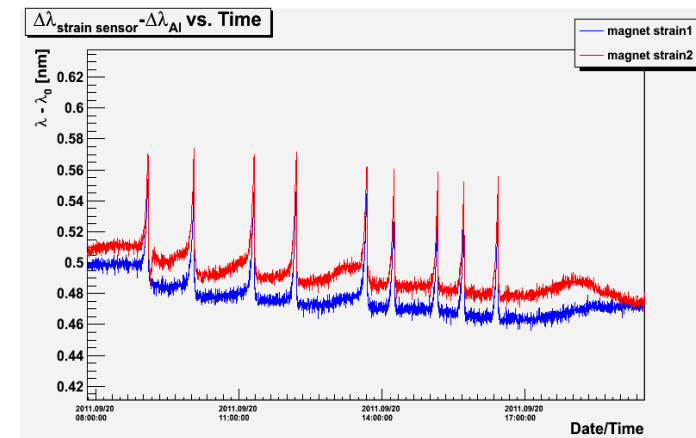


Resistive
strain
gauges

Fiber Optic
strain
sensors

Aluminum shell

Magnet fixed to the insert of
the cryostat



All quenches are clearly seen on the FBG strain sensors: the quench monitoring can help in preventing damages of the magnet due to the high temperature reached during the phenomena

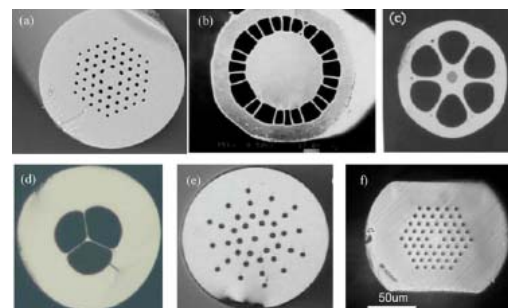
ADDING FUNCTIONALITIES

Microstructured Fiber Bragg Gratings Sensors for Chemical and Biological Applications

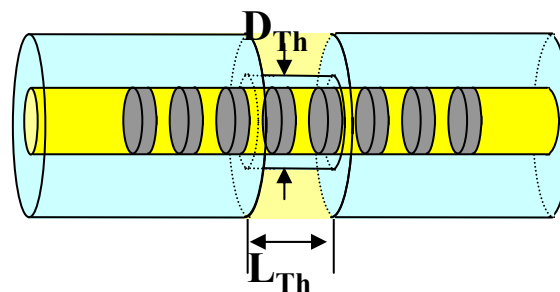
1) FBG realization within unconventional fiber structures

- Microstructured Optical Fiber (MOFs)

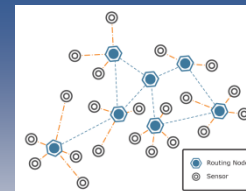
J. Canning *et al.*, Laser Chemistry 2008, 239417 (2008)



2) Conventional FBGs post-processed for structuring the host fiber in localized micro-sized regions: sensitization to surroundings



A. Cusano *et al.*, Journal of Lightwave Technology 27, 1663 (2009)

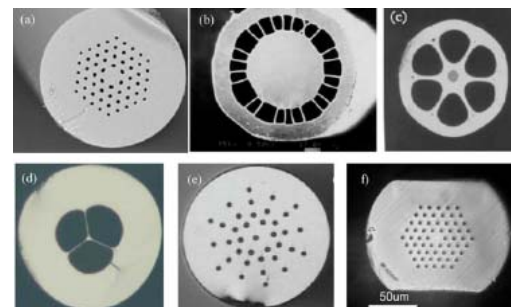


Microstructured Optical Fibers

- 1974: Kaiser and Astle Proposed for the First Time MOFs

P. V. Kaiser and H. W. Astle, Bell System Technical Journal 53, 1021
(1974)

- 1996: Knight *et al.* Reinvigorated This Area of Research:
 - Peculiar Holey Structure
 - New Degrees of Functionality



October 1, 1996 / Vol. 21, No. 19 / OPTICS LETTERS

All-silica single-mode optical fiber with photonic crystal cladding

J. C. Knight,* T. A. Birks,* P. St. J. Russell* and D. M. Atkin

Optoelectronics Research Centre, University of Southampton, Southampton, SO17 1BJ, UK

FIRST DEMONSTRATION OF FBG WRITING IN MOFs

OPTICS LETTERS / Vol. 24, No. 21 / November 1, 1999

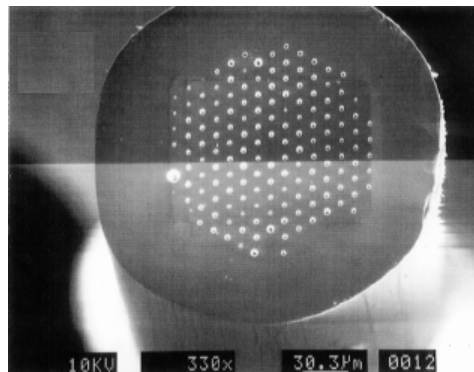
Grating resonances in air-silica microstructured optical fibers

B. J. Eggleton, P. S. Westbrook, R. S. Windeler, S. Spälter, and T. A. Strasser

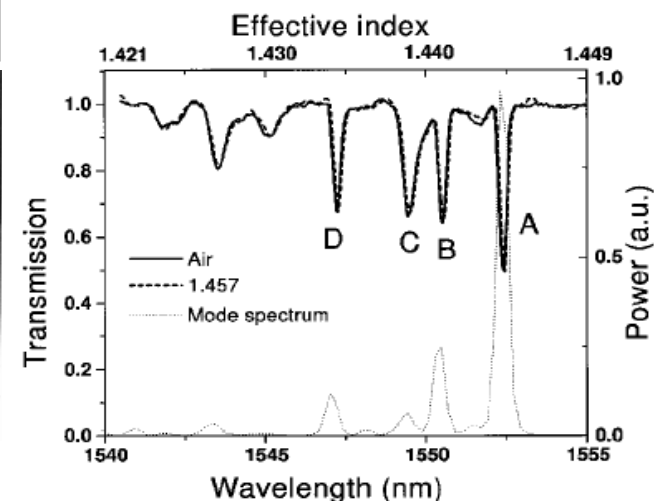
Bell Laboratories, Lucent Technologies, Murray Hill, New Jersey 07974

Single-photon writing at 242 nm: absorption band of the germanium- oxygen-deficient centers

- Conventional writing technique
- Scattered light from the holes
- Higher-Order Modes (HOMs)

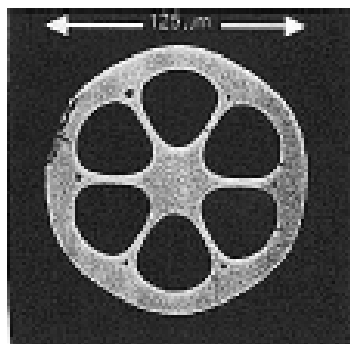


Ge-doped photosensitive solid core MOF



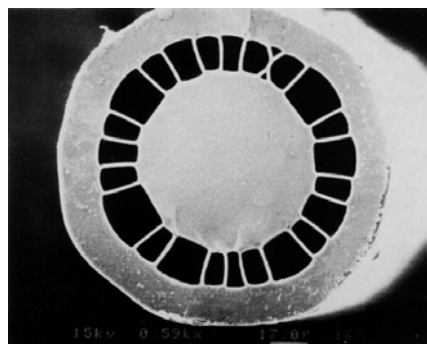
Other FBGs written Ge-doped core MOFs:

Grapefruit Fiber



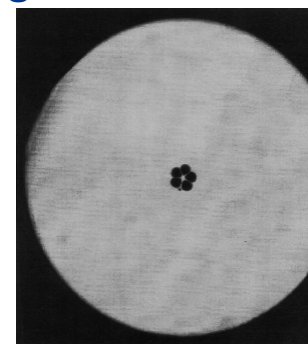
P. S. Westbrook *et al.*, IEEE
Photonics Technology Letters 12, 495

Air-Clad Fiber



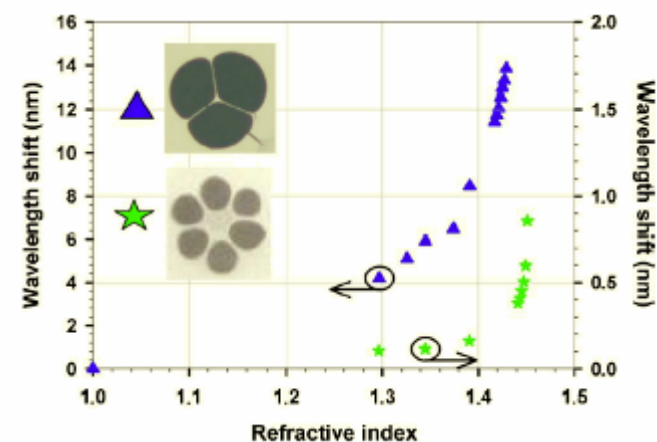
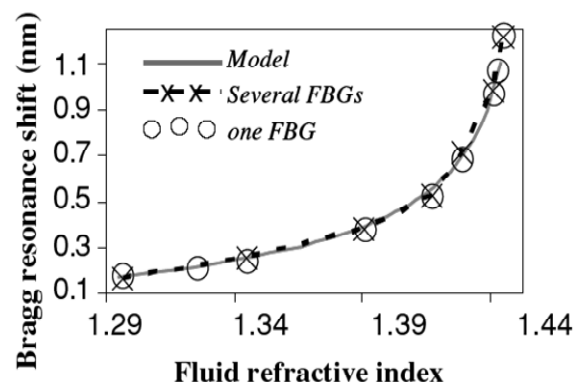
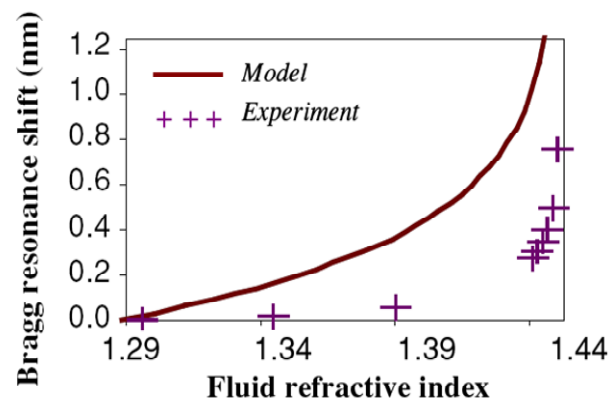
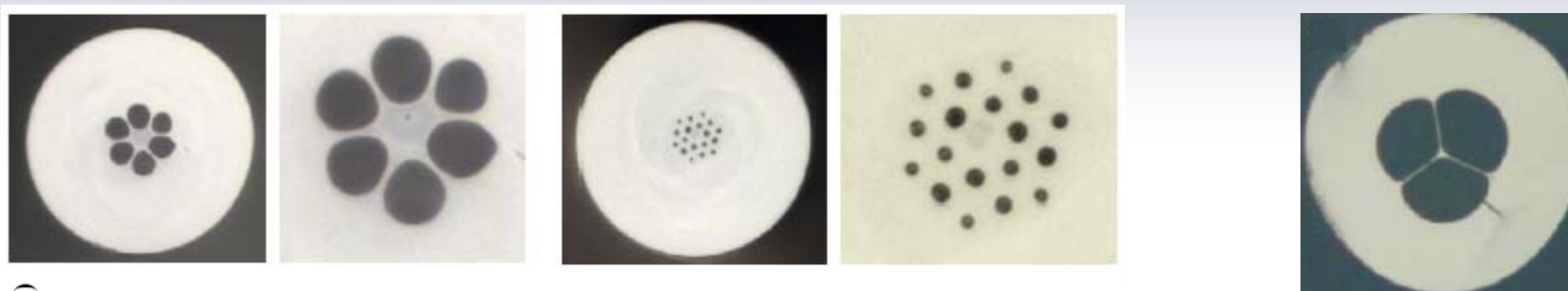
B. J. Eggleton *et al.*, Journal of
Lightwave Technology 18, 1084

High-Delta MOF



B. J. Eggleton *et al.*, Optics Express
9, 698 (2001)

MOF-BASED MSFBGs APPLICATIONS: RI Sensitivity



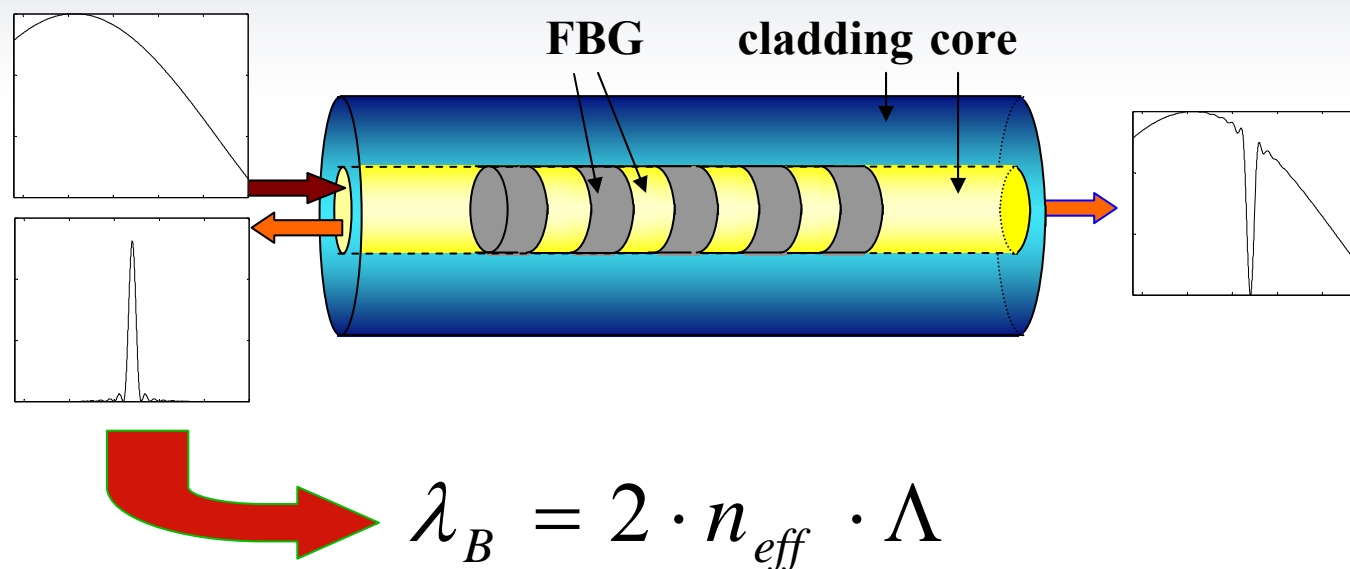
M. C. Phan Huy *et al.*, Measurements Science and Technology 17, 992 (2006)

M. C. Phan Huy *et al.*, Optics Letters 32, 2390 (2007)

$\Delta\lambda=1\text{pm}$	Refractive Index Resolution		
RI	6-hole MOF	2-ring triangular MOF	3-hole MOF
~ 1.33	4×10^{-3}	7×10^{-4}	3×10^{-5}
$\sim 1.40-1.41$	2.1×10^{-4}	1.8×10^{-4}	6×10^{-6}
~ 1.44	7×10^{-5}	2×10^{-5}	-
~ 1.45	6.8×10^{-6}	-	-

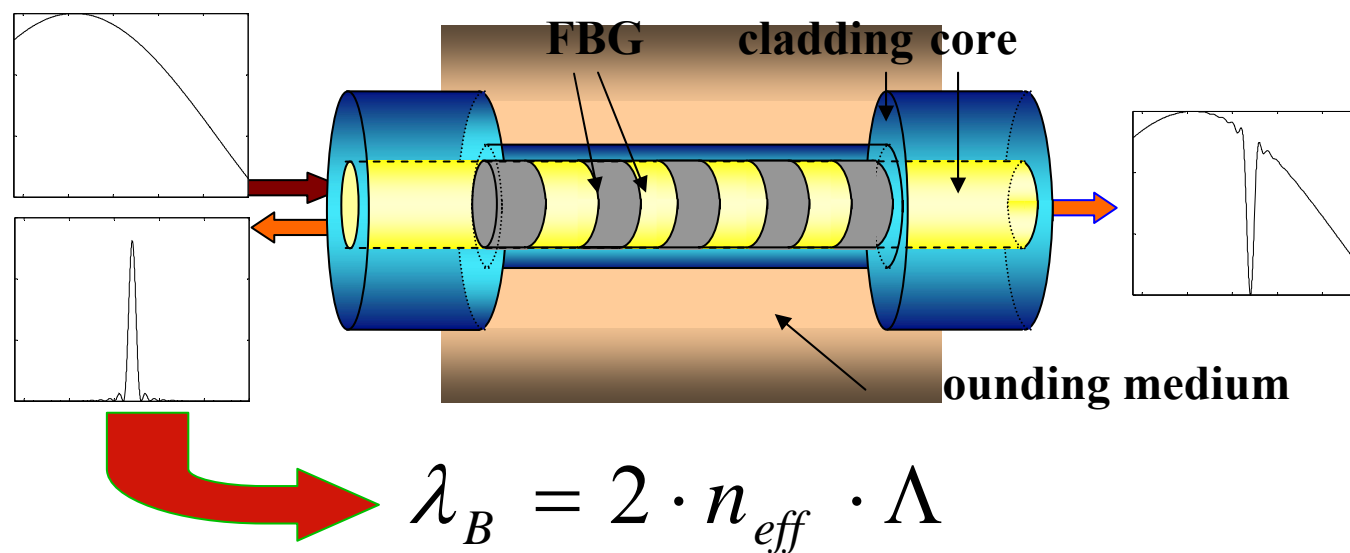
Resume of the different RI resolution with the assumption that 1 pm spectral variations are detectable

In Standard Fiber Bragg Grating (FBG):



The fundamental mode is well shielded from the environment through the cladding layer thus no sensitivity to external refractive index is expected

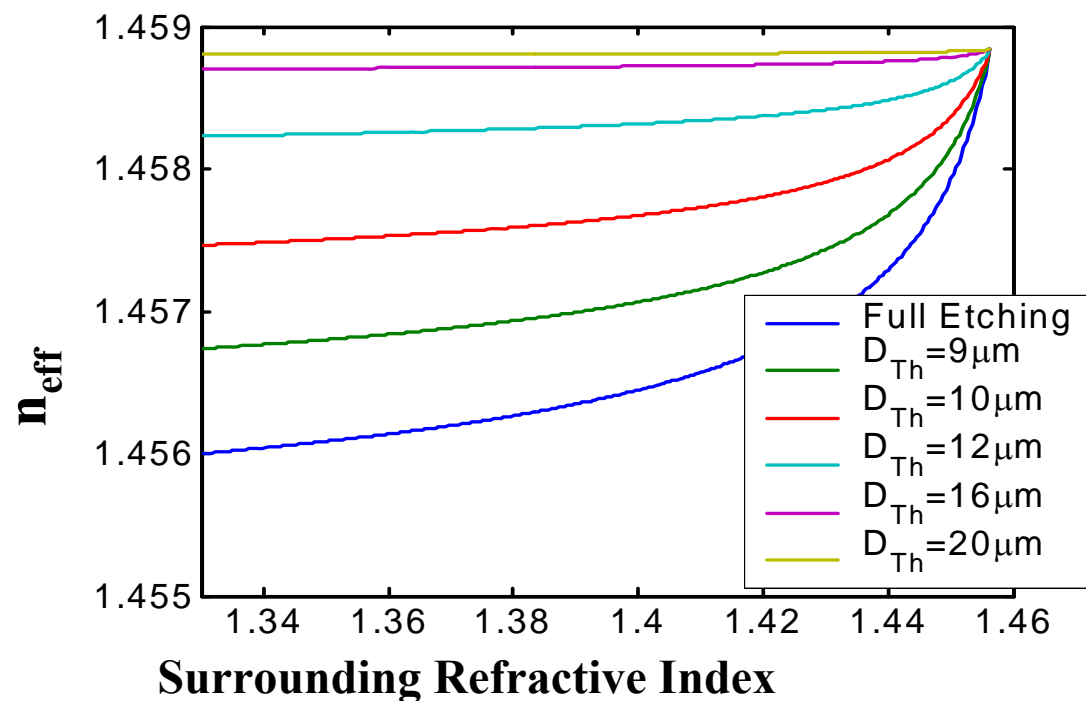
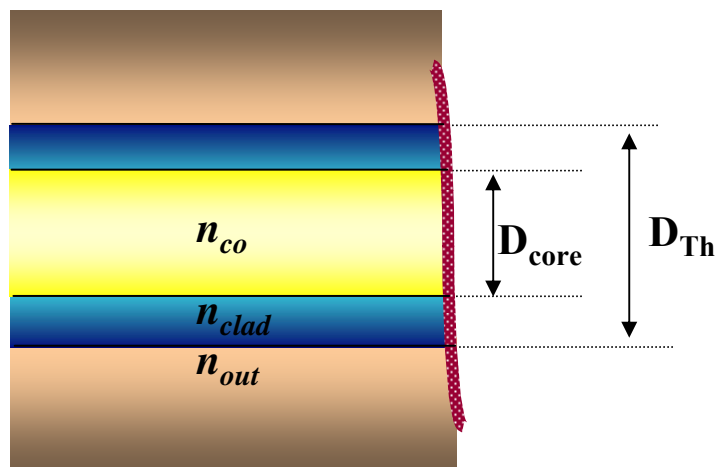
In Thinned Fiber Bragg Grating (ThFBG):



n_{eff} is significantly affected by surrounding medium
refractive index

leading to a shift in the Bragg resonance

Effective Index Sensitivity

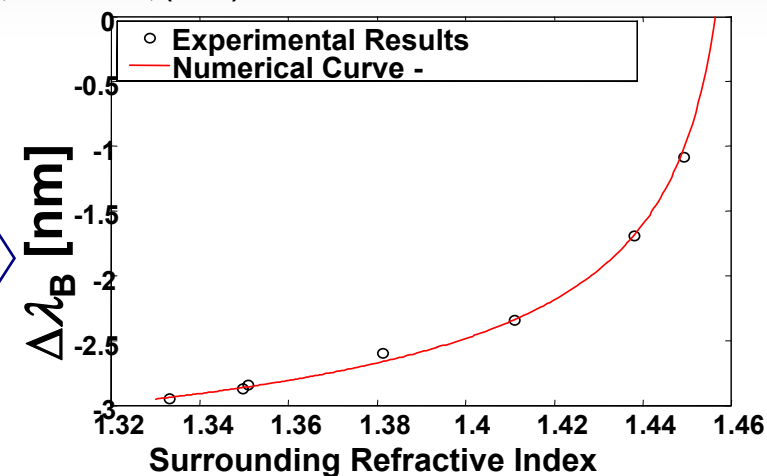
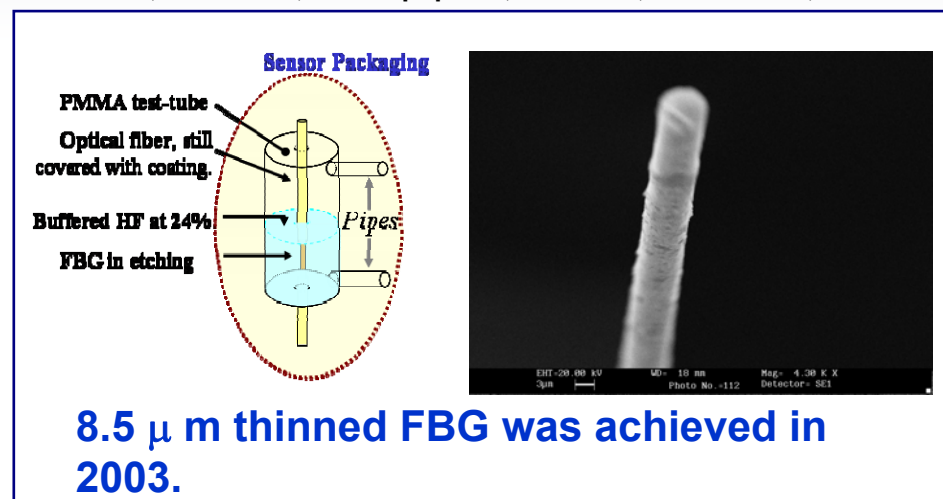


*Maximum sensitivity is obtained by
a complete removal of the cladding layer*

ThFBG demonstrations

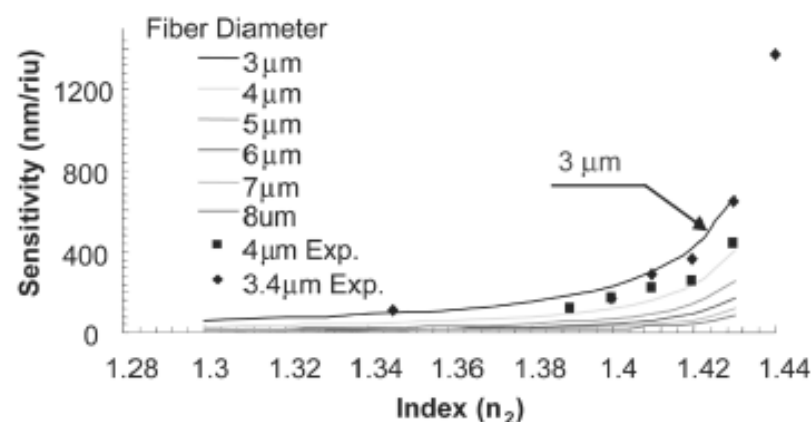
A. Iadicicco, A. Cusano, A. Cutolo, R. Bernini, M. Giordano, IEEE Phot. Techn. Letters 16(4), 1149 – 1151 (2004)

A. Iadicicco, A. Cusano, S. Campopiano, A. Cutolo, M. Giordano, IEEE Sens. J. 5(6), 1288–1295, (2005)



Enhancement of sensor sensitivity by ultra-thinned FBGs was demonstrated

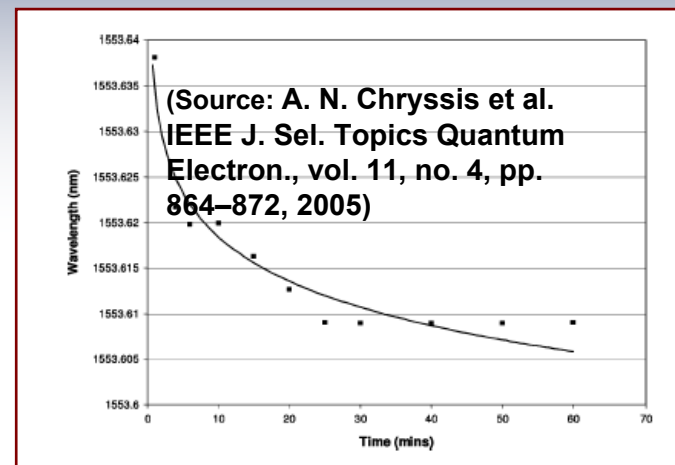
(Source: A. N. Chryssis, et al. IEEE Phot. Technol. Lett., vol. 17, no. 6, pp. 1253–1255, (2005))



ThFBG: Enhanced configurations

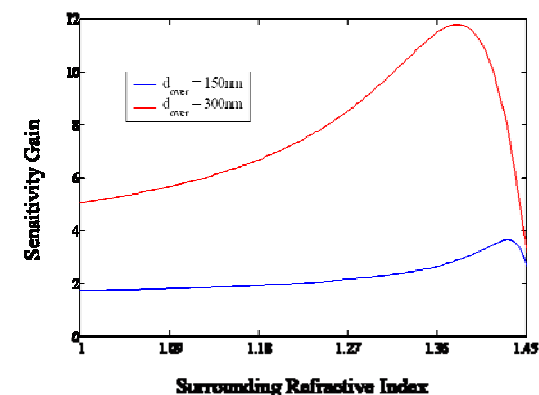
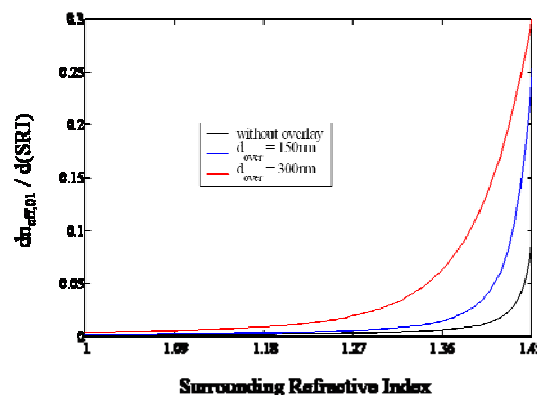
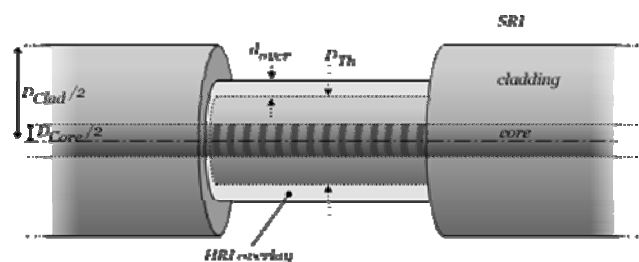
ThFBG based biosensor

Single stranded DNA oligonucleotide probes of 20 bases were immobilized on the surface of the fiber grating using relatively common glutaraldehyde chemistry. Hybridization of a complimentary target single strand DNA oligonucleotide was monitored in situ and successfully detected.



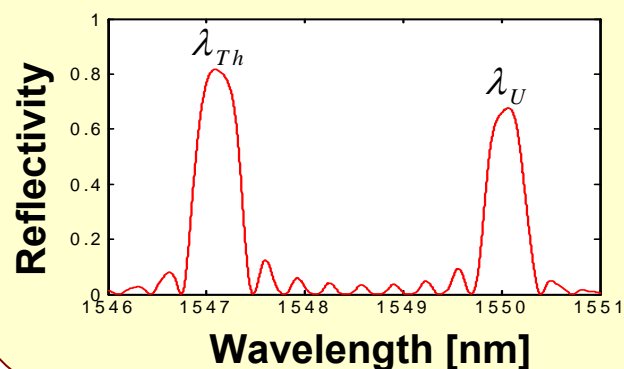
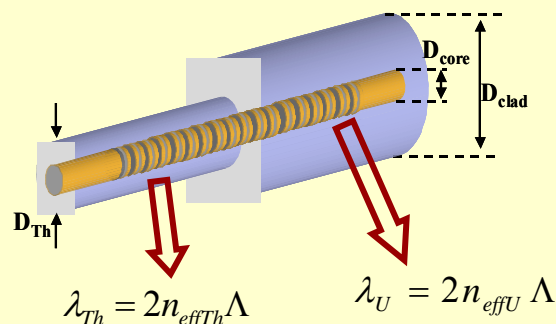
Bragg wavelength shift of a 5 μm core etched grating during the hybridization of the target

HRI coated ThFBG for enhancing sensitivity

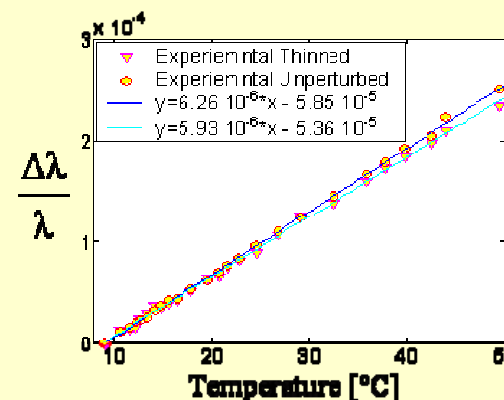
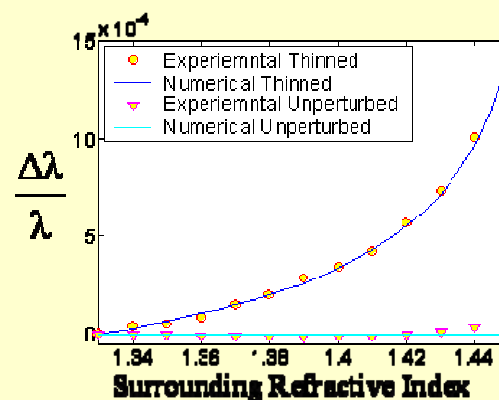


D. Paladino, A. Iadicicco, A. Cutolo, S. Campopiano, M. Giordano, A. Cusano,
Proceedings of the 18th Optical Fiber Sensors
Confer-ence SPIE Cancún, México (2006)

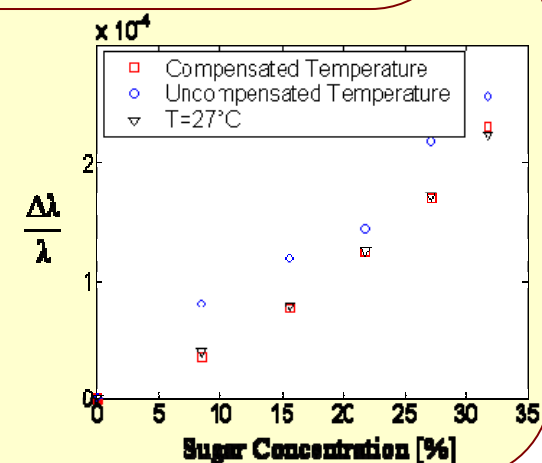
Self-temperature compensation



Relative Bragg wavelength sensitivity to surrounding refractive index and local temperature



Sugar concentration measurements by non uniform ThFBGs with and without temperature self-referencing compensation

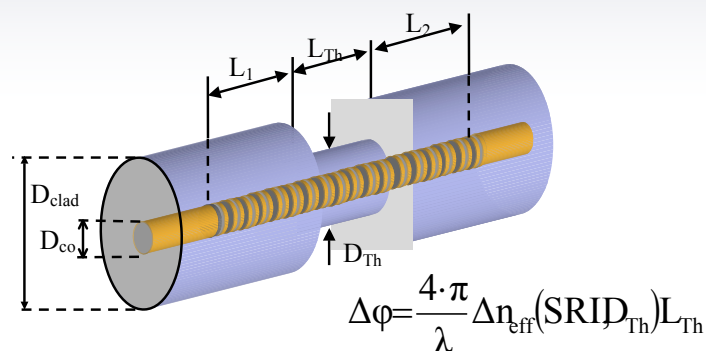


A. Iadicicco, S. Campopiano, A. Cutolo, M. Giordano, A. Cutolo, IEEE Photon Technol Lett, 17(7), 1495-1497 (2005).

A. Iadicicco, S. Campopiano, A. Cutolo, M. Giordano, A. Cusano, Sensors and Actuators B: Chemical 120(1), 231-237 (2006)

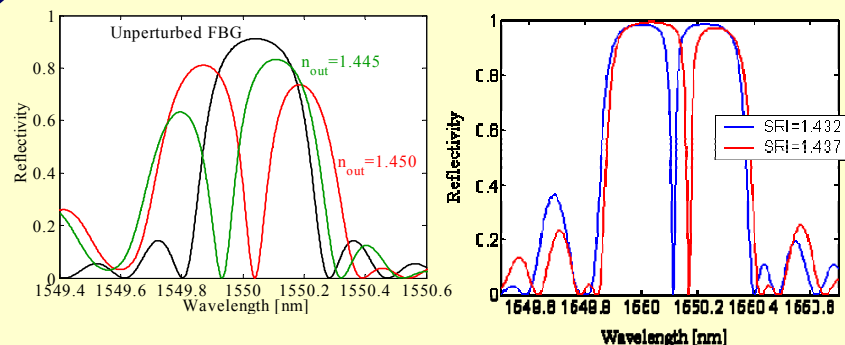
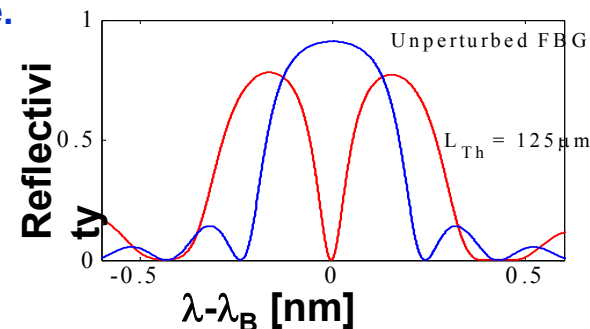
A. Iadicicco, S. Campopiano, A. Cutolo, M. Giordano, A. Cusano Proceedings of SPIE 5855, 479-482 (2005)

Micro-Structured FBGs

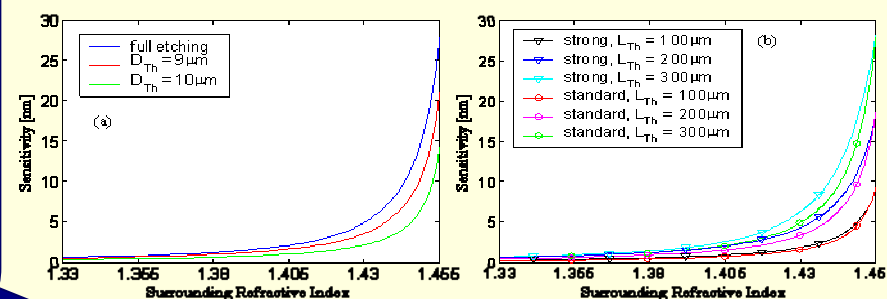


The main effects of the localized perturbation of the periodic structure are:

- the increasing of the stop-band
- the formation on a narrow allowed band, or defect state.



- Defect state bandwidth depends on FBG reflectivity
- Defect state wavelength depends on SRI

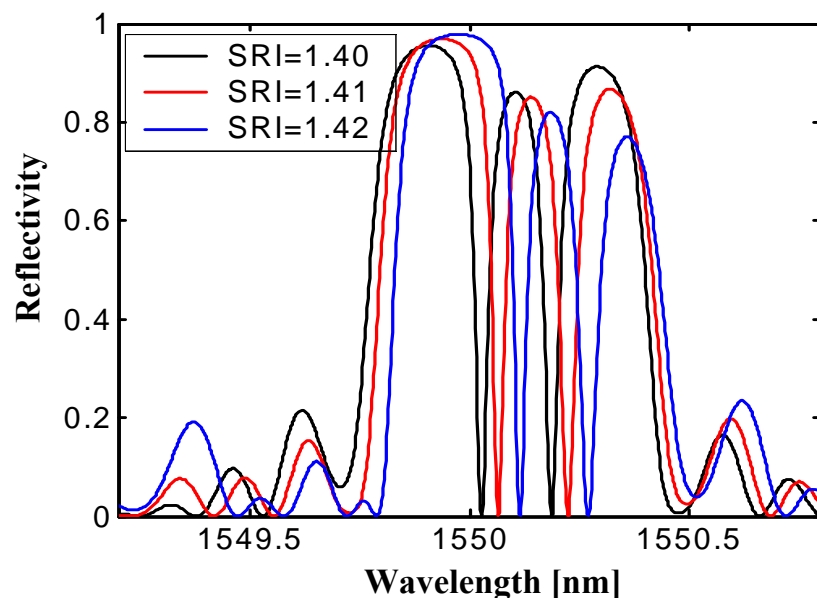
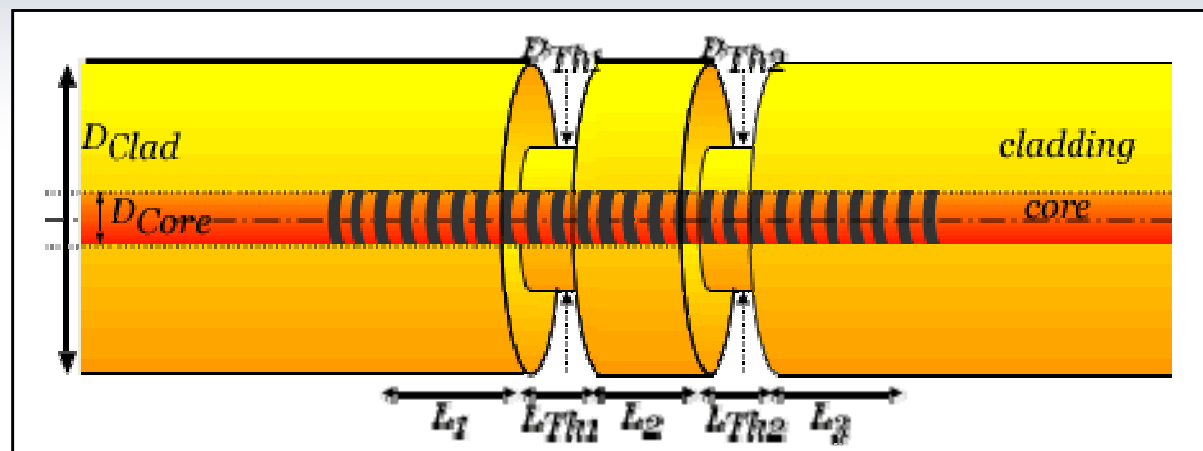


- A.Iadicicco, A.Cusano, S.Campopiano, A.Cutolo, M.Giordano IEEE Electronics Letters 41(8), 466-468 (2005)
A.Iadicicco, A.Cusano, S.Campopiano, A.Cutolo, M.Giordano, IEEE Photonics Technology Letters 17(5), 1250-1252 (2005)
A. Cusano, A. Iadicicco, S. Campopiano, M. Giordano, A. Cutolo, J. of Opt. A: Pure and App. Optics 7, 734-741 (2005)
A. Cusano, A. Iadicicco, D. Paladino, S. Campopiano, A. Cutolo, M. Giordano, Optical Fiber Technology 13(4), 281-290 (2007)

MULTI-DEFECT STRUCTURE

A. Cusano *et al.*, Journal of Optics A: Pure and Applied Optics 7, 734 (2005)
A. Cusano *et al.*, Optical Fiber Technology 13, 291 (2007)

More structural defects can correspond to more allowed bands or defect states



1. Increasing sensitivity
2. Each allowed band results sensitive to the Surrounding RI (SRI) in correspondence of all the structural defects along the grating

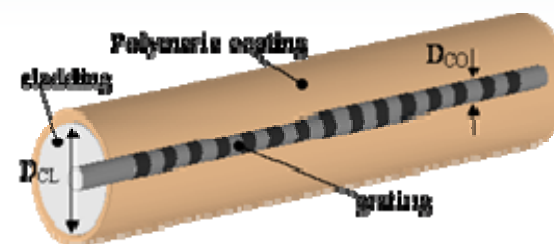
Lithographic Fabrication Procedure

Three-steps procedure:

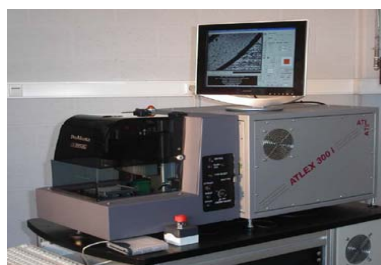
1. Uniform Coating Deposition



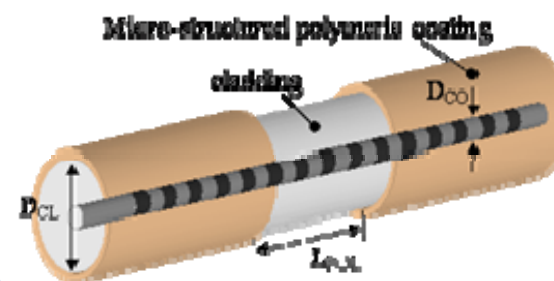
An uniform polymeric coating is cast on the grating fiber region by fiber recoater machine



2. UV Laser Micromachining ($\lambda = 193$ nm)

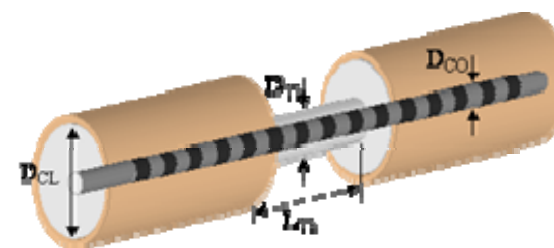


Excimer laser permits fine control of the polymeric coating microstructuring, controlling and accurately defining the etched region length



3. HF Based Etching

HF based wet chemical etching and consequent cladding thinning along the unmasked FBG region



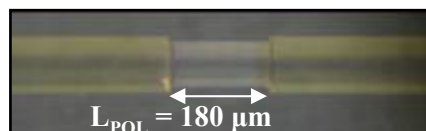
LITHOGRAPHIC FABRICATION PROCEDURE

1. Uniform Overlay Deposition

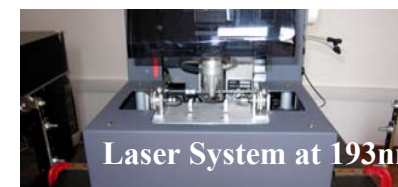


Polyamide coatings
with $D=165 \mu\text{m}$

2. UV Laser Micromachining

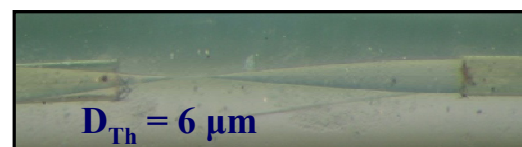


$L_{POL} = 180 \mu\text{m}$

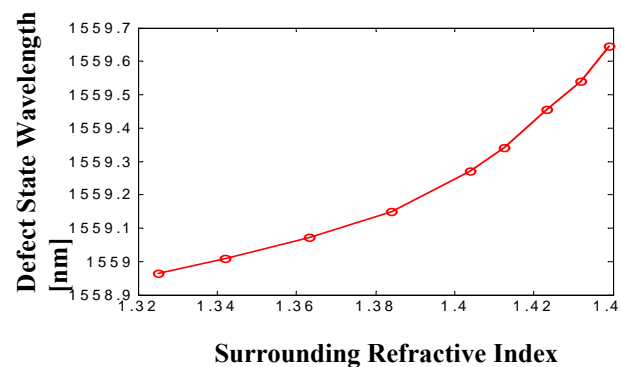
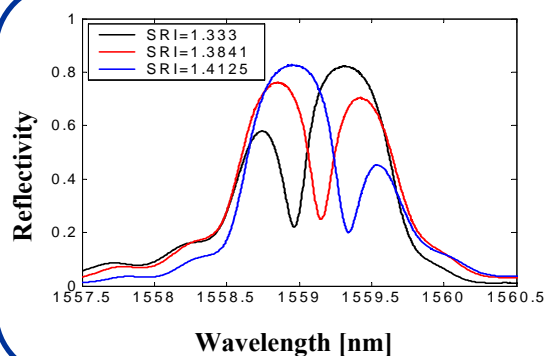
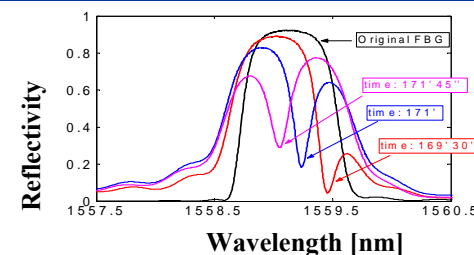


Laser System at 193nm

3. HF Etching



$D_{Th} = 6 \mu\text{m}$



Sensitivity of:
2.5nm/RIU for
SRI=1.33
14.5nm/RIU for
SRI=1.44

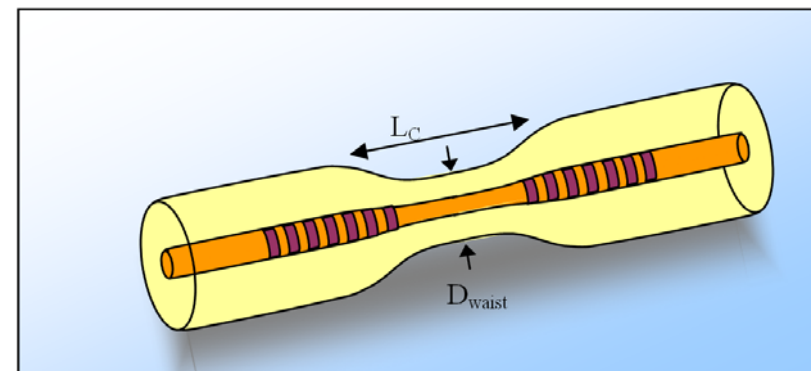
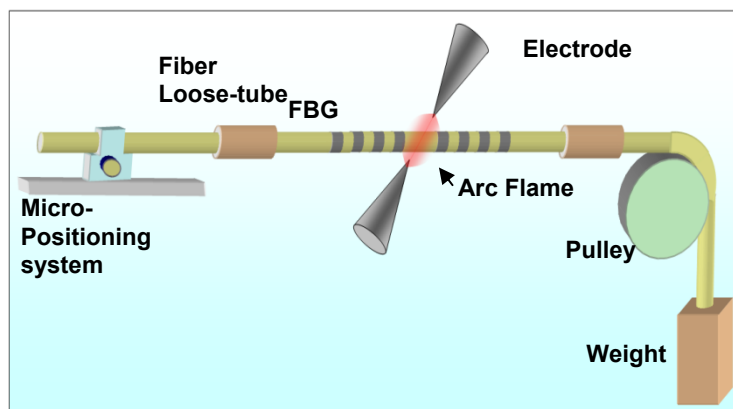
Heat & Pulling Technique

Locally heating and
contemporarily pulling it



Non-adiabatic
cavity tapering

$$\phi(\lambda) = \frac{4\pi}{\lambda} n_c L_c$$



Biconical taper features are mainly determined by:

- ✓ Arc Power (Arc Current)
- ✓ Arc Duration
- ✓ Pulling Weight (4÷20 g)

NOT-LITHOGRAPHIC FABRICATION PROCEDURE

1. Biconical Taper by Electric Arc Discharge (EAD)

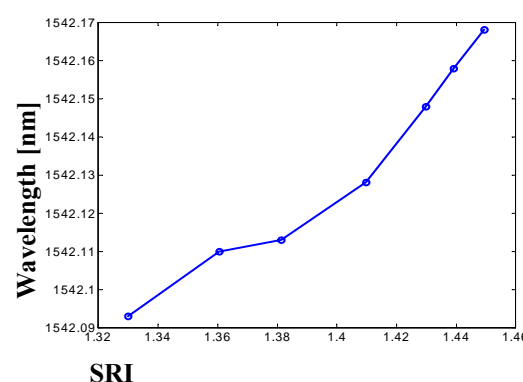
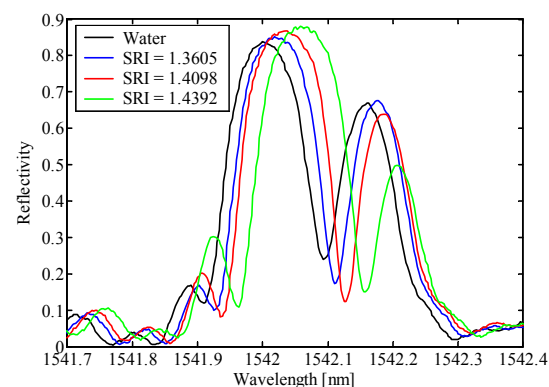
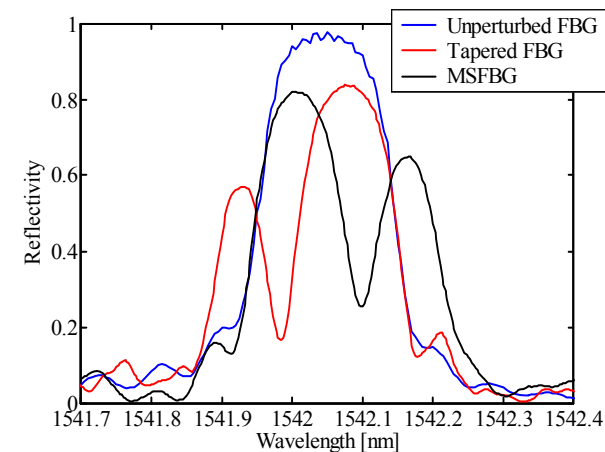


Here a diameter mismatch of 20 μm is requested

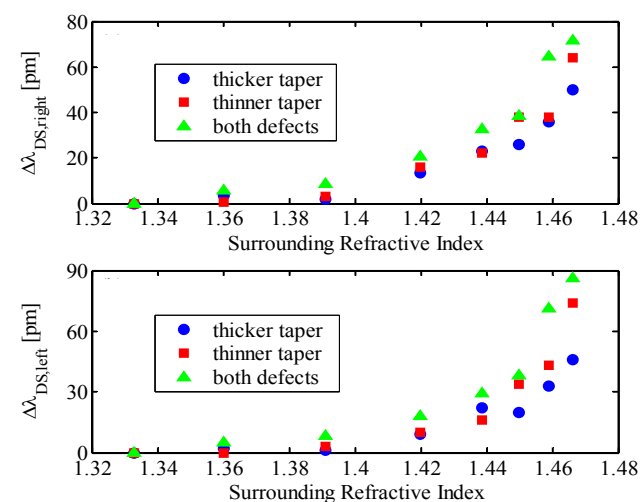
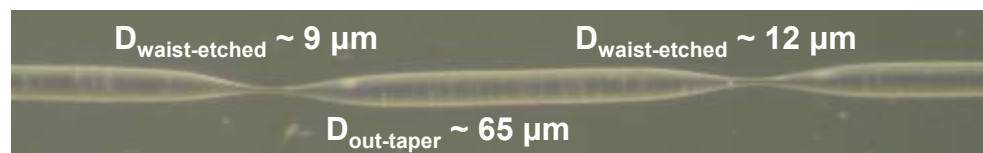
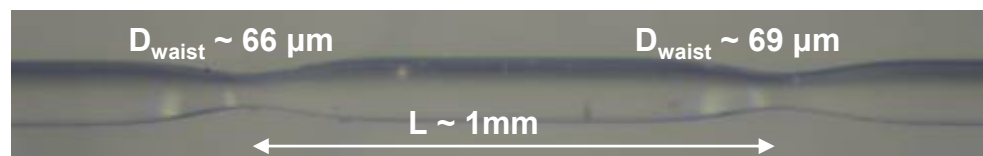
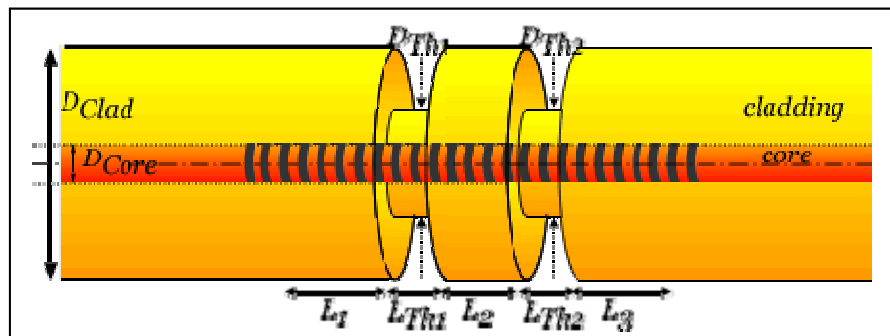
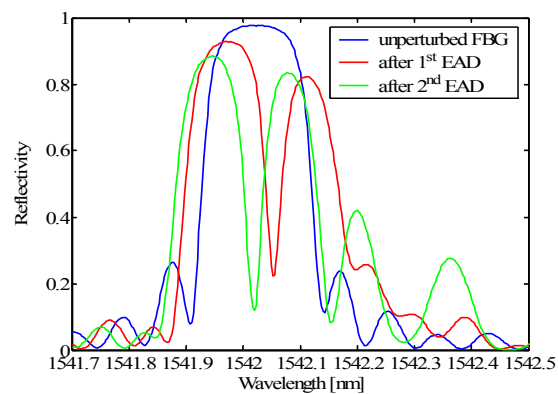
2. Maskless HF Etching



Wet chemical etching in HF allows a uniform fiber thinning

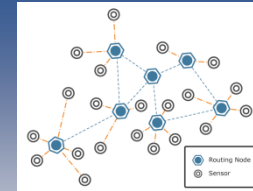


MULTI-DEFECT MSFBG



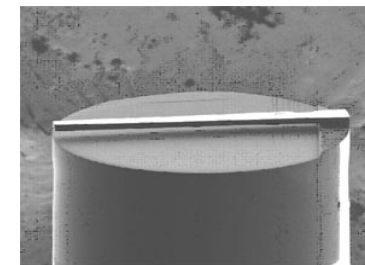
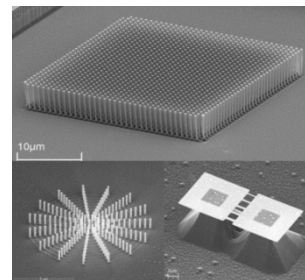
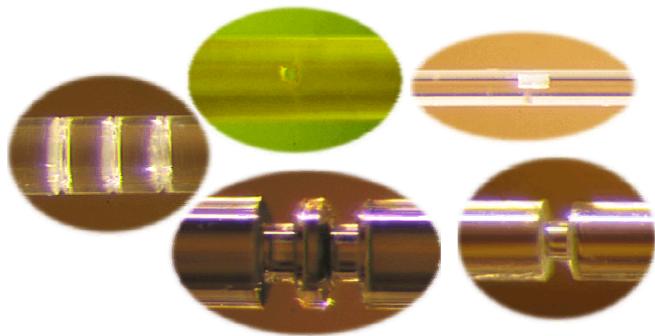
D. Paladino *et al.*, Optics Express 17, 1042 (2009)

A. Cusano *et al.*, Optical Fiber Technology 13, 291 (2007)



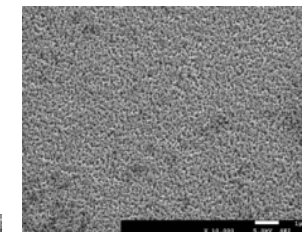
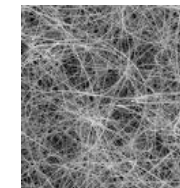
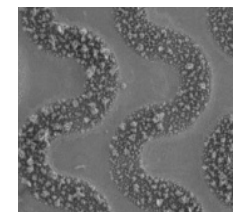
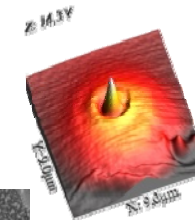
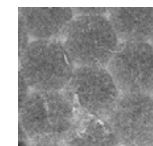
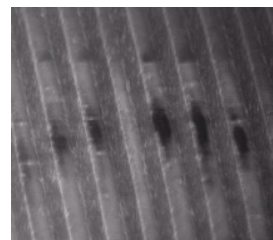
NEW TREND: LAB ON FIBER VISION towards integrated and multifunctional micro and nanodevices

- Integration and patterning (at the micro and nano-scale) of different functional materials with desired optical, mechanical, magnetic, electrical, acoustic, chemical and biological properties



A. Cusano et al.,
“Lab on fiber technology
and related devices”,
Invited Paper
Proc. SPIE, vol. 8001
(2011)

Increased light matter interaction and creation of a technological world completely integrated within optical fibers with significant advantages in terms of functionality, performances, miniaturization, robustness, cost effectiveness and power consumption

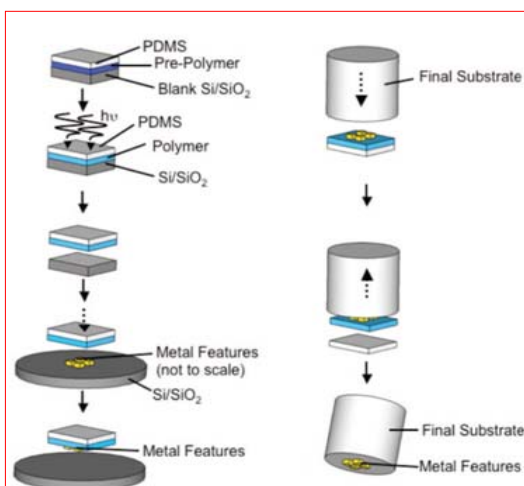


MAIN ISSUE: Definition of a reliable *fabrication procedure able to integrate and process, at micro- and nano-scale*, several materials onto unconventional substrates such as the optical fibers.

Integration with Optical Fibers

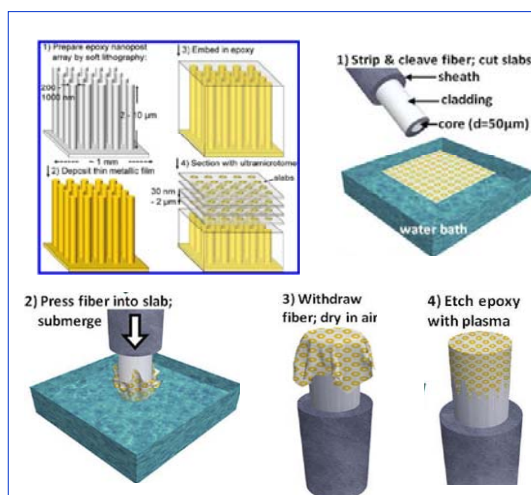
Nano-fabrication on planar substrates and transferring onto optical fibers

EBL and soft lithography



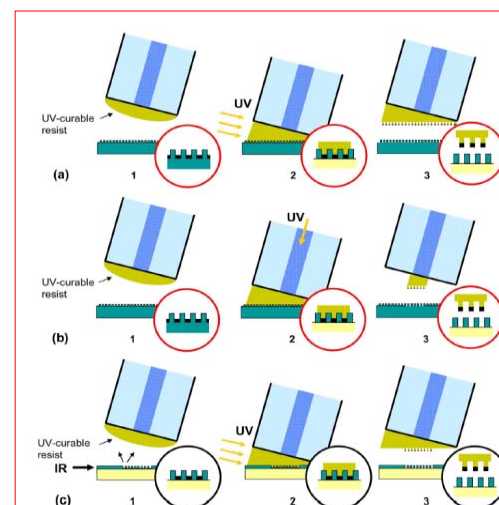
E. J. Smythe, F. Capasso et al.,
ACS Nano, 2009, 3 (1), 59-65

Soft lithography, nano-skiving and dipping



D. J. Lipomi, F. Capasso et al.,
Nano Lett. 2011, 11(2) 632-6

UV nano imprint and transfer lithography (NITL)

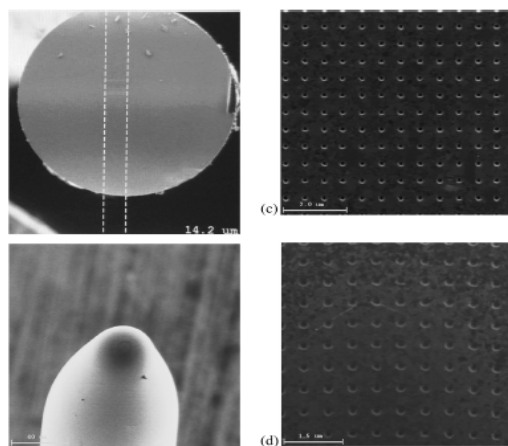


S. Scheerlinck, R. Baets et al., J.
Light. Tech., pp.1415-1420, 2009

Integration with Optical Fibers

Direct-writing approaches

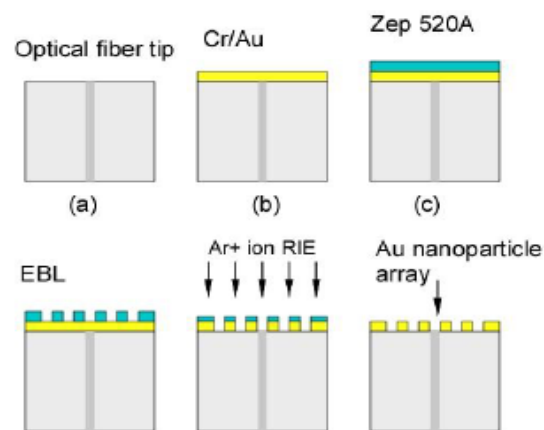
FIB milling



A. Dhawan et al., Sens. J. IEEE
2008, 8, 942-950



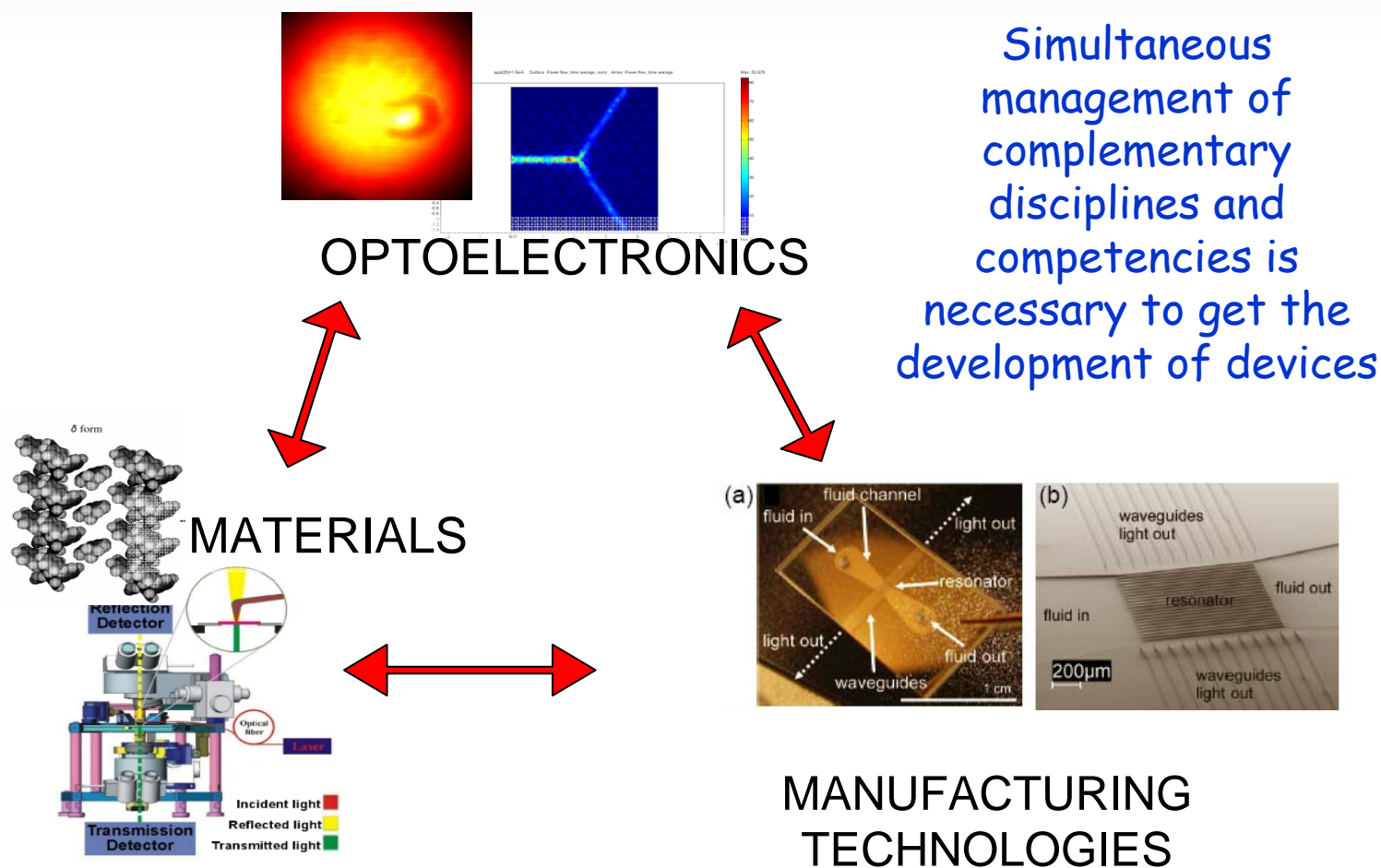
EBL and Reactive Ion Etching



Y. Lin, R. G. Lindquist et al., Biomed
Opt Express. 2011; 2(3): 478-484.



Multidisciplinary Approach





**Ente Nazionale per
l'Energia e l'Ambiente,
Portici (NA) Italy**



**Plasma Enhanced
Chemical Vapor
Deposition (PE-CVD)**



Focused Ion Beam (FIB)



**Excimer Laser
Micromachining
Systems (193
nm)**



**Optical
Characterization**



**Modified
Spin coater**



**Excimer Laser
Micromachining
Systems (248
nm)**



**Magnetron
Sputtering
System**

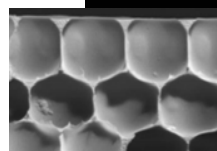
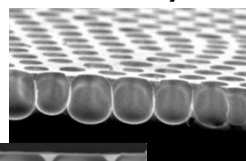


**Istituto di Cibernetica "E.
Caianiello", CNR, Pozzuoli (NA)
Italy**



**Electron Beam Lithography
EBL RAITH 150**

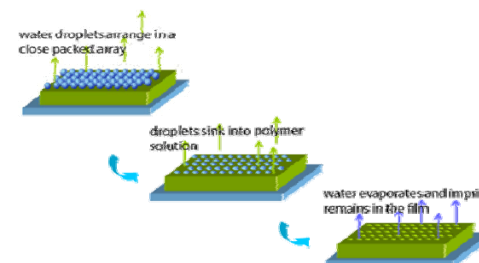
Monolayer



Multilayer



Self-assembling techniques



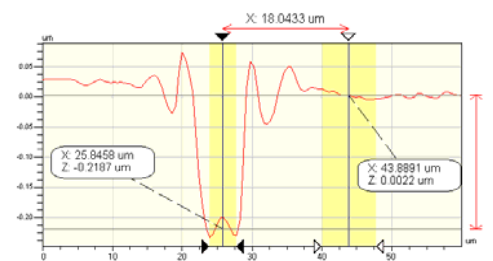
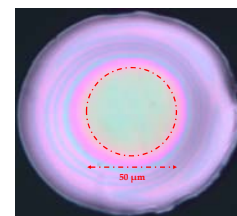
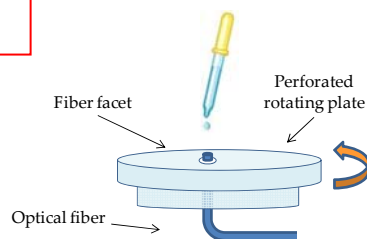
A New Fabrication Process

Direct fabrication of metallic and dielectric nanostructures on the optical fiber tip

A. Cusano et al., **ACS Nano**. 2012, vol. 6(4), pp. 3163–3170.

1) Electron resist (ZEP520A) deposition

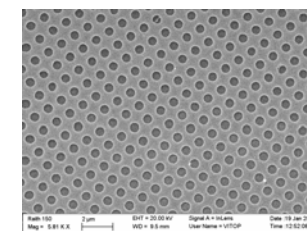
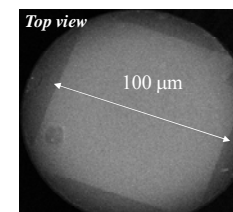
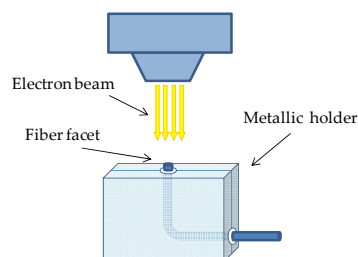
Customized spin coating for optical fibers



100-400nm thick (ZEP) overlay can be reproducibly obtained with high uniformity on the fiber core

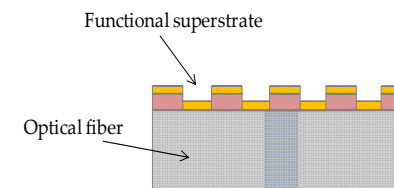
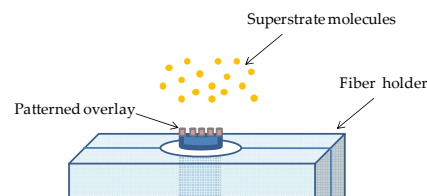
2) Nano-scale patterning of the overlay

Customized EBL for optical fibers



3) Functional superstrate deposition

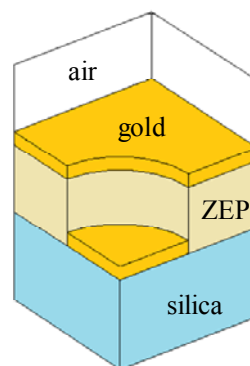
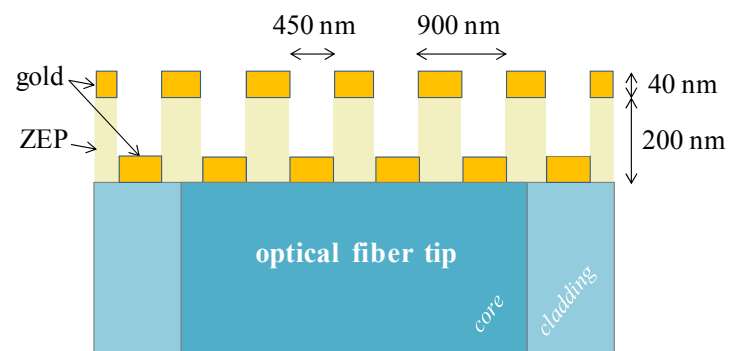
Customized sputtering, thermal evaporation, etc.



Different functional materials (metallic or non-metallic) can be easily deposited by various techniques, properly customized to operate with optical fibers

Nanoplasmonics within Optical Fibers

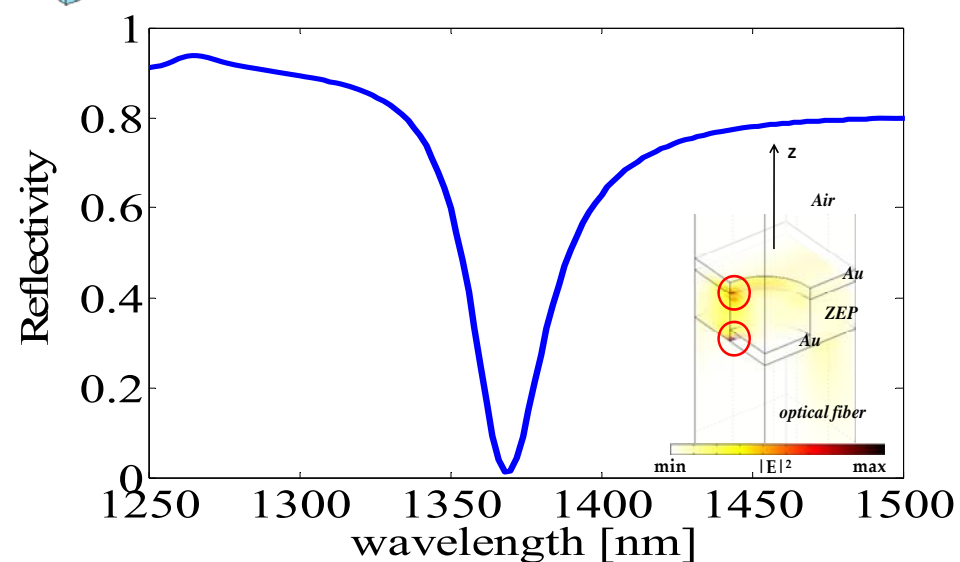
A first technological platform based on a 2D metallo-dielectric nanostructure



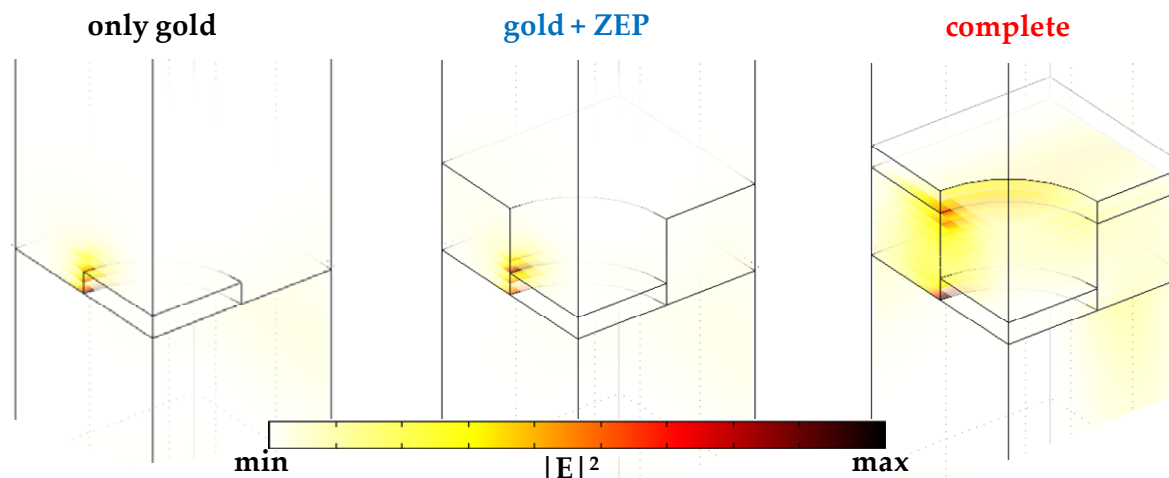
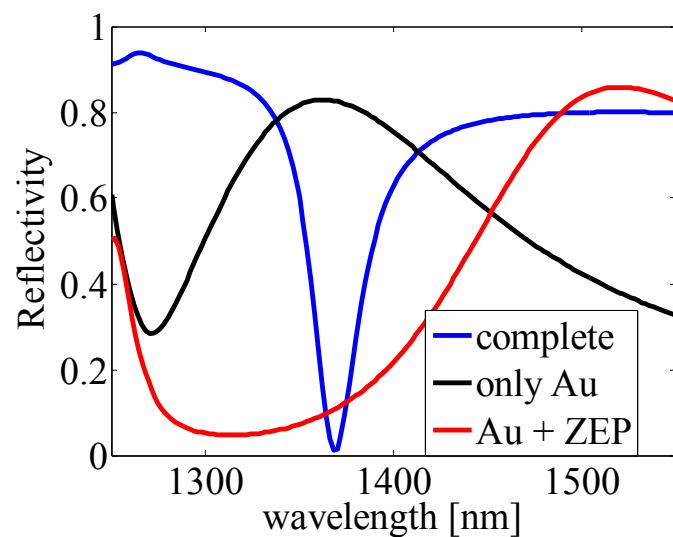
Full-wave simulations have been carried out
via the finite-element-based commercial
software package COMSOL Multiphysics

Refractive index at 1350 nm:

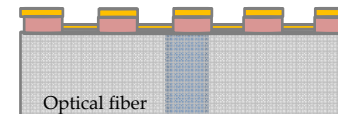
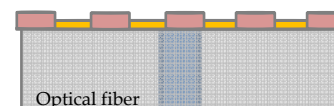
$$\begin{aligned} n_{\text{ZEP}} &= 1.54 && \text{[from datasheet]} \\ n_{\text{Au}} &= 0.5 - 7j && \text{[E.D. Palik, Academic Press, New York, 1985]} \\ n_{\text{SiO}_2} &= 1.44 \end{aligned}$$



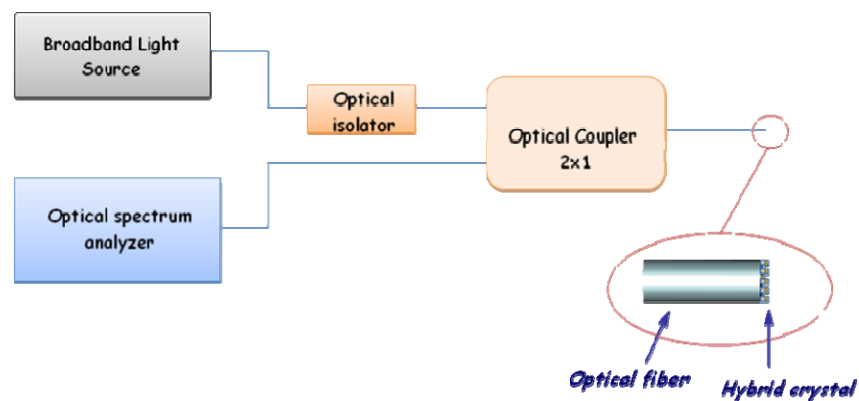
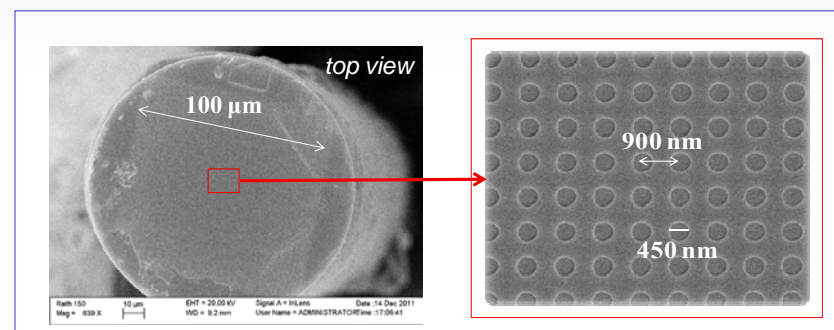
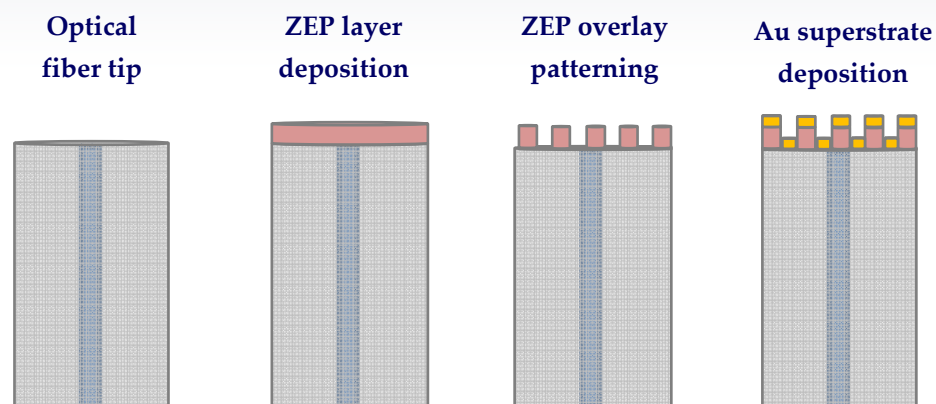
THE WHOLE IS BETTER THAN THE SINGLE PARTS



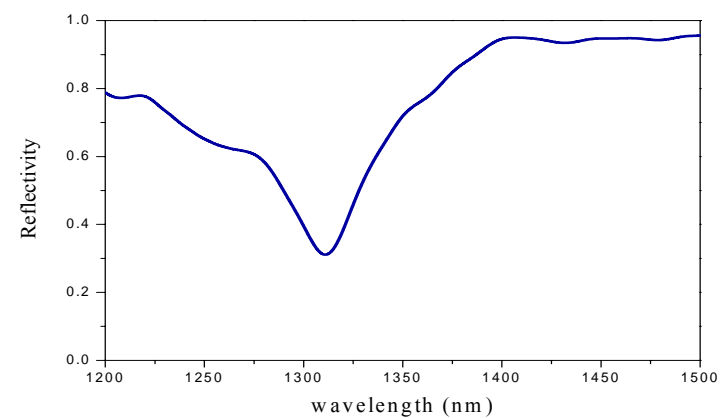
Enhancement of Field Intensity up to 7 times



Device Fabrication



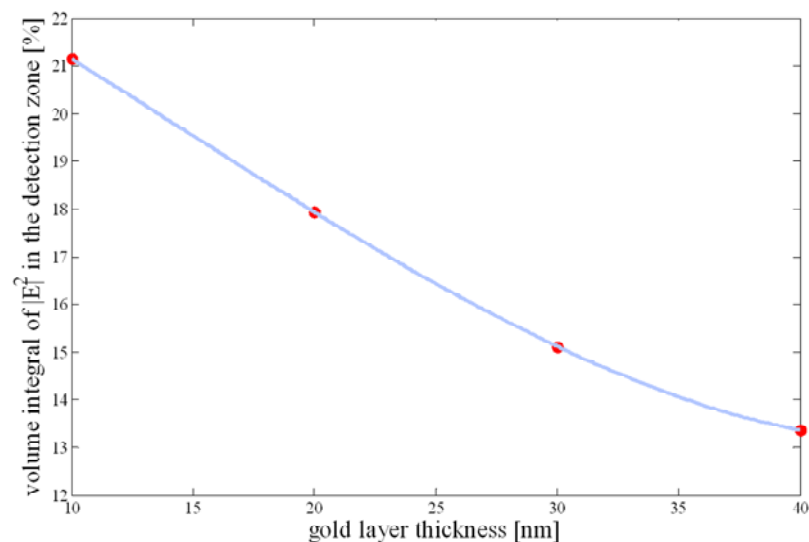
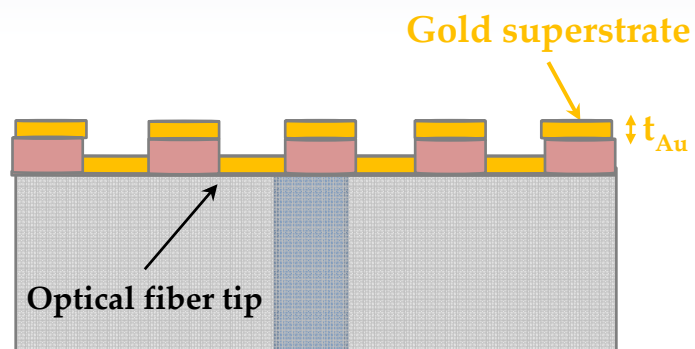
Experimental setup for spectral characterizations of fabricated samples



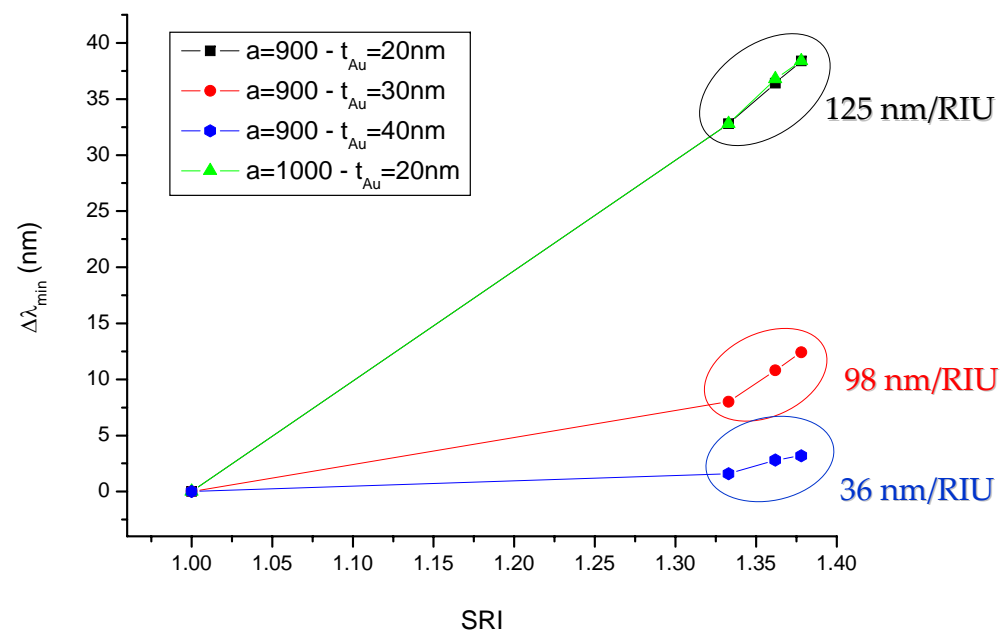
Reflectivity spectrum of a hybrid crystal with period $a=900 \text{ nm}$ ($r/a=0.25$)

A resonance dip centered at 1311 nm was found with a Q-factor of ~ 23

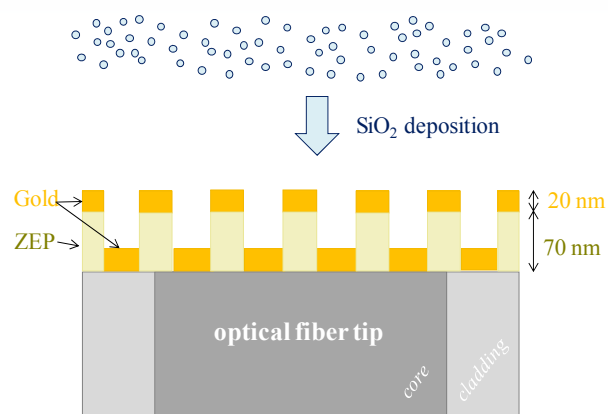
LIGHT-MATTER INTERACTION ENHANCEMENT



Decreasing gold thickness provides a useful tool to improve light matter interaction with the surrounding environment



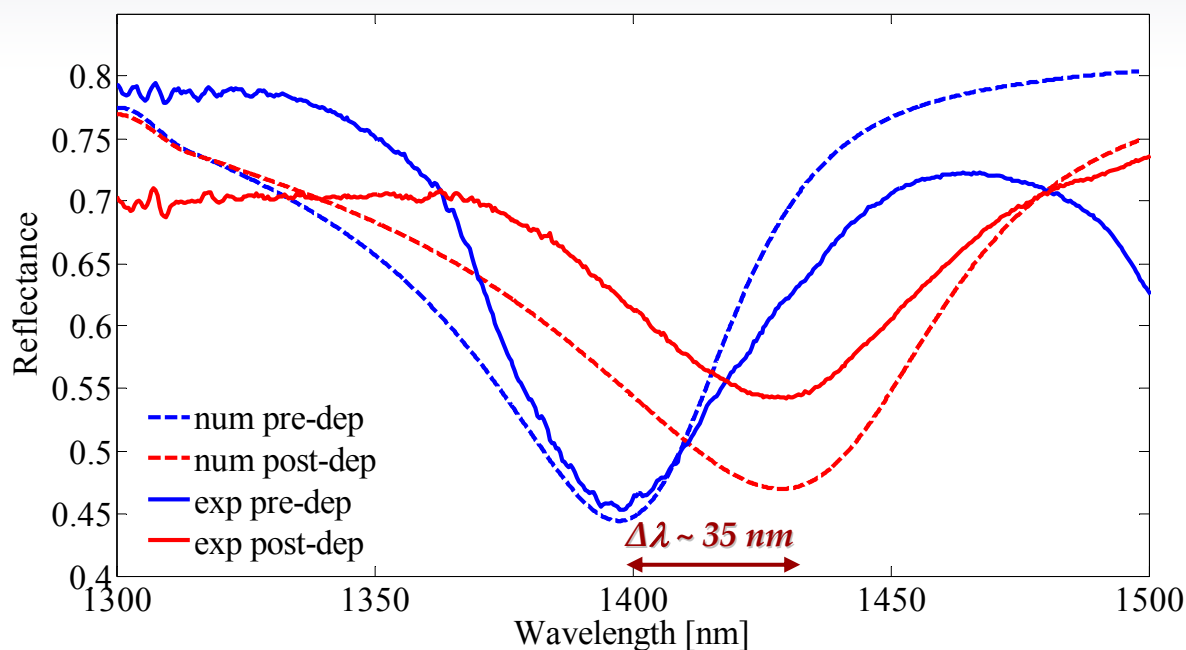
SURFACE REFRACTIVE INDEX SENSITIVITY



$$d_{ZEP} = 70\text{nm} , d_{Au} = 20\text{nm}$$

$$d_{SiO_2} = 100\text{nm}$$

$$n_{SiO_2} = n_{biolayers} \sim 1.45$$

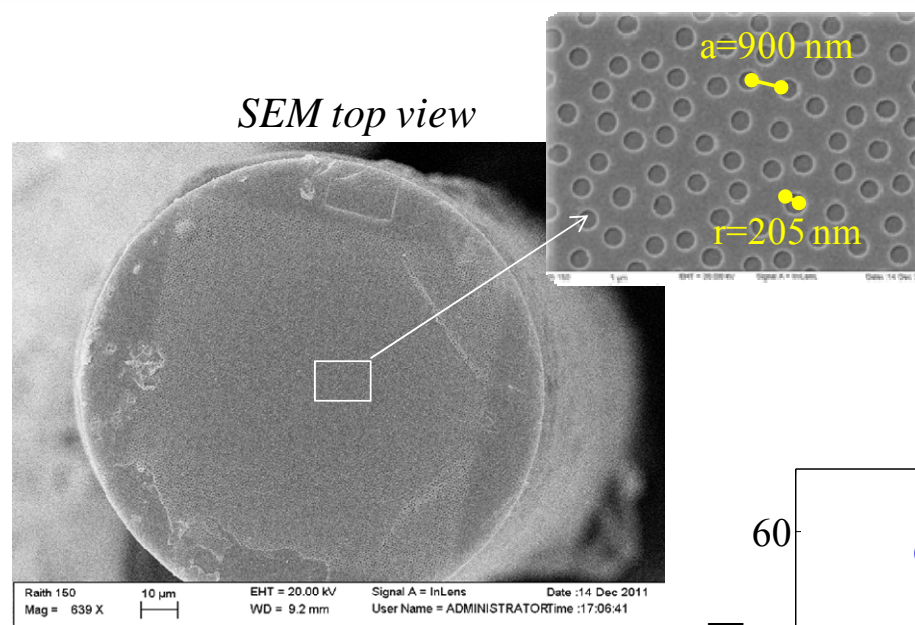


Numerical and experimental spectra before and after the deposition of a 100nm-thick SiO_2 overlay

The surface sensitivities (in terms of resonance shift per nanometer of SiO_2 overlay) resulted as high as 0.35 nm /nm of deposited overlay

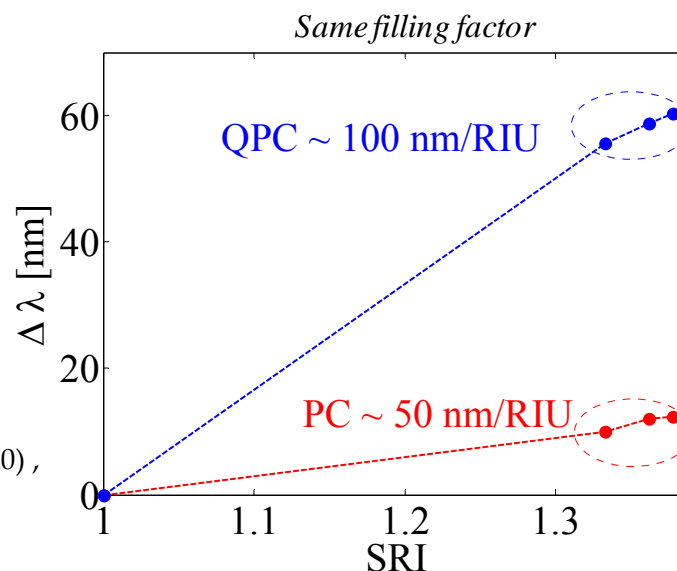
Further optimization margins exist taking advantages from the large set of degrees of freedom exhibited by the platform

REFRACTIVE INDEX SENSITIVITY ENHANCEMENT USING PALSMONIC RESONANCES IN HYBRID METALLO-DIELECTRIC QUACRYSTALS INTEGRATED ONTO OPTICAL FIBERS

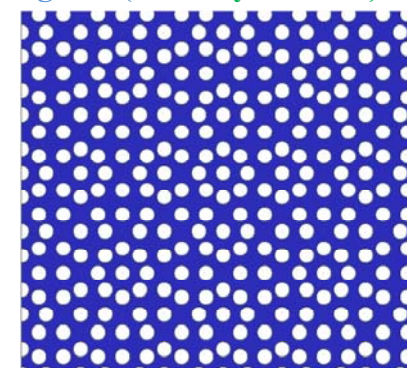


For a given filling factor QCs outperform the periodic counterpart

A. Cusano et al, *Advanced Functional Materials*, 22 (20), 4389-4398 (2012)



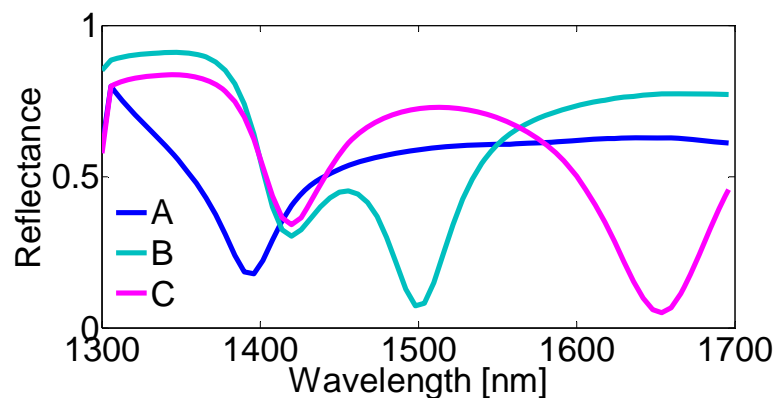
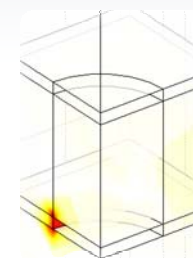
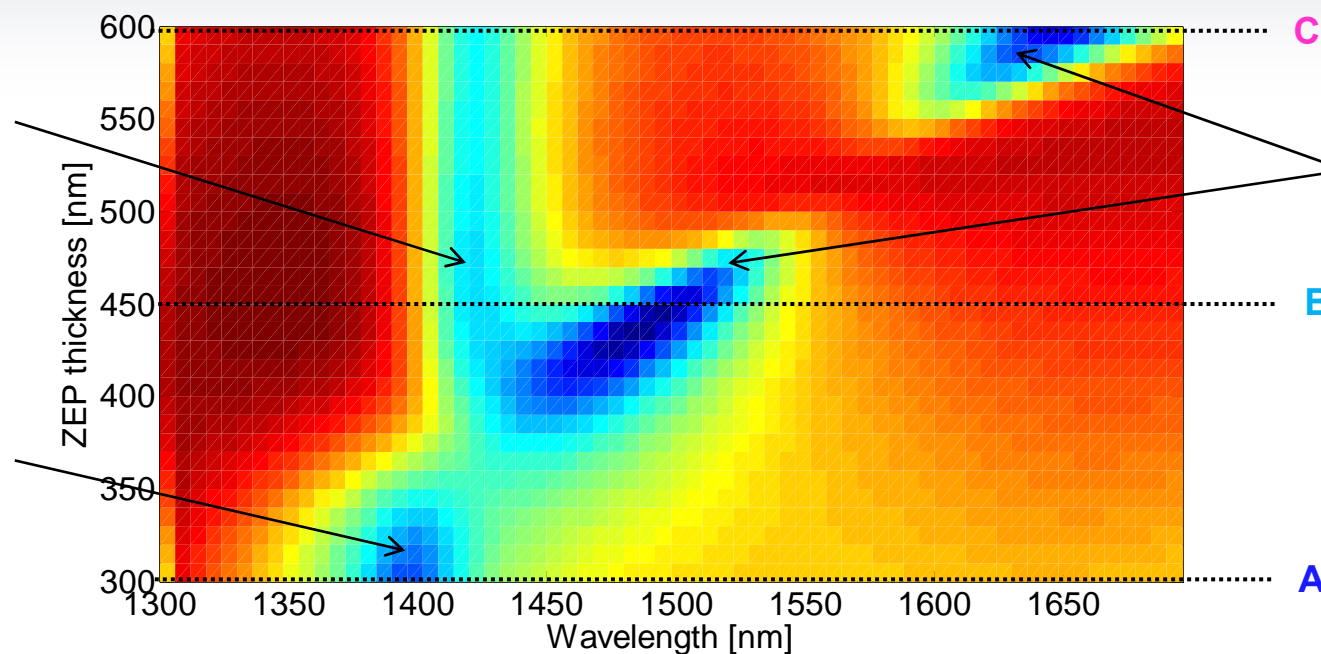
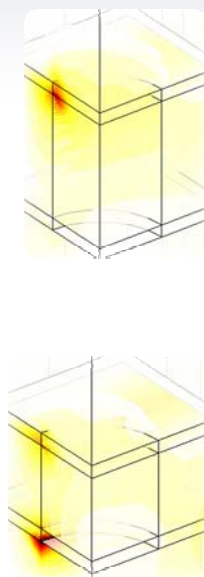
Ammann-Beenker
octagonal (8-fold symmetric) tiling



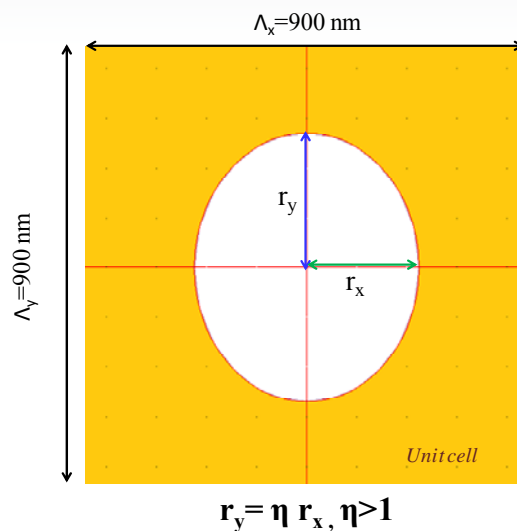
Rotational symmetry for $\phi=2\pi/8$

Using the large set of available parameters (gold and resist thickness, lattice tiling) SRI sensitivities of the order of 500nm/RIU are expected with active regions of less than 100 μm^2

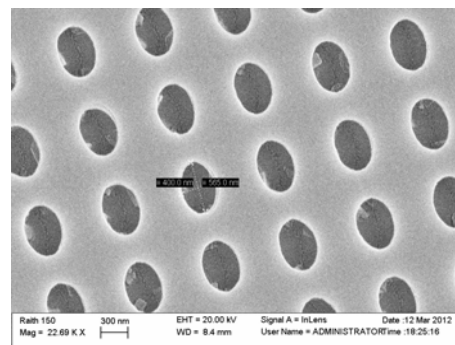
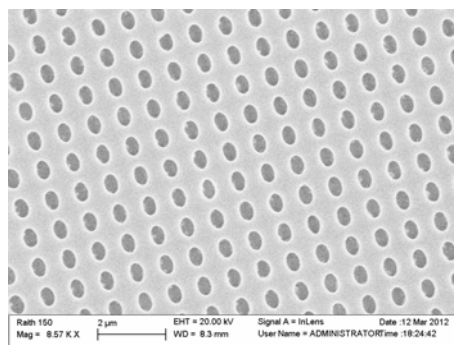
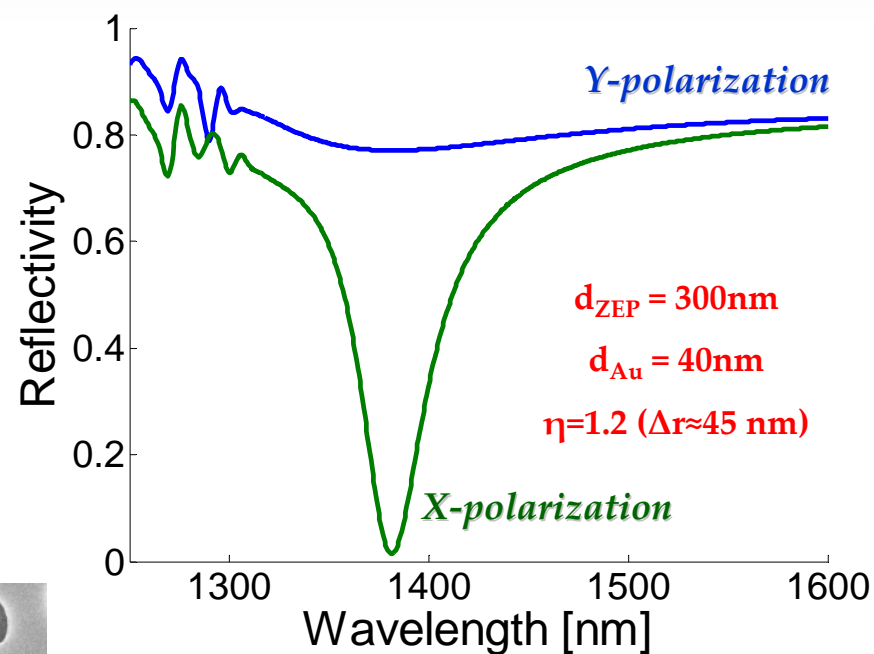
DIELECTRIC THICKNESS TUNING : TOWARDS RESONANCES ENGINEERING



TOWARDS POLARIZATION DEPENDENCE-BASED DEVICES



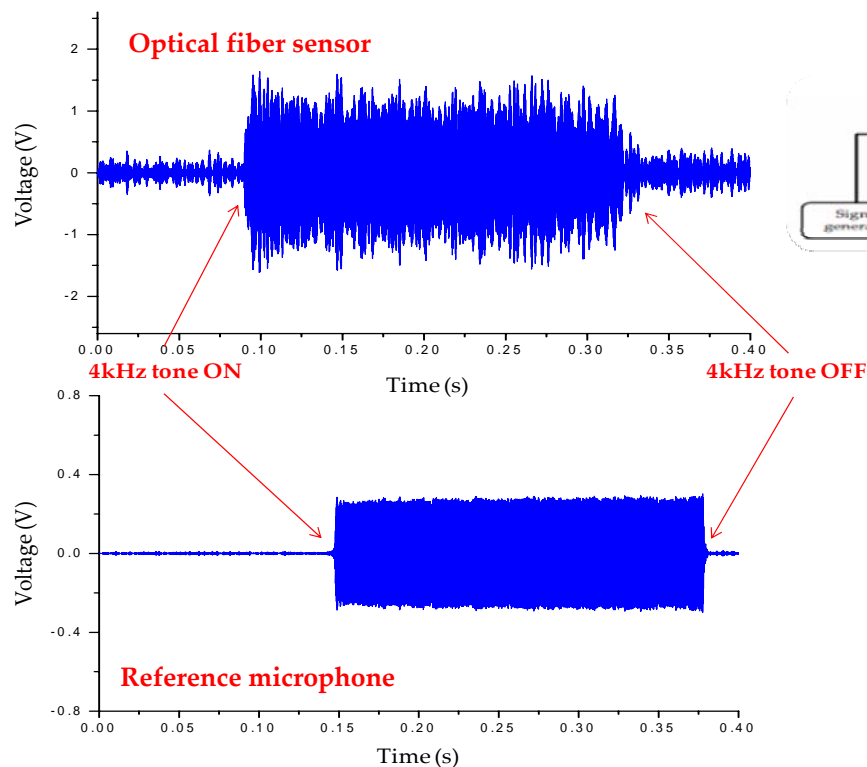
Ellipticity
 $\eta = r_y / r_x$



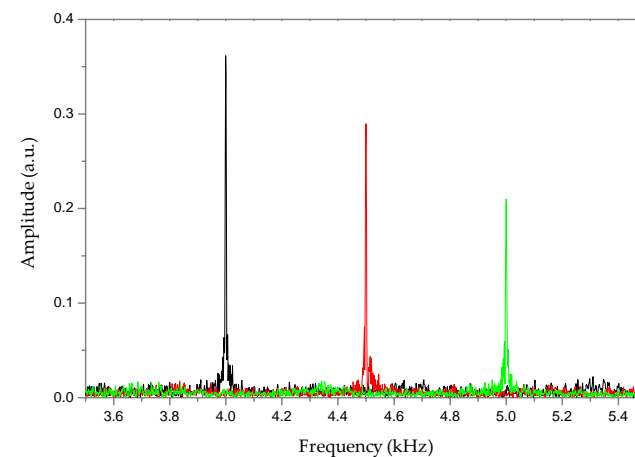
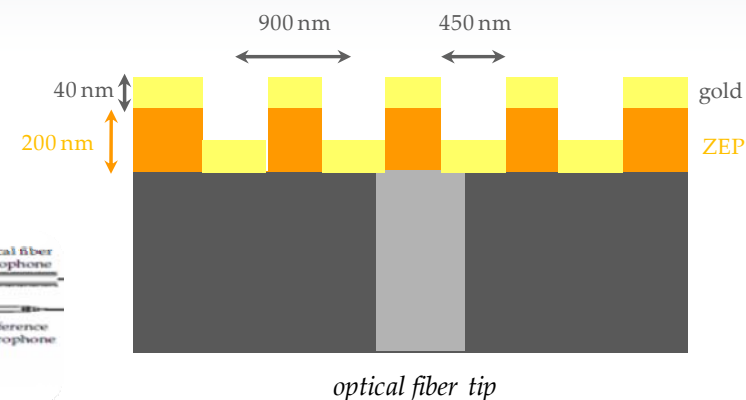
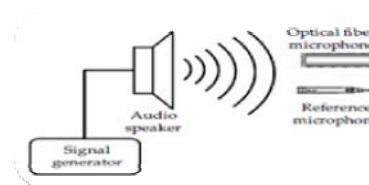
Numerical spectra of the two orthogonal polarization (X- and Y-polarizations) when $\eta = 1.2 (\Delta r \approx 45 \text{ nm})$

MULTIPARAMETER SENSING: ACOUSTIC WAVE DETECTION

Active role of the polymeric layer: Incident acoustic pressure wave modulates either the geometric features of the low elastic module polymer producing a resonance dip shift at the same frequency of the acoustic wave.



Typical time response for a 4kHz tone



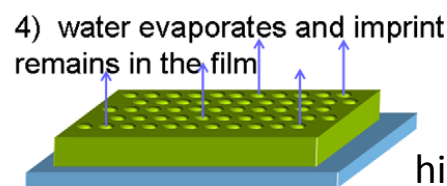
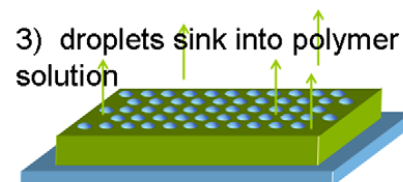
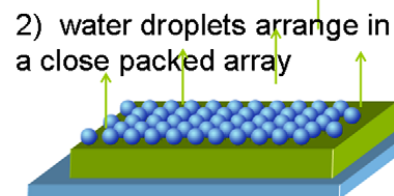
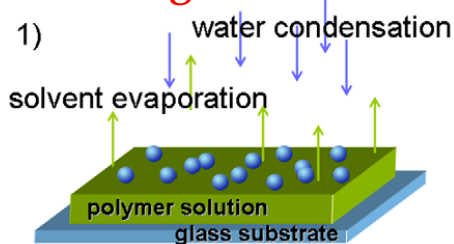
Sensor response to tones having different frequency

LAB ON FIBER BY SELF ASSEMBLY: BREATH FIGURE TECHNIQUE

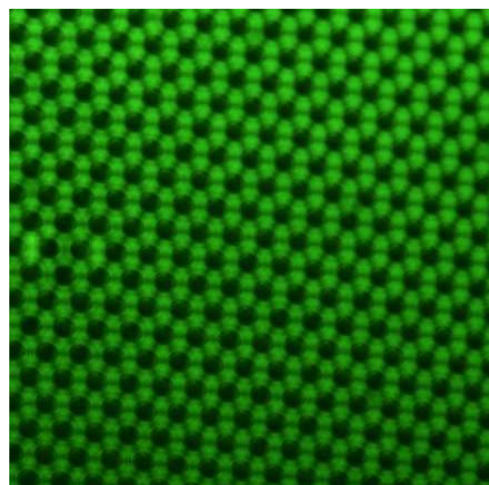
In collaboration with

Self assembly techniques enable the deposition of polymeric periodic pattern on glass substrates

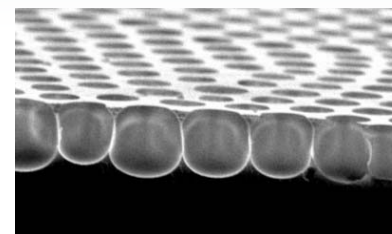
Breath figure (BF) technique



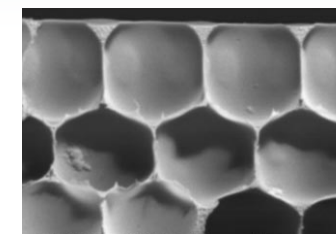
deposition conditions:
1.5-5 mg/mL polystyrene
in CS₂
moist N₂: 60 % R.H. at
25 °C
2 L/min flow



highly ordered breath figure patterns



monolayer



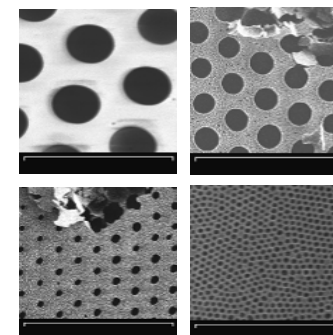
multilayer

tunable
structures

cavity size : nm → μm

Galeotti F et al. Self-functionalizing Polymer Film Surfaces Assisted by Specific Polystyrene End-tagging. *Chemistry of Materials*, **2010**, 22, 2764-2769.

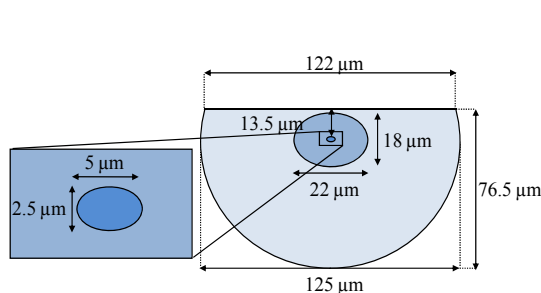
Galeotti F. et al, CdTe nanocrystal assemblies guided by breath figure templates. *Soft Matter*, **2011**, 7, 3832-3836.



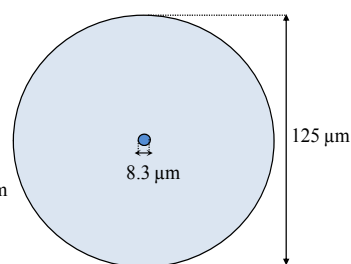
scale bar is 10 μm

FIB-ASSISTED NANOFABRICATION FOR LAB-ON-FIBER TECHNOLOGY

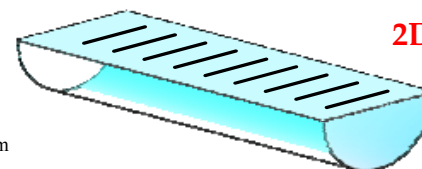
D-shaped fiber



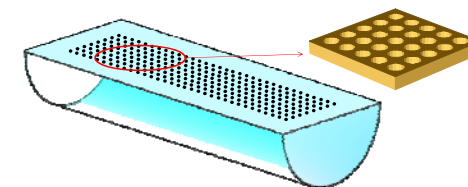
Standard fiber



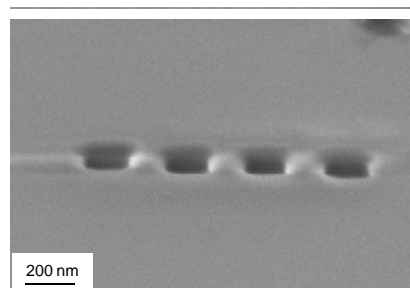
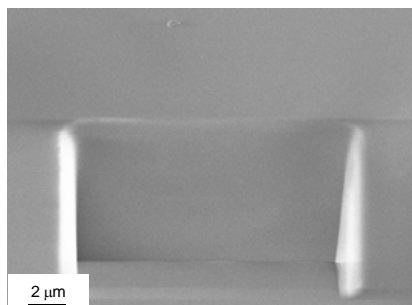
New Fiber Gratings (1D)



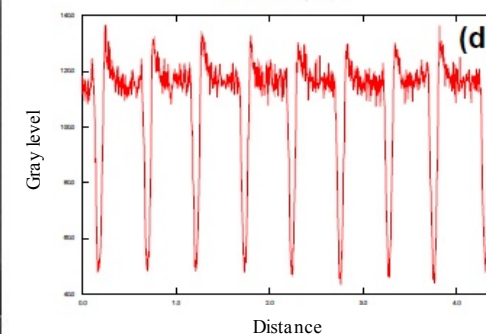
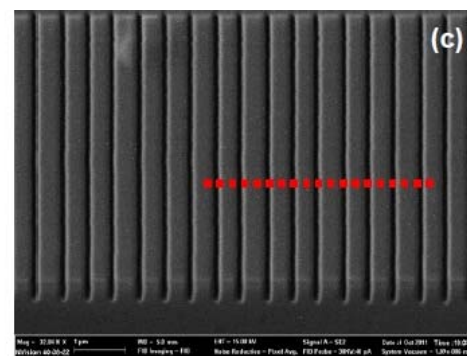
2D In-Fiber Photonic-Plasmonic Crystals



1D metallic (Pt) grating realized on the core of a D-shaped optical fiber (the grating period is 500 nm)



SEM images of a $13 \times 13 \mu\text{m}^2$ dig (depth = $13.5 \mu\text{m}$) and of a row of $150 \times 150 \text{ nm}^2$ holes FIB milled inside the fiber core.



SEM image of a Pt 1D grating created on the core of a D-shaped fiber by FIB. The contrast line-scan profile shows the regularity of the pattern.

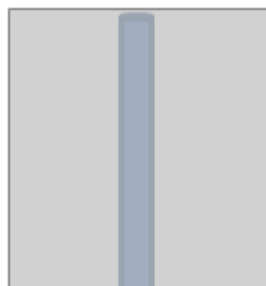
Lab on Fiber by Focused Ion Beam (FIB)

Fabrication steps for creating a photonic crystals slab on the fiber tip

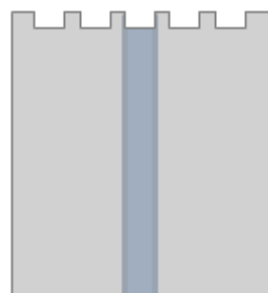


Italian National Agency for New Technologies,
Energy and Sustainable Economic Development

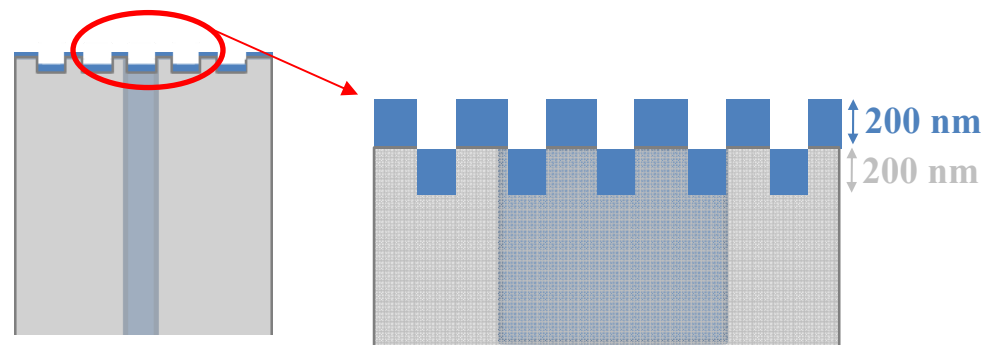
1. Optical fiber tip



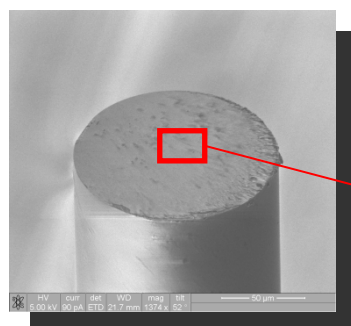
2. Optical fiber nano-pattern (FIB)



3. nSiOx deposition (PECVD)

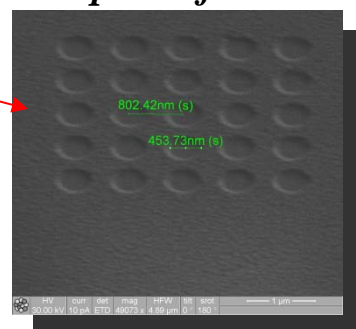


Preliminary experimental results

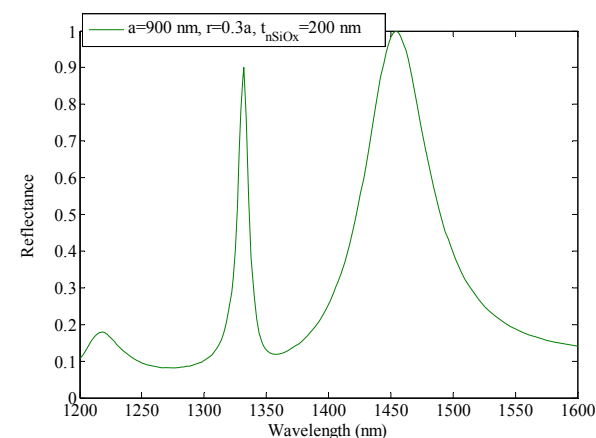


SEM image

Nano-pattern onto the optical fiber



Numeric Reflectance



STARTING RESEARCH PROJECT: “SMART HEALTH 2.0”

- Supported by Italian Ministry of University and Research
- Call: PON Smart Cities
- Funding : 30M€
- Duration: 3 years



Optoelectronics Framework

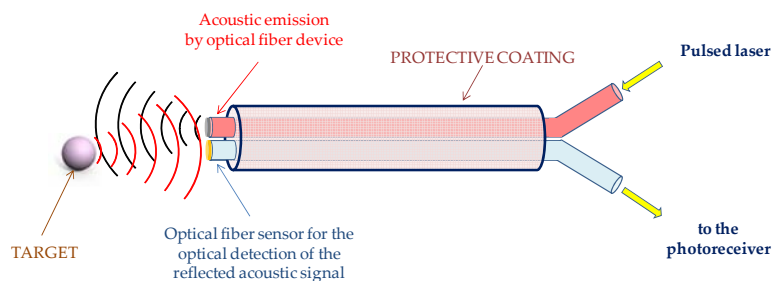
*To develop innovative optical fiber sensors
for real time and continuous
detection of clinically relevant
parameters
for the invasive diagnostics*



CENTRO REGIONALE
INFORMATION COMMUNICATION TECHNOLOGY
CERICT SCRL



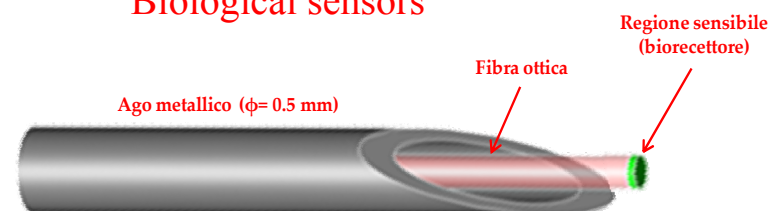
Acoustic Sensors



Magnetic sensors



Biological sensors



A NEW PUBLIC-PRIVATE AGGREGATION "TOP-IN"

- Supported by Italian Ministry of University and Research
- Call: PON *LABORATORI PUBBLICO-PRIVATI E RELATIVE RETI*
- Funding : 20.6M€ for 3 Industrial Research Projects
- Partners: 30 (industries, research centers, universities, SME)



Tecnologie
Optoelettroniche
per l'Industria

Mission: Research and development of optoelectronic technologies for industrial applications

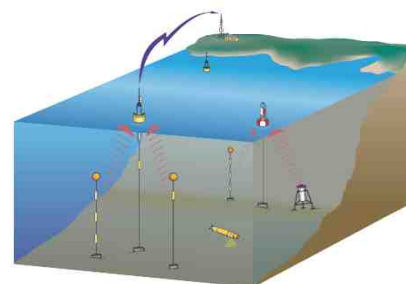
Nanophotonics Laboratory

Main lines of action (priorities)

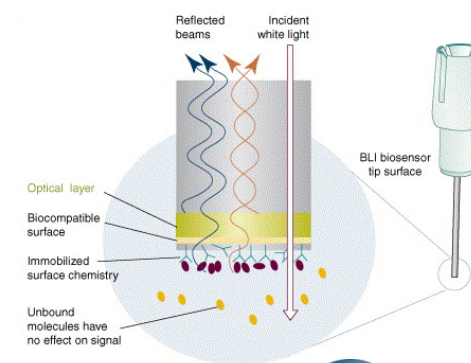
Railway monitoring



Water monitoring

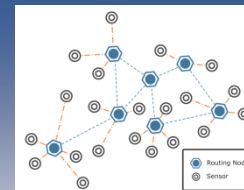


Biomedical sensors





Optoelectronics Group, Engineering Department
University of Sannio, Benevento (Italy)



**THANKS FOR YOUR
ATTENTION**

